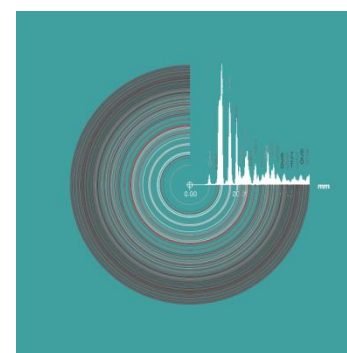
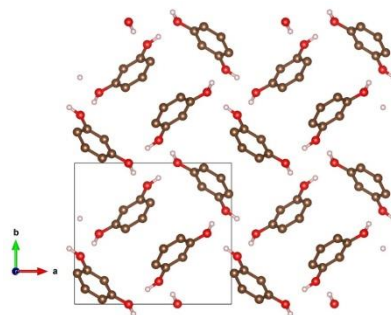


CRYSTAL STRUCTURE ANALYSIS OF PHARMACEUTICALS WITH ELECTRON DIFFRACTION



Dr. Stavros Nicolopoulos

Consultant IUCr Electron Crystallography Commission



This document was presented at PPXRD - Pharmaceutical Powder X-ray Diffraction Symposium

Sponsored by The International Centre for Diffraction Data

This presentation is provided by the International Centre for Diffraction Data in cooperation with the authors and presenters of the PPXRD symposia for the express purpose of educating the scientific community.

All copyrights for the presentation are retained by the original authors.

The ICDD has received permission from the authors to post this material on our website and make the material available for viewing. Usage is restricted for the purposes of education and scientific research.



PPXRD Website – www.icdd.com/ppxrd

ICDD Website - www.icdd.com

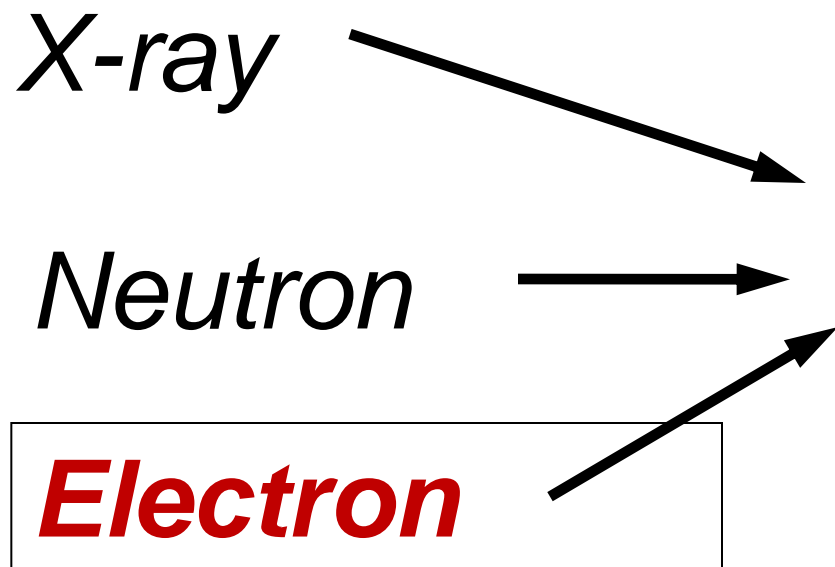
Free transnational access

to the most advanced TEM equipment
and skilled operators for HR(S)TEM,
EELS, EDX, Tomography, Holography and
various in-situ state-of-the-art
experiments

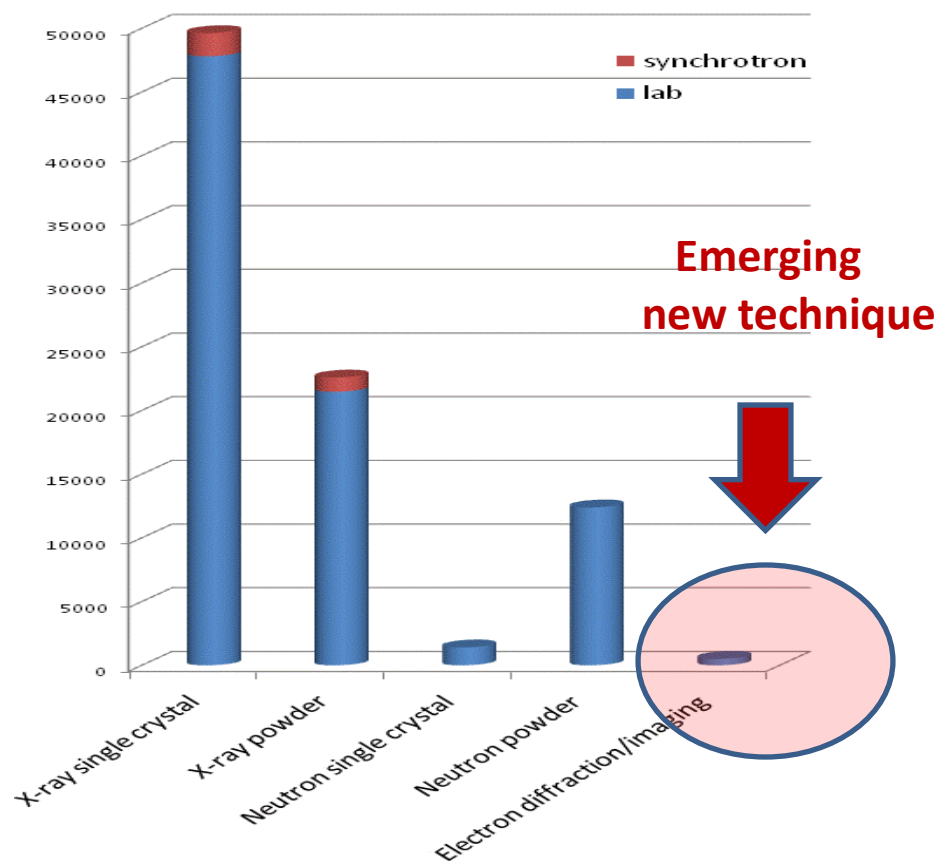
X 2 SME participate

CEOS
NanoMEGAS





Crystallography



Why electrons?

- **10^{4-5} times stronger interaction with matter compared with X-ray**
 - *single crystal data on powder sample*
 - *short data collection time*
- Phases are present in high resolution electron microscopy (HREM) images
 - **for nm- and micro-sized crystals**

Comparison X-Ray powder diffraction /electron diffraction: Limitations X-Ray powder

Ovelapping of reflections

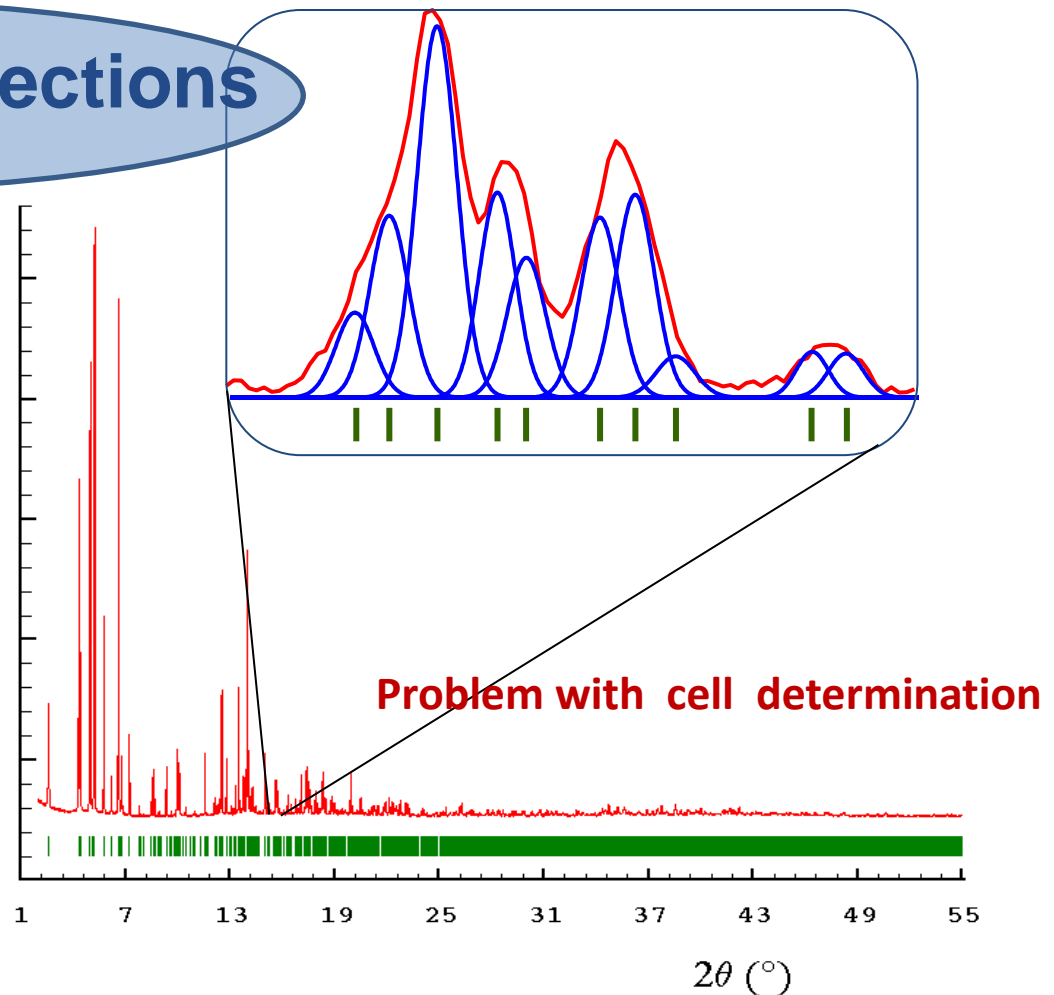
stacking intergrowth

Preferential orientation

Nanocrystals

Impurities

Light atoms (Li, Be)



X- Ray powder diffraction limitations

overlapping

Stacking intergrowth

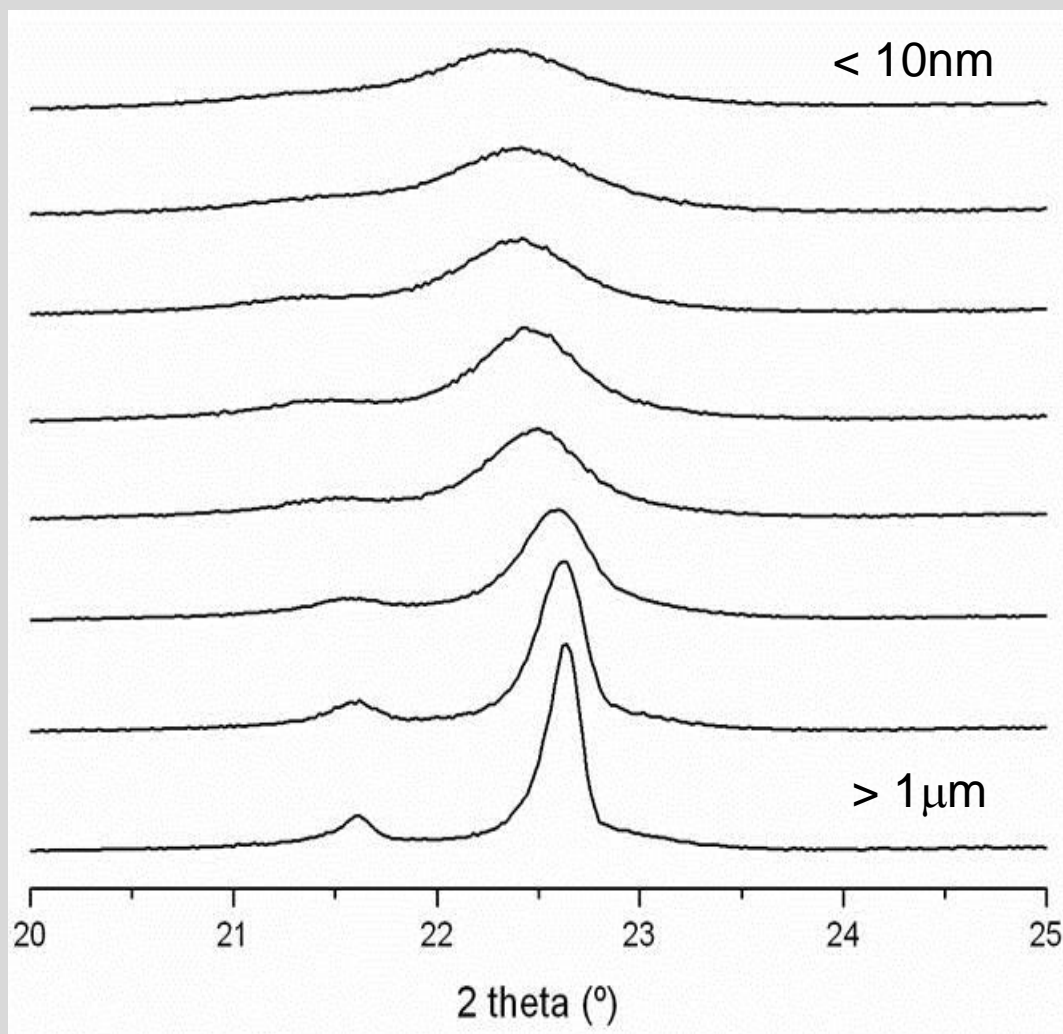
Preferential orientation

Nanocrystals

Impurities

Light atoms (Li, Be)

X-Ray “amorphous”

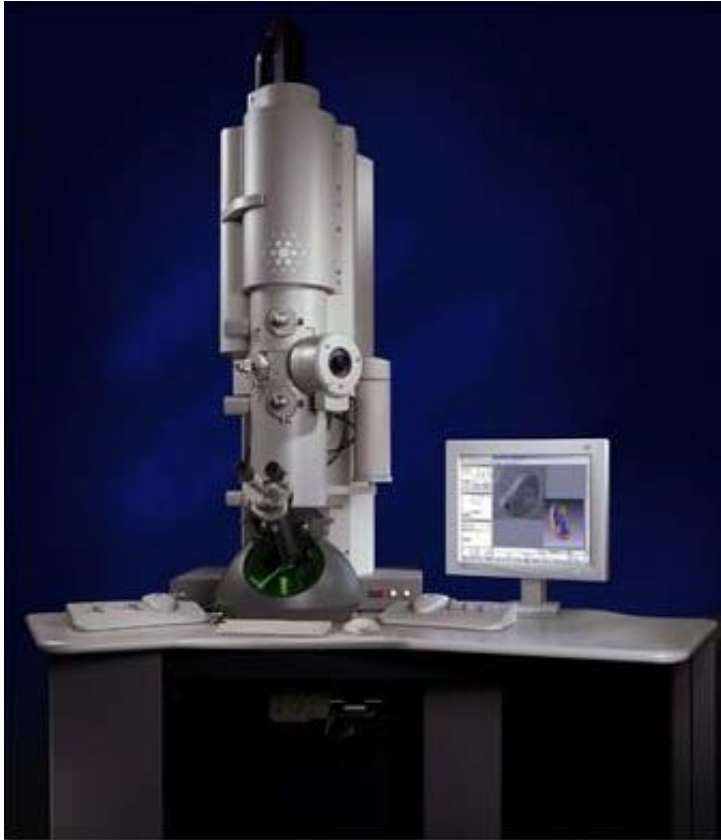


NanoMEGAS

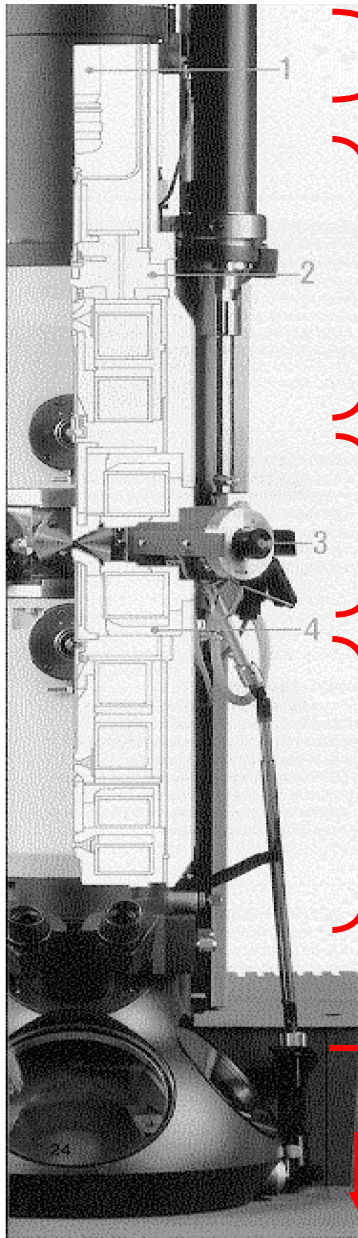
Advanced Tools for electron diffraction

Transmission electron microscopy

TEM



- **Diffraction** – selected area, nano- and convergent beam electron diffraction
- **Imaging** – conventional, high resolution
- **Chemical analysis** – EDS and EELS



Source (Gun)

TEM : It can be **thermionic** or **field emission**

Illumination system

Two condenser lenses C1 and C2
C1 : different **spot sizes**
C2 : **convergence** of the beam

Objective Lens

It creates the **first image** of the sample

Projection system

Intermediate lens: to change from **image** mode to **diffraction** mode

Projection lens: to change the **magnification**

Screen

CCD or Photographic plates

TEM : Image resolution

With TEM microscopes we can obtain images of **crystalline materials** with atomic resolution:

Acceleration voltage (kV)

120

200

300

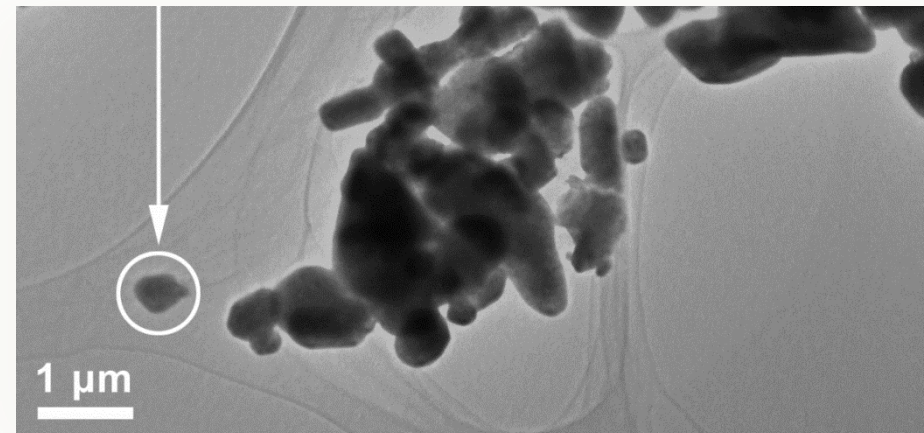
Point resolution (Å)

~3

2.0

1.7

We can see nano-crystals



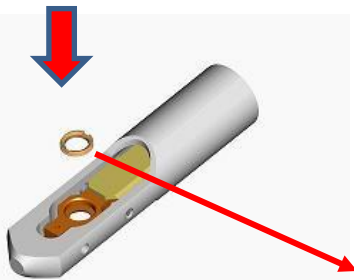
TEM : Brightness and beam size

FEG Guns have a higher brightness (10^3):

we can use beams with a smaller diameter having enough current for obtaining a detectable signal

	Thermionic	FEG
Smallest beam size	10nm	<1nm

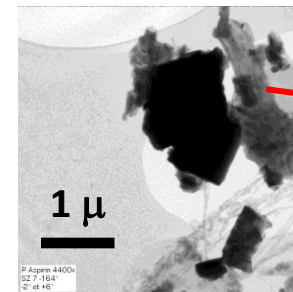
TEM grid
4 mm size



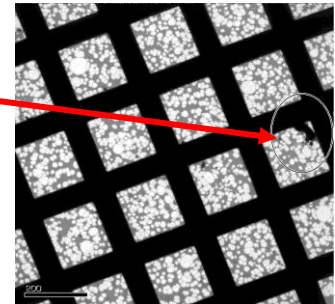
We have a nano-probe!

**Very small quantity
of sample !**

aspirin crystals

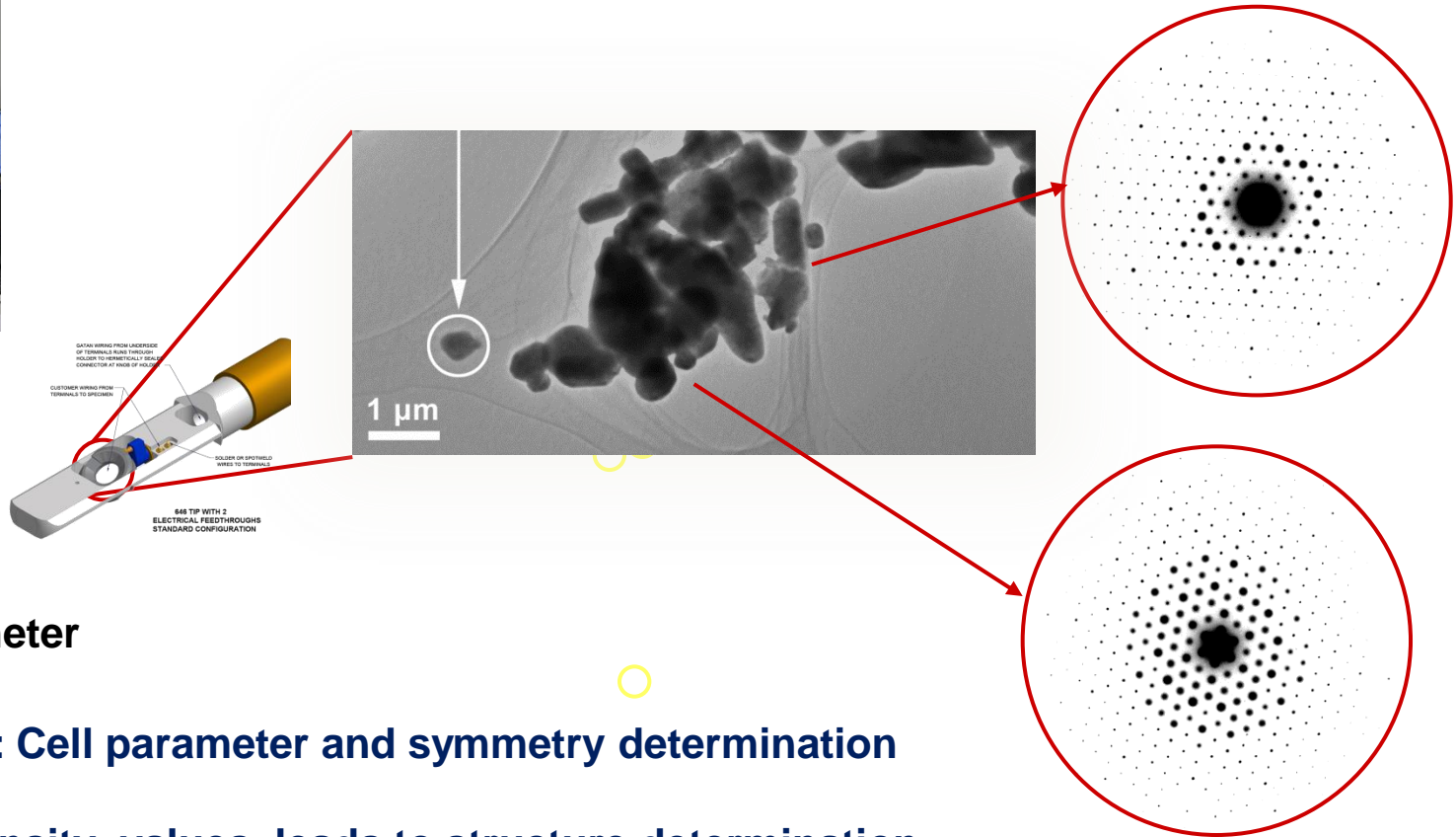
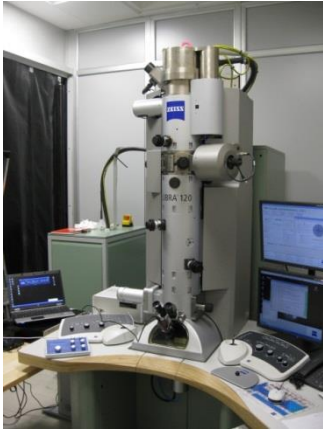


TEM grid



TEM : Electron diffraction advantages

Every TEM (electron microscope) may produce ED patterns and HREM from individual single nanocrystals

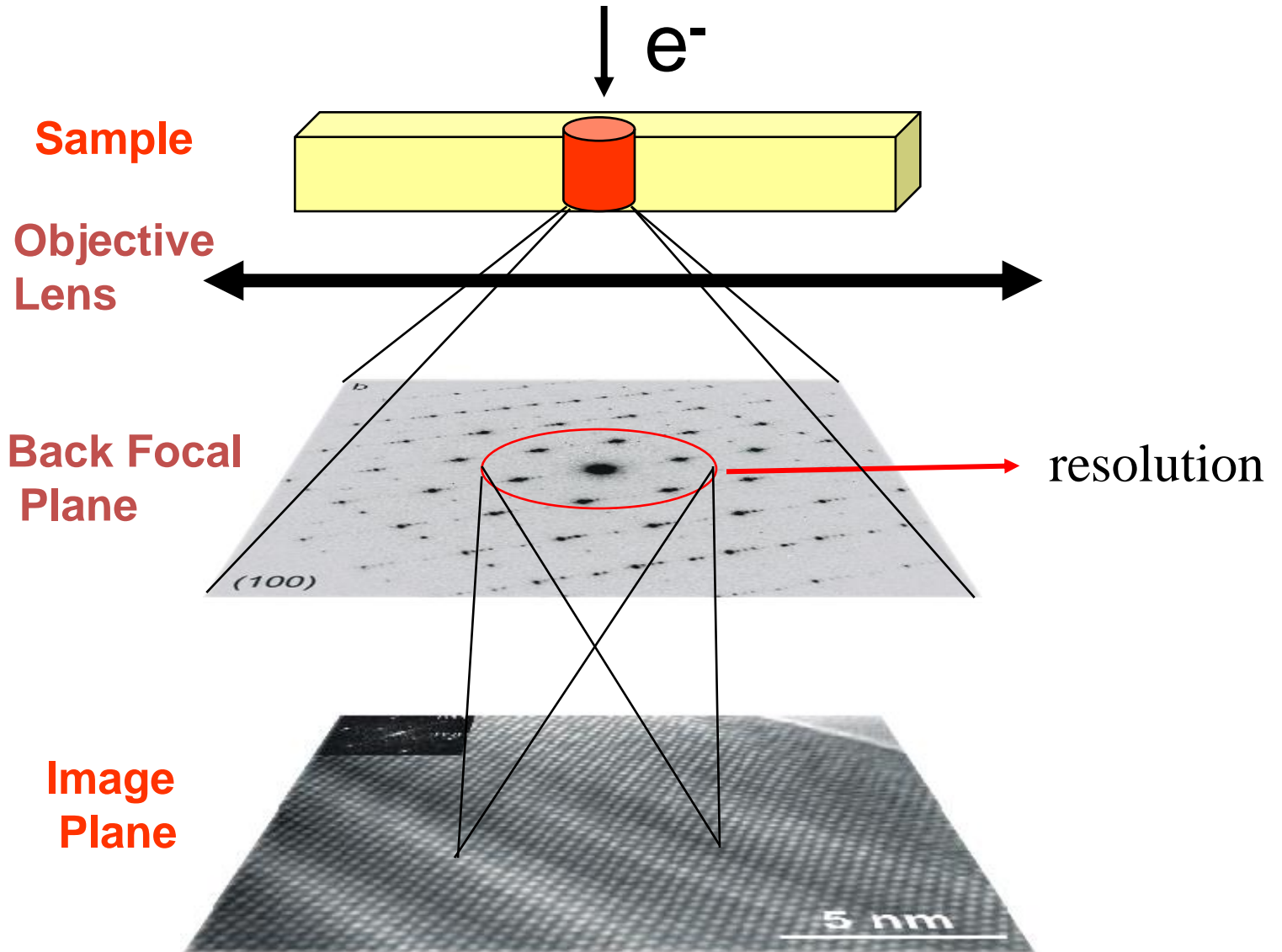


TEM goniometer

ED information: Cell parameter and symmetry determination

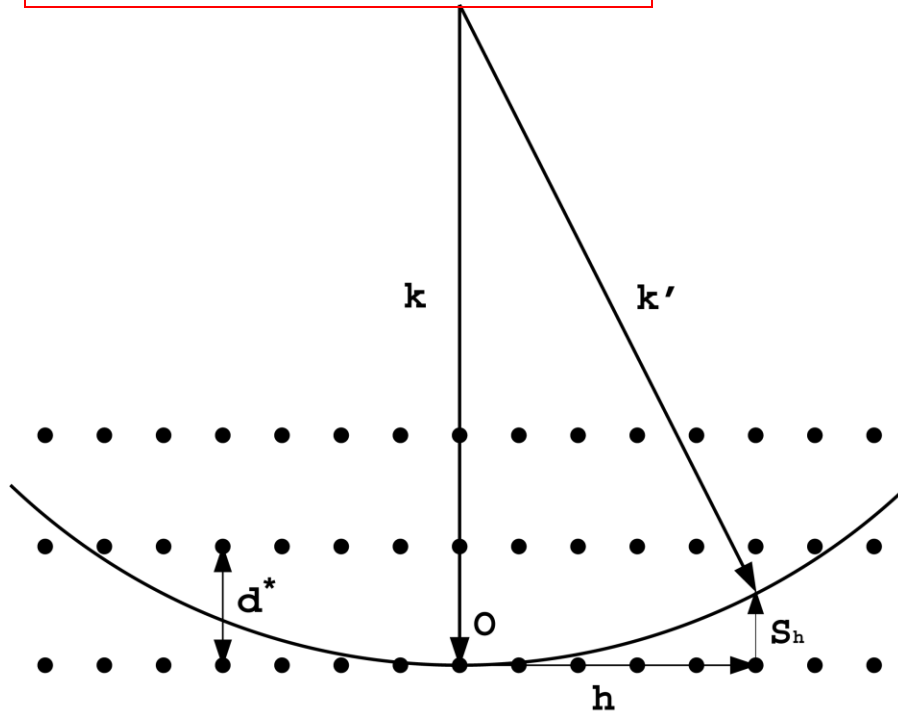
Measuring intensity values leads to structure determination

Image formation

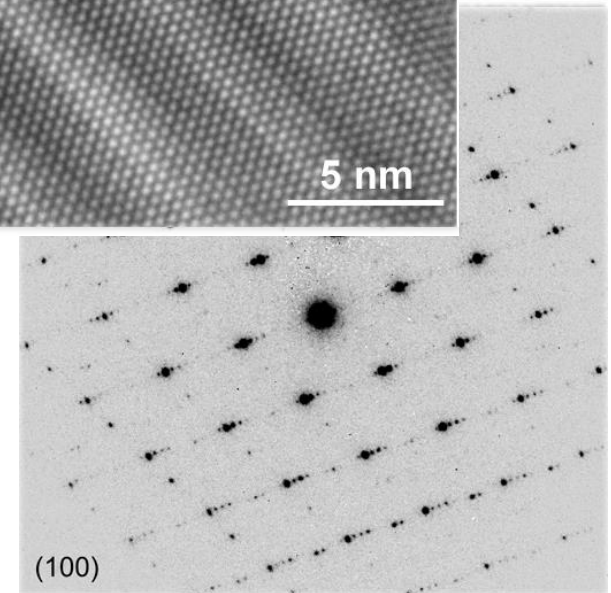
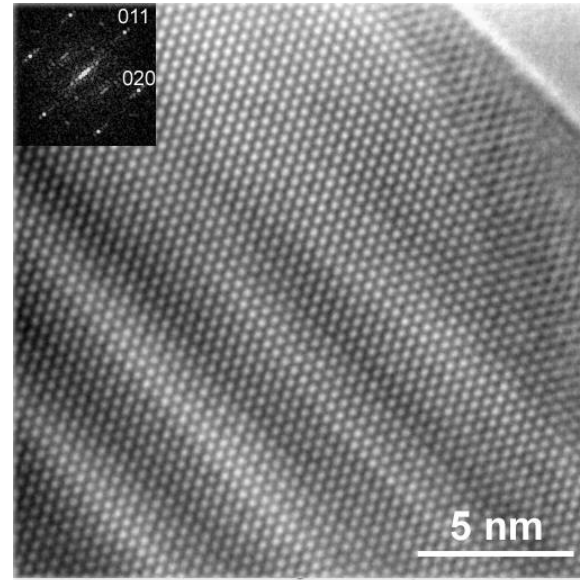


Electron diffraction

RECORD RECIPROCAL SPACE - TEM



VOLTAGE IN KV	λ IN Å
100	0.0370
300	0.0197
1000	0.0087

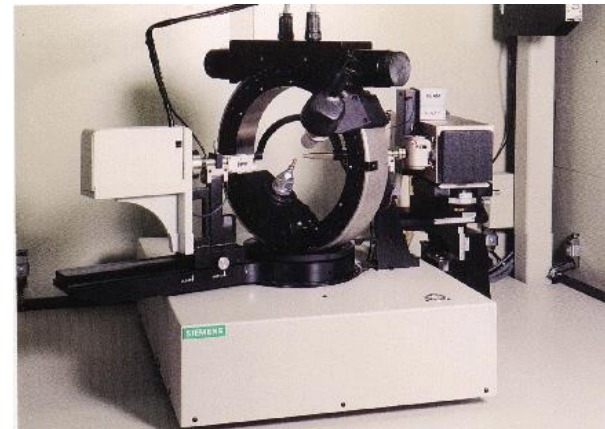
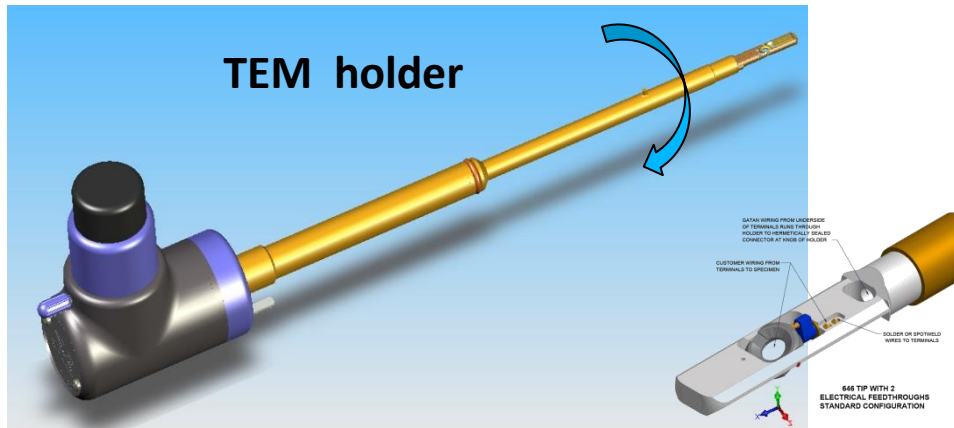


The Ewald sphere is flat!

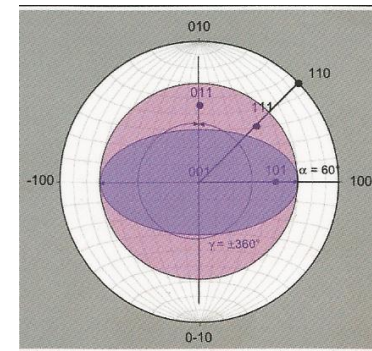
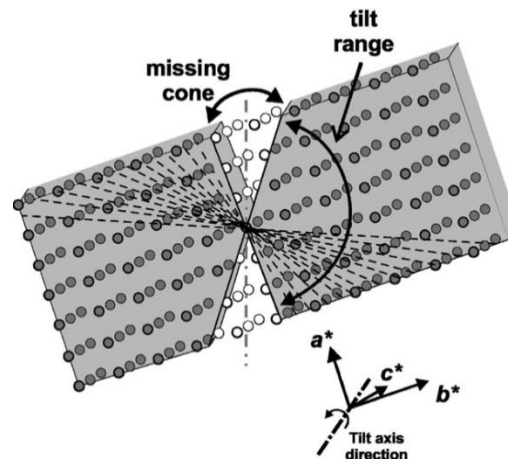
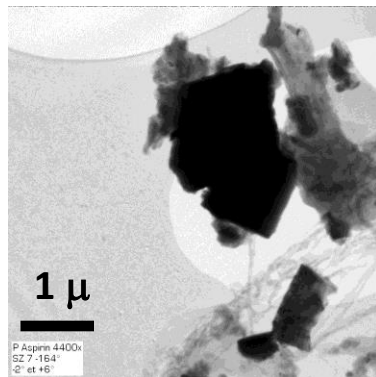


In one shot we record a reciprocal lattice plane

TEM goniometer (single /double tilt, tilt rotation, tomography)

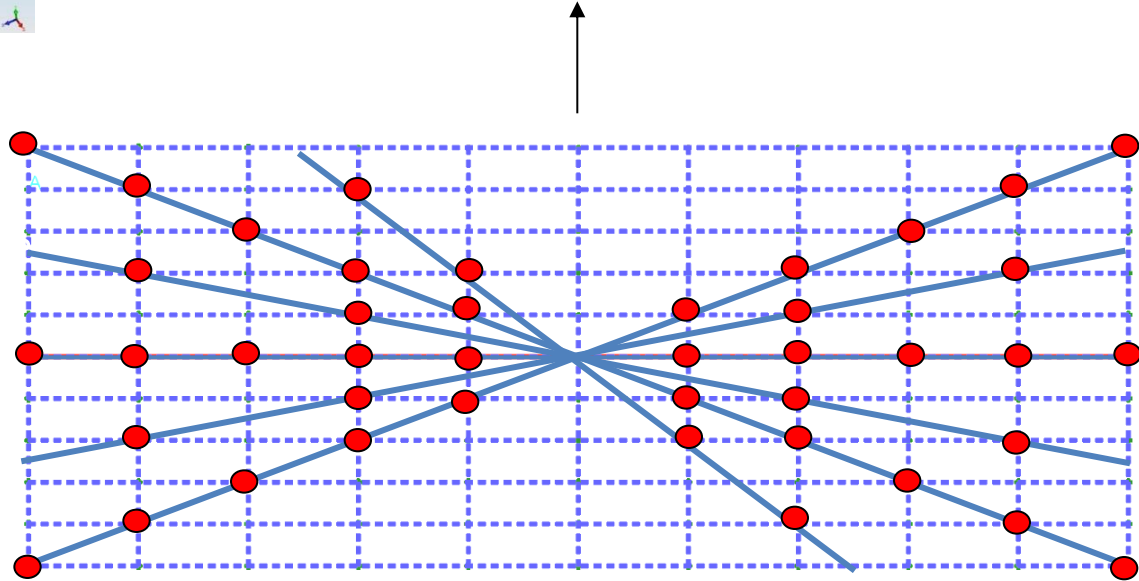
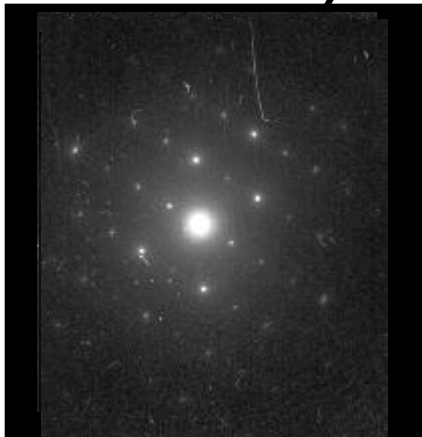
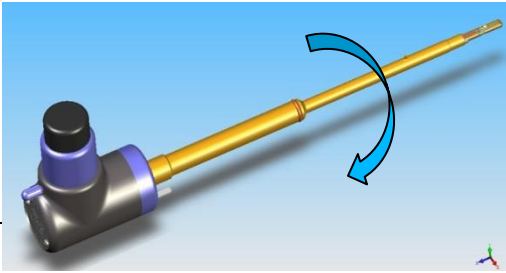


all goniometers work according to same principles, goniometry of direct or reciprocal lattice vectors of individual crystals can be easily treated by matrices and visualized by stereographic projections

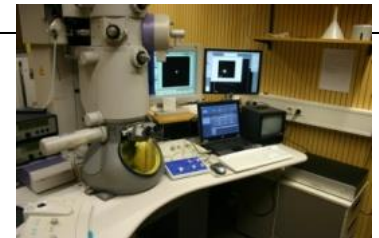
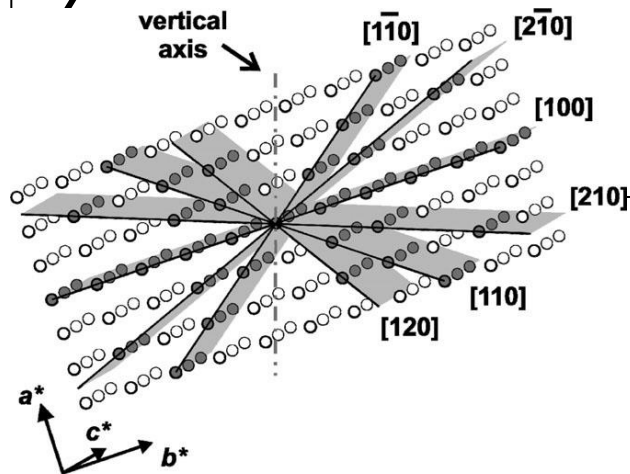


Find crystal cell parameters

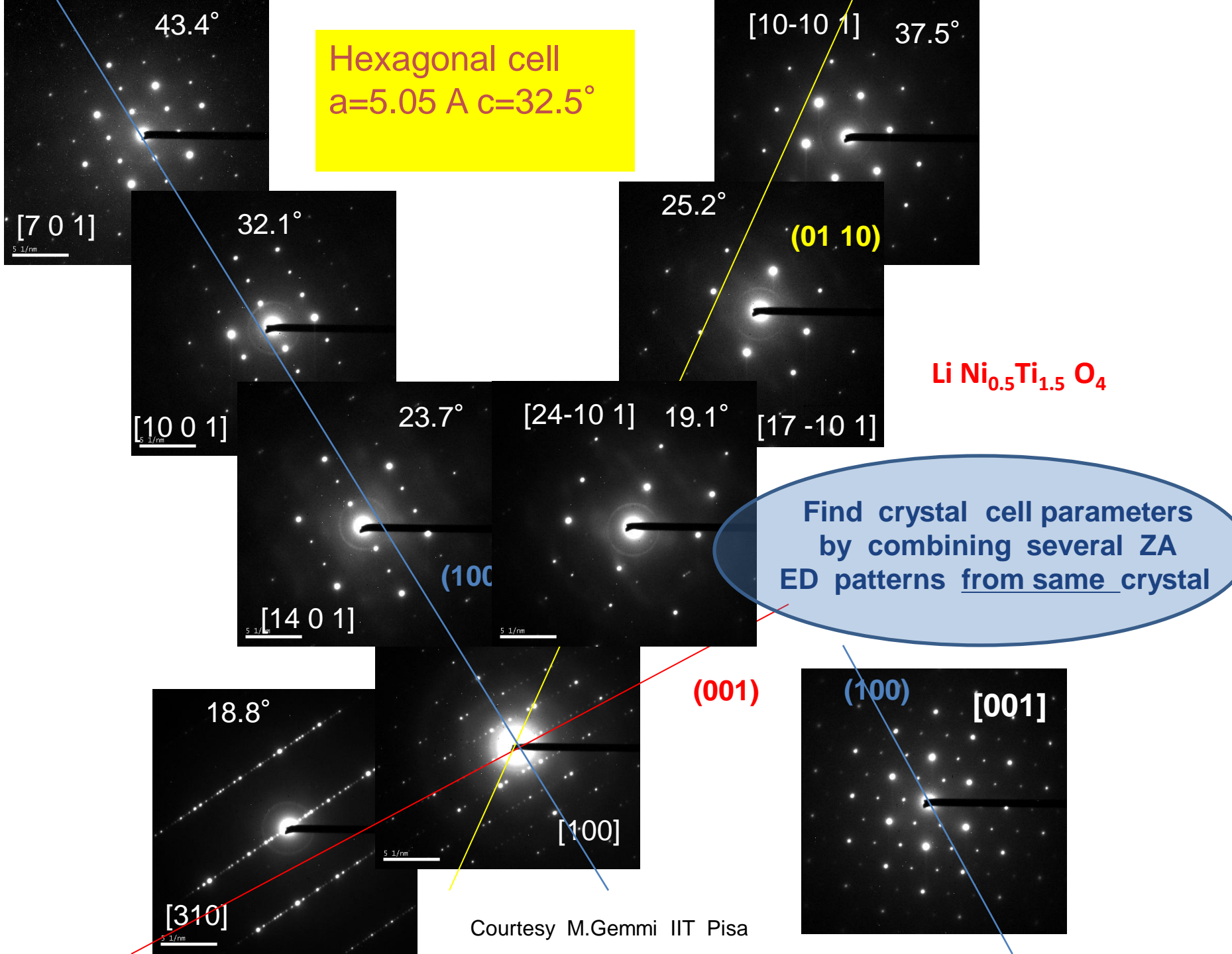
TEM : manual tilt series acquisition



Problem : "missing cone" = lost data



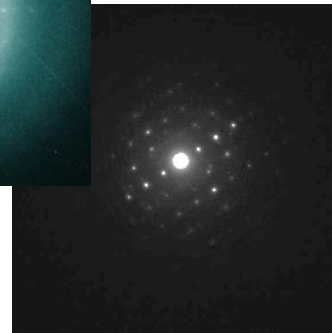
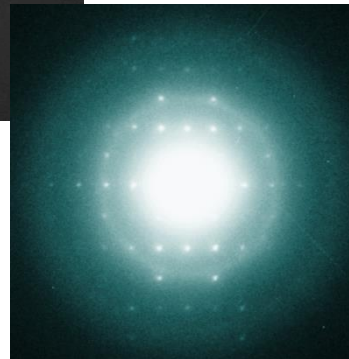
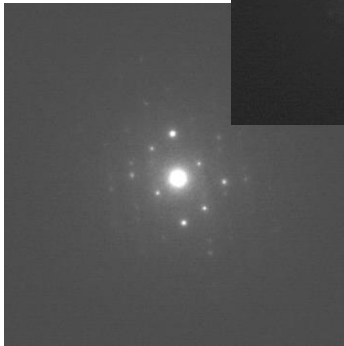
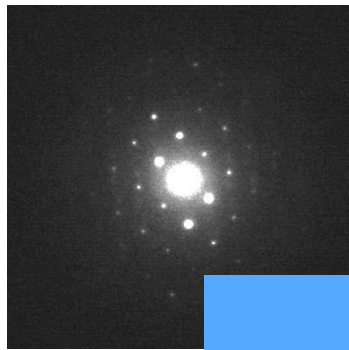
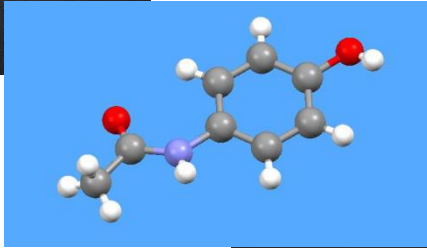
Courtesy : Prof. U Kolb UMainz



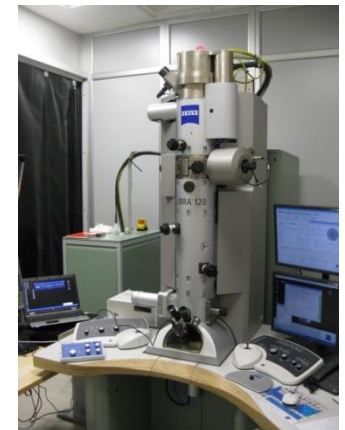
ORGANIC crystals : beam sensitive

*Only possible to collect several
(non ZA oriented ED patterns)*

from different crystals

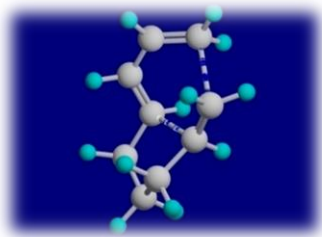
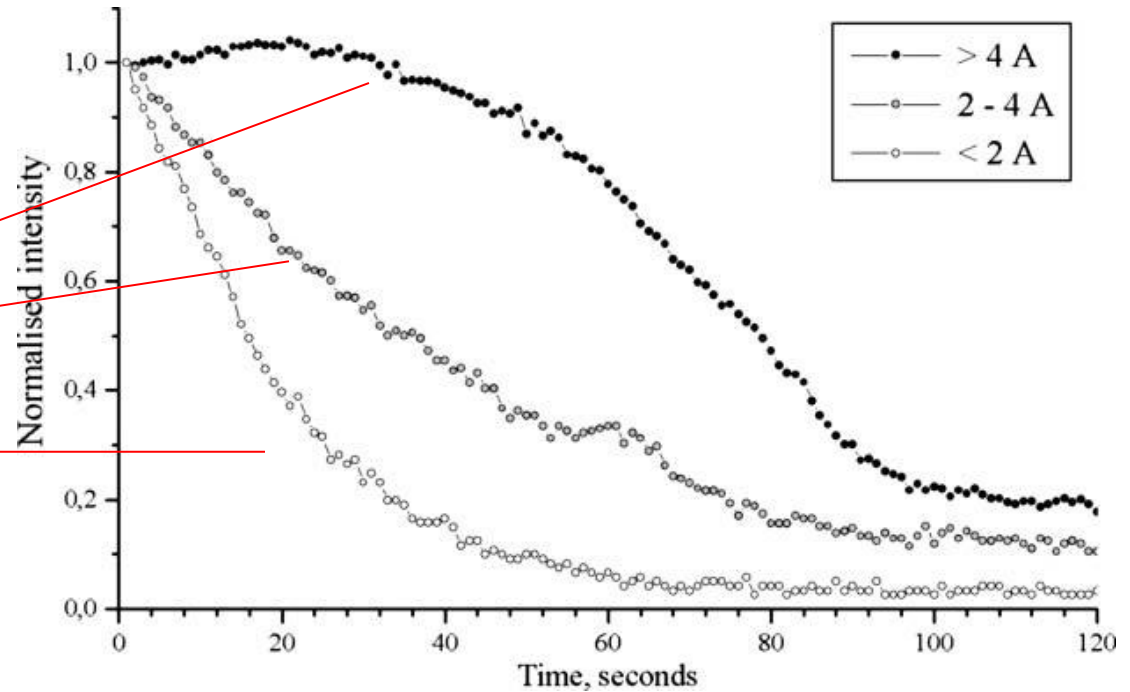
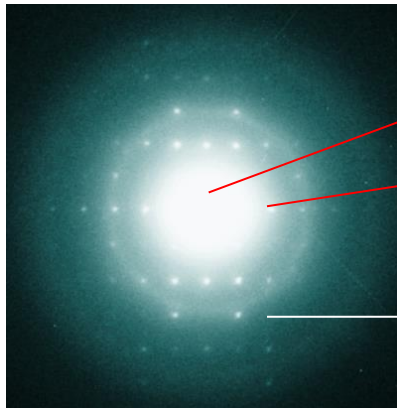


*CRYSTAL UNIT CELL can be calculated
from several patterns (oriented or not)*

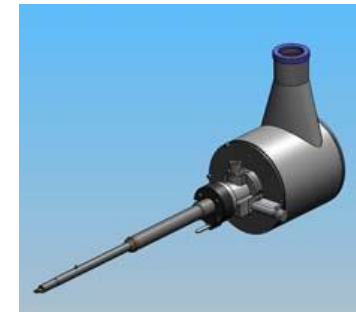


TEM - organic samples

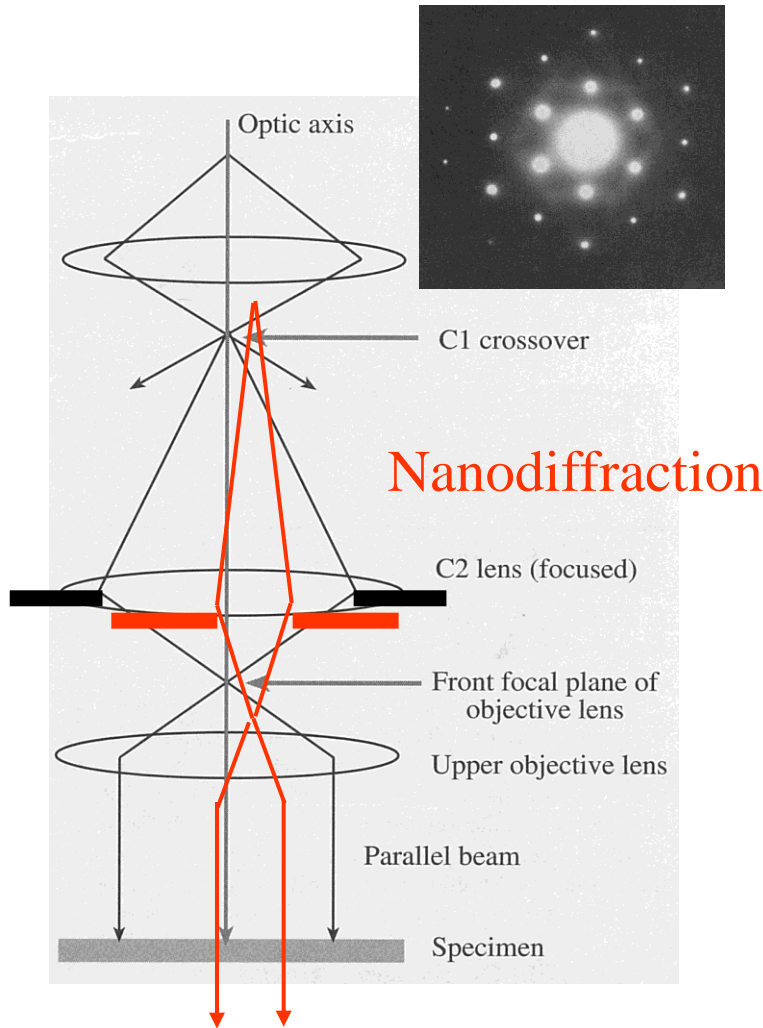
Keeping crystals deep-frozen: cryo techniques



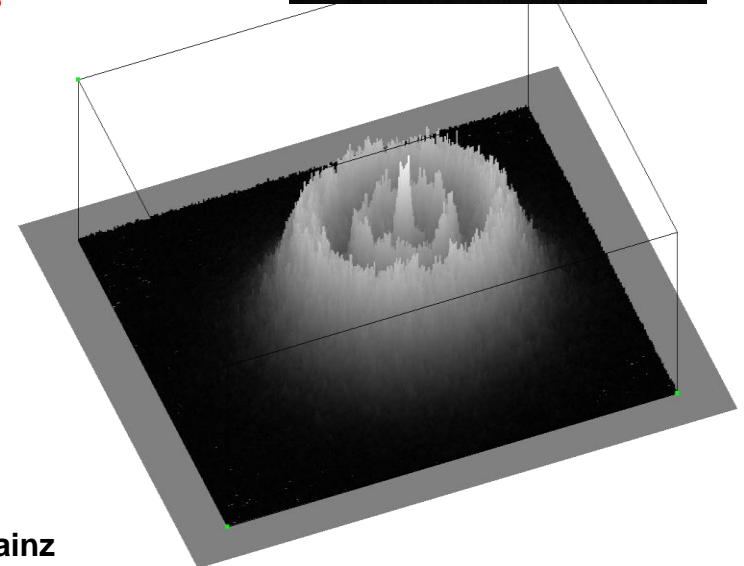
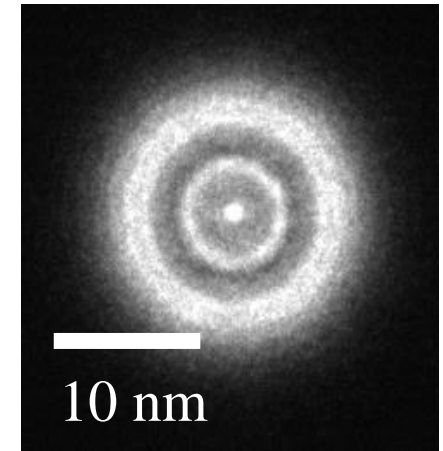
Organic samples degrade fast under the beam – cooling sample at Liquid Nitrogen is mandatory



TEM for organic samples : use small probe and low dose



Convergence angle:
0.2 mrad
Electron dose rate:
 $\sim 3 \text{ e}/\text{A}^2\text{s}$



ORGANIC CRYSTALS & ELECTRON DIFFRACTION - EARLY BEGINNINGS 1950-1990

Some electron diffractionists were persistent -
Group in Moscow claimed that structures could be solved from e. d. data



Рис. 1. Коллектив кафедры электрографии (1957 г.) и лаборатория электрографии ИГиЛ. Сверху направо: И.К. Балабанов, З.Т. Павлов, Л.С. Тарнополь, П.Н. Дорсет, И.В. Роман.

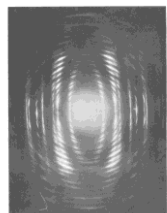


Figure 1 shows electron diffraction pattern of the clay mineral muscovite.

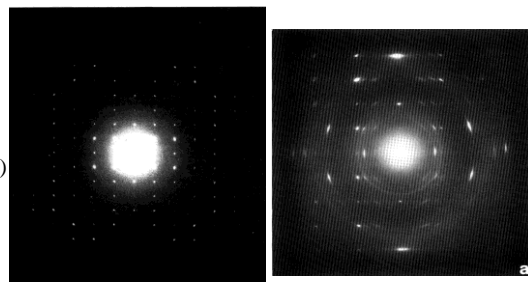
Oblique texture patterns from mm diameter areas:

Multiple scattering effects supposedly minimized by averaging over several orientations. Dynamical deviations addressed by 2-beam theory, permitting *ab initio* analysis.

ExxonMobil
 Research and Engineering

Example 2: Poly(butene-1), polymorph III

Epitaxy by lattice matching is understandable for relatively simple linear polymer chains. However, helical structures can also be oriented with specialized organic substrates - e. g. the polymorphs of isotactic poly(butene-1). (See: S. Kopp, et al., Polymer 35 (1994) 908, 916.)



hk0

polymer on epitaxial substrate

$a = 12.38$, $b = 8.88$, $c = 7.56$ Å

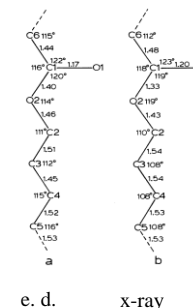
From D.Dorset lecture ElCryst 2005 Brussels

Application to the determination of linear polymer structures

1. Poly ϵ -caprolactone

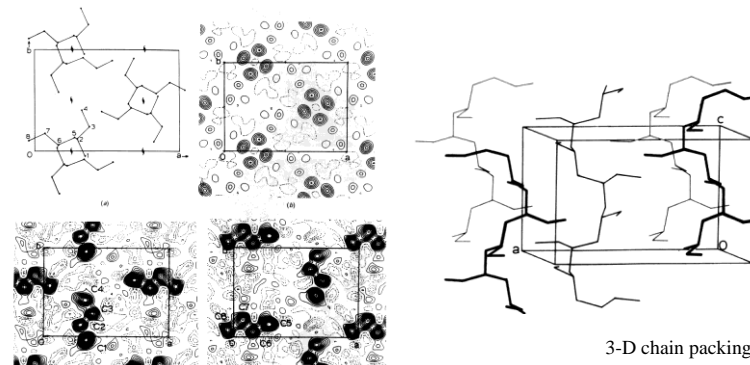
Data from solution-crystallized lamellae and epitaxially oriented material. Space group $P2_12_12_1$, $a = 7.48$, $b = 4.98$, $c = 17.26$ Å, 47 unique data. The analysis used symbolic addition via algebraic unknowns to yield 30 phases. (D. L. Dorset, Proc. Natl. Acad. Sci. USA 88 (1991) 5499.) Potential maps were interpretable. Bond distances and angles agree well with the best x-ray structure.

The electron crystallographic determination distinguished between two conflicting powder diffraction models, one with a planar molecular conformation (H. Bittiger, et al., Acta Cryst. B26 (1970) 1923) and the other with a twist around the ester linkage (Y. Chatani, et al., Polym. J. 1 (1970) 555), in favor of the latter. This solution was later verified by a direct methods solution with published powder x-ray data (D. L. Dorset, Polymer 38 (1997) 247.)



Poly(butene-1), polymorph III

The crystal structure could be determined by a number of direct methods and the atomic positions were observable in potential maps. (D. L. Dorset, M. P. McCourt, S. Kopp, J. C. Wittmann, and B. Lotz, Acta Cryst. B50 (1994) 201.)



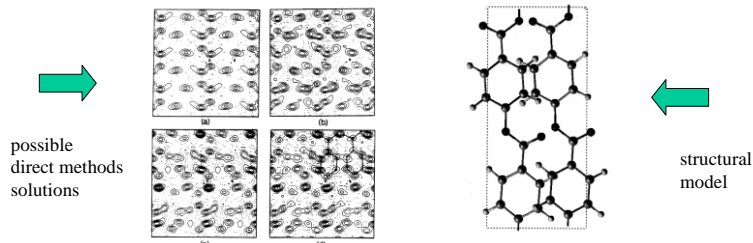
3-D chain packing

A molecular 4_1 axis was found to be oriented along the space group 2_1 axes in the c-direction. The structure could then be refined by restrained least squares.

ORGANIC CRYSTALS & ELECTRON DIFFRACTION - EARLY BEGINNINGS 1950-1990

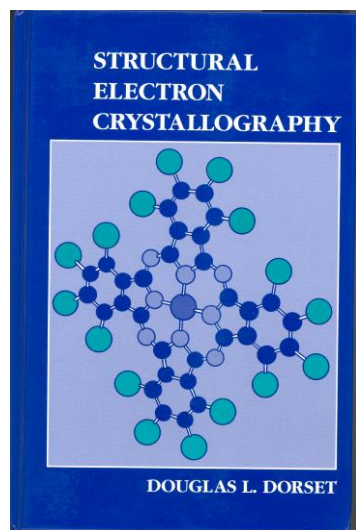
Example 3: Poly (*p*-oxybenzoate)

When epitaxial substrates are not obvious, it is possible sometimes to employ other crystallization techniques to obtain the proper orientation. For example, whiskers are produced from high temperature polymerization in dilute solutions (J. Liu and P. H. Geil, *J. Macromol. Sci. Phys.* B31 (1992) 163)



Whisker crystals of this polymer can be used with normal lamellar preparations for 3-D data collection. The phase 1 form, $a = 7.45$, $b = 5.64$, $c = 12.47 \text{ \AA}$, was solved in space group $P2_12_12_1$ by direct methods. (J. Liu, B. L. Yuan, P. H. Geil, and D. L. Dorset, *Polymer* 38 (1997) 6031.)

Other polymer structure analyses also reported.



Other structures determined from electron diffraction data:

- Light atom inorganics - e. g. boric acid
- Lipid bilayers
- Linear polymers
- Zeolites - accompanying lecture

Sometimes structure determination difficult despite all measures

Example 4: triphenylene

Space group: $P2_12_12_1$
 $a = 13.20$, $b = 16.73$, $c = 5.26 \text{ \AA}$

Crystals grown by orientation on naphthalene - also epitaxial view to provide 3-D data set. Crystals flatter than if grown from solution.

Data set very sparse, however. Traditional direct methods not useful. Structure solved by lattice energy minimization. (Dorset, McCourt, Li, Voigt-Martin, *J. Appl. Cryst.* 31 (1998) 544.)

More recently solved by maximum entropy and likelihood. Only molecular envelope obtained - similar to structures solved by U. Kolb and I. Voigt-Martin at U. Mainz

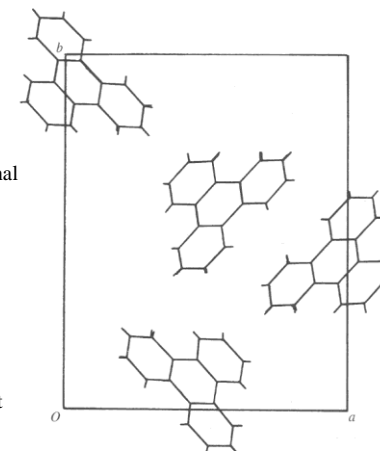
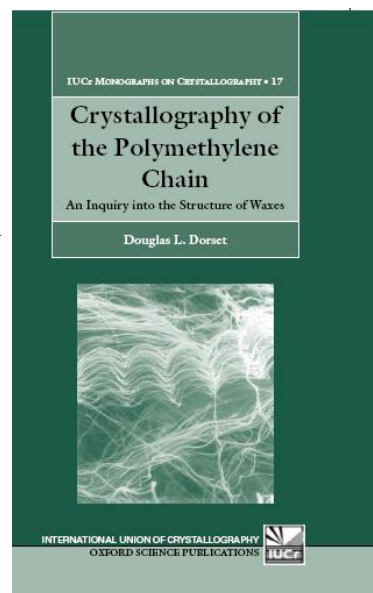


Fig. 4. Packing diagram, oriented along (001), showing the c -axis.



Major application area of organic electron crystallography:

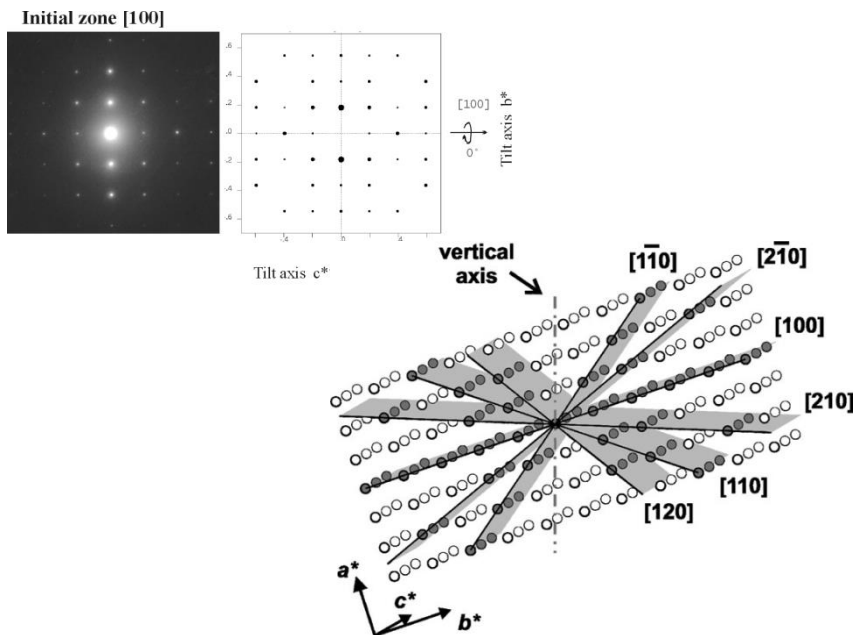
Structure of polydisperse chain arrays (including chain branching):

- binary solid solutions
- miscibility gap
- eutectics
- petroleum waxes
- low MW linear polyethylene

TEM : manual tilt to obtain ED patterns

organic pigments , drugs etc..

ORGANIC CRYSTALS & ELECTRON DIFFRACTION - 1990 - 2000



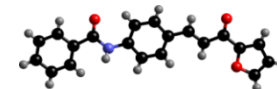
1-(2-furyl)-3-(4-aminophenyl)-2-propene-1-one
(FAPPO)

Cell parameter from electron diffraction

$$a = 28.51 \text{ \AA}$$

$$b = 5.043 \text{ \AA}$$

$$c = 11.025 \text{ \AA}$$



Cell parameter from Pawley Fit:

$$Rwp = 5.18\%, Rp = 3.83\%$$

$$a = 28.4885 \text{ \AA}$$

$$b = 5.0563 \text{ \AA}$$

$$c = 11.0191 \text{ \AA}$$

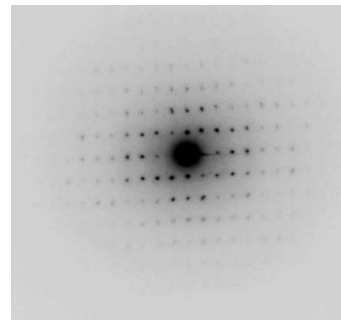
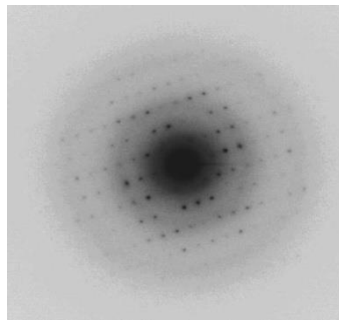
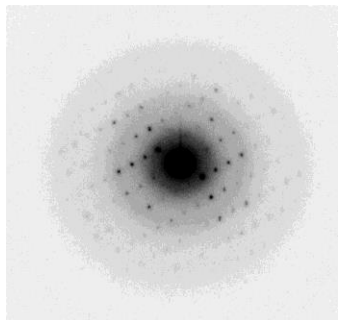
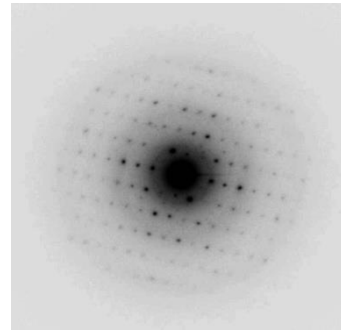
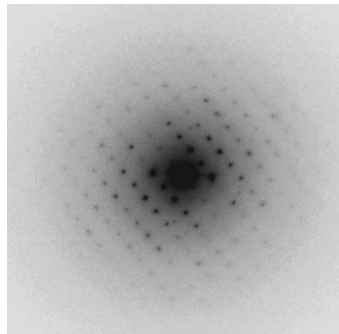
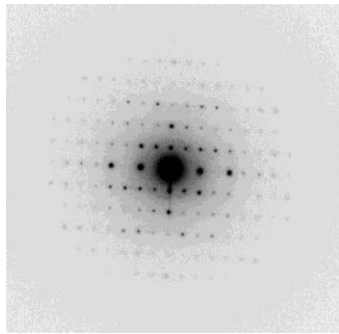
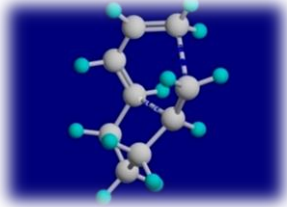
Intensity



FWHM: $\hat{u}=0.410$ $\hat{v}=-0.225$ $\hat{w}=0.050$

TEM : Manual random search for oriented ED patterns

Penicillin G – potassium



Laue class	Zone axes						
CUBIC CRYSTAL SYSTEM							
m-3m	<111>	<001>	<110>	<uv0>	<uuv>	<uvw>	
WP	3m	4mm	2mm	M	m	1	
ZOLZ	(6mm)	(4mm)	(2mm)	(2mm)	(2mm)	(2)	
m-3	<111>	<001>	<uv0>	<uuv>			
WP	3	2mm	m	1			
ZOLZ	(6)	(2mm)	(2mm)	(2)			
HEXAGONAL CRYSTAL SYSTEM							
6/mmm	<0001>	<11-20>	<1-100>	<uv 0>	<uu.w>	<u-u.w>	<uvw>
WP	6mm	2mm	2mm	m	m	m	1
ZOLZ	(6mm)	(2mm)	(2mm)	(2mm)	(2mm)	(2mm)	(2)
6/m	<0001>	<uv 0>	<u.v.w>				
WP	6	m	1				
ZOLZ	(6)	(2mm)	(2)				
TRIGONAL CRYSTAL SYSTEM							
-3m	<0001>	<11-20>	<u-u.w>	<uv.w>			
WP	3m	2	m	1			
ZOLZ	(6mm)	(2)	(2mm)	(2)			
-3	<0001>	<uv.w>					
WP	3	1					
ZOLZ	6	2					
TETRAGONAL CRYSTAL SYSTEM							
4/mmm	<001>	<100>	<110>	<u0w>	<uv0>	<uuvw>	<uvw>
WP	4mm	2mm	2mm	m	m	m	1
ZOLZ	(4mm)	(2mm)	(2mm)	(2mm)	(2mm)	(2mm)	(2)
4/m	<001>	<uv0>	<uvw>				
WP	4	m	1				
ZOLZ	(4)	(2mm)	(2)				
ORTHORHOMBIC CRYSTAL SYSTEM							
mmm	<100>	<010>	<001>	<0vw>	<u0w>	<uv0>	<uvw>
WP	2mm	2mm	2mm	m	m	m	1
ZOLZ	(2mm)	(2mm)	(2mm)	(2mm)	(2mm)	(2mm)	(2)
2/m	<010>	<u0w>	<uvw>				
WP	2	m	1				
ZOLZ	(2)	(2mm)	(2)				
MONOCLINIC CRYSTAL SYSTEM (unique axis b)							
-1	<uvw>						
WP	1						
ZOLZ	(2)						
TRICLINIC CRYSTAL SYSTEM							

Easier to find crystal cell parameters from “randomly oriented” PED patterns
 Orthorombic a = 6.4 Å b = 9.4 Å c = 30 Å

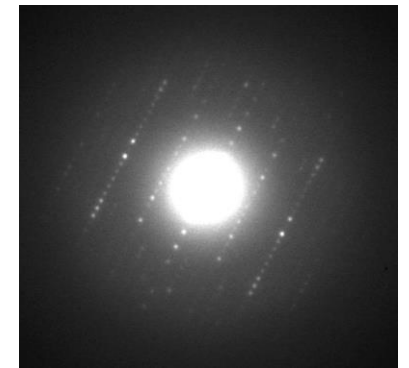
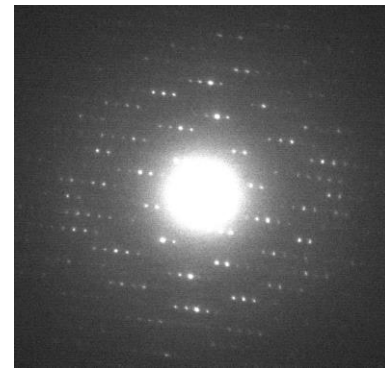
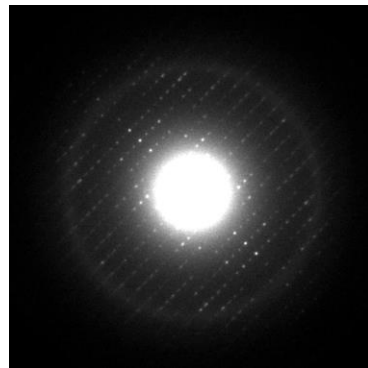
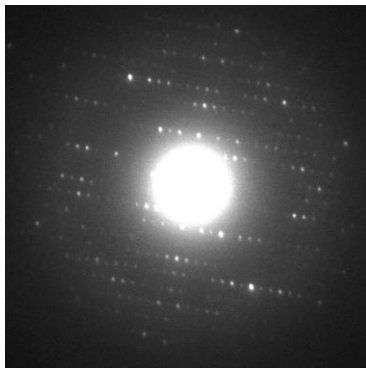
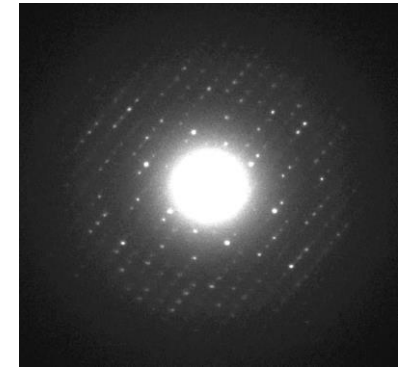
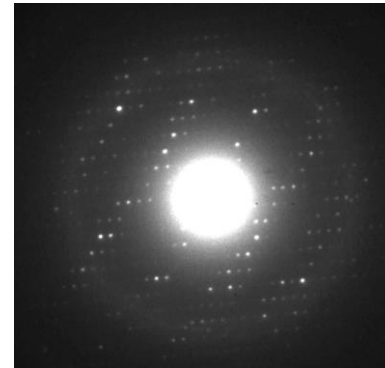
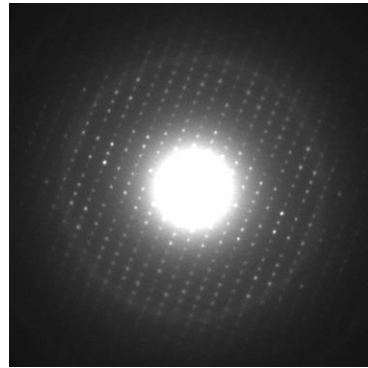
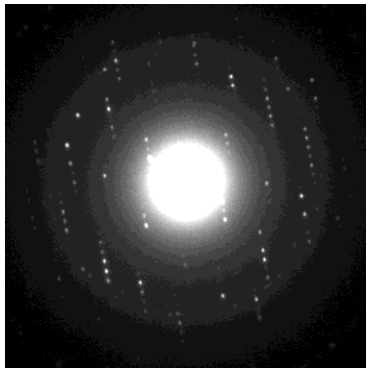
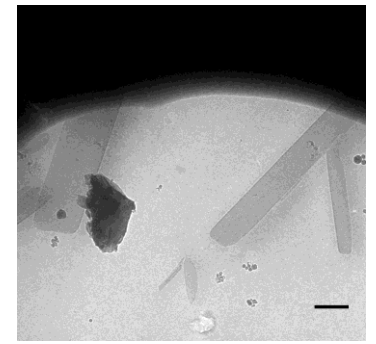
TEM : high resolution electron diffraction of proteins



- We can grow sub-micron crystals of different proteins reproducibly
- These protein nano-crystals are small enough for electron diffraction
- Crystals can be frozen successfully: diffraction so far $\sim 2.1 \text{ \AA}$
- Unit cell parameters can be calculated from the electron diffraction data
- Problems:
 - limiting factor is the beam damage, BUT electrons are more than 1000 times less damaging than X-rays, so we should be able to do better than synchrotron radiation...

Electron diffraction pattern of a 3D lysozyme nano-crystal recorded on an image plate

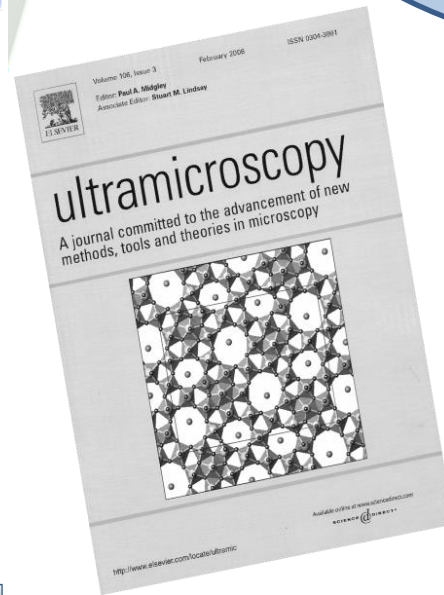
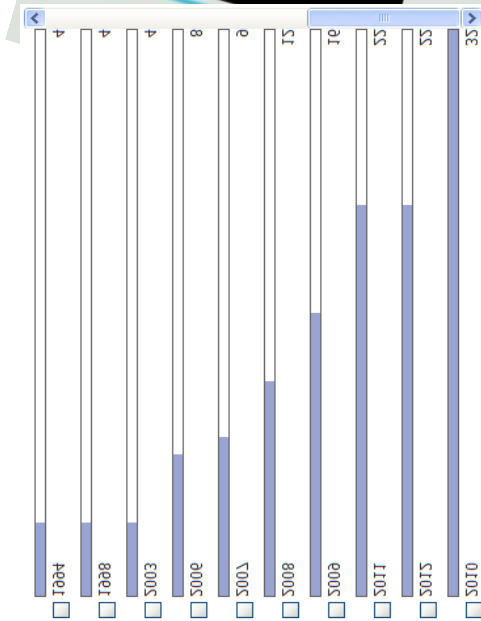
TEM : manual random search for oriented
electron diffraction patterns from lysozyme
nanocrystals $P4_32_12$ $a=b=79.2$ A $c=38.0$ A



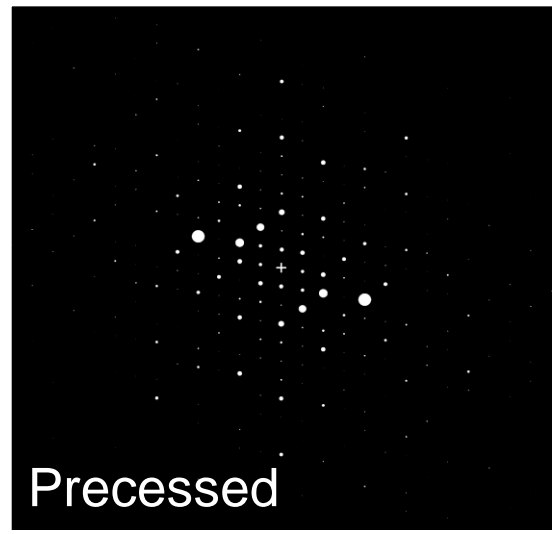
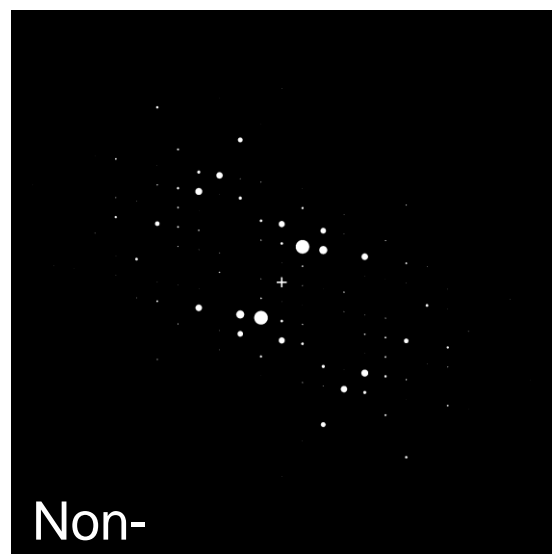
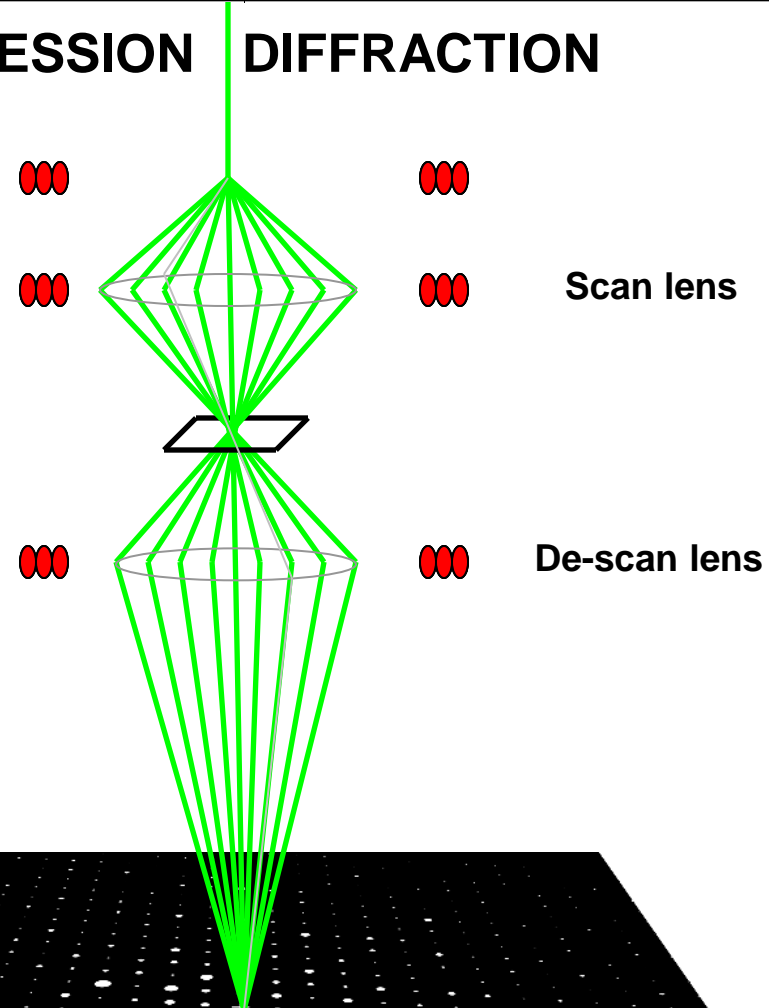
PRECESSION ELECTRON DIFFRACTION

NEW structure analysis
technique for TEM

- > 150 articles in 8 years
- > 75 installations world-wide in TEM



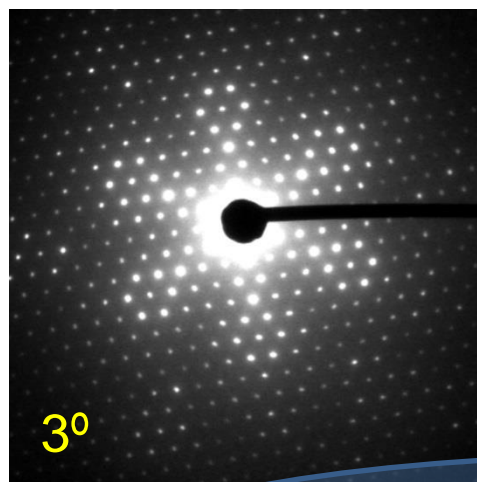
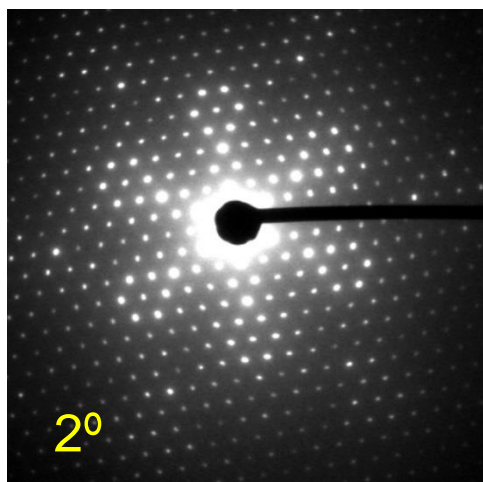
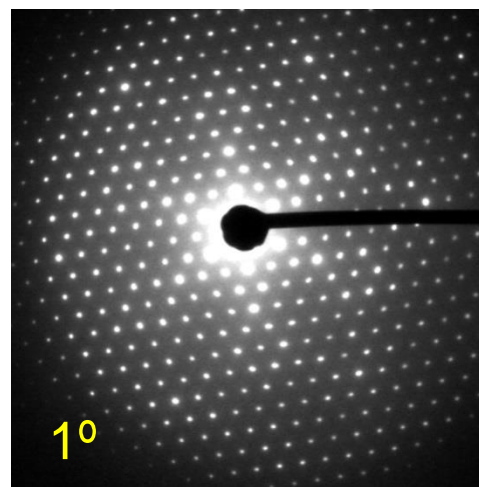
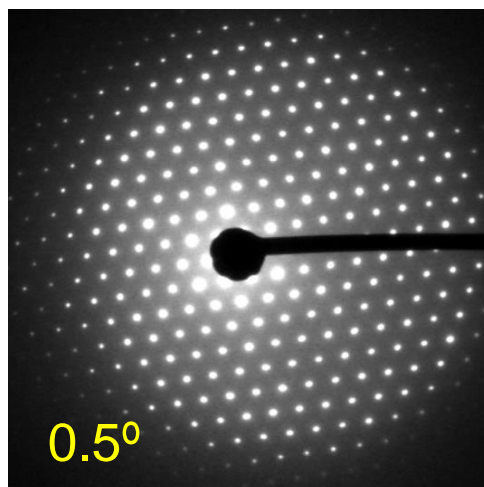
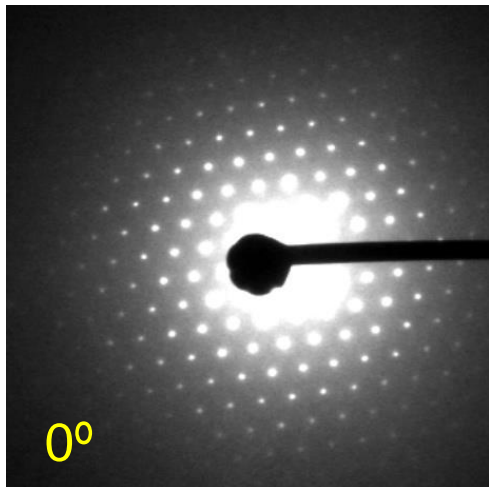
PRECESSION DIFFRACTION



Precession...

(Diffracted amplitudes)

TEM : with precession electron diffraction (PED) ED intensity data are closer to kinematical values (X-Ray like)

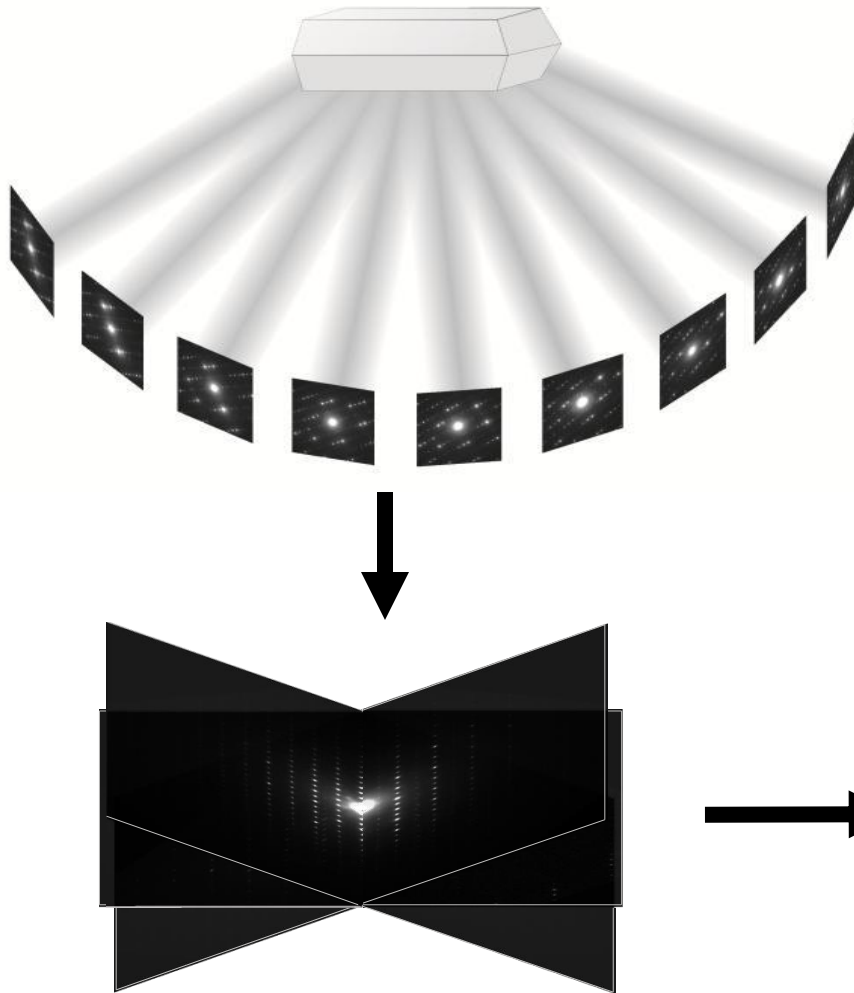


As the precession angle increases from 0° to 3°, the diffraction pattern goes to higher resolution (i.e. more diffraction spots are seen).

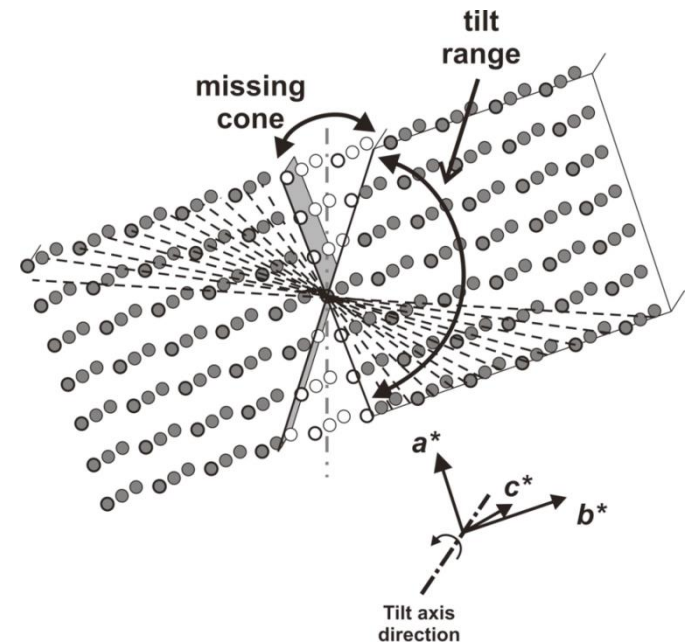
Mayenite $\text{Ca}_{12}\text{Al}_{14}\text{O}_{33}$
Cubic **$a = 11,89 \text{ \AA}$**

WE CAN USE PED DATA TO SOLVE STRUCTURES !

New Technique for cell & structure determination : Automatic precession diffraction tomography (ADT 3D)

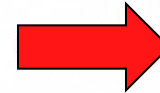
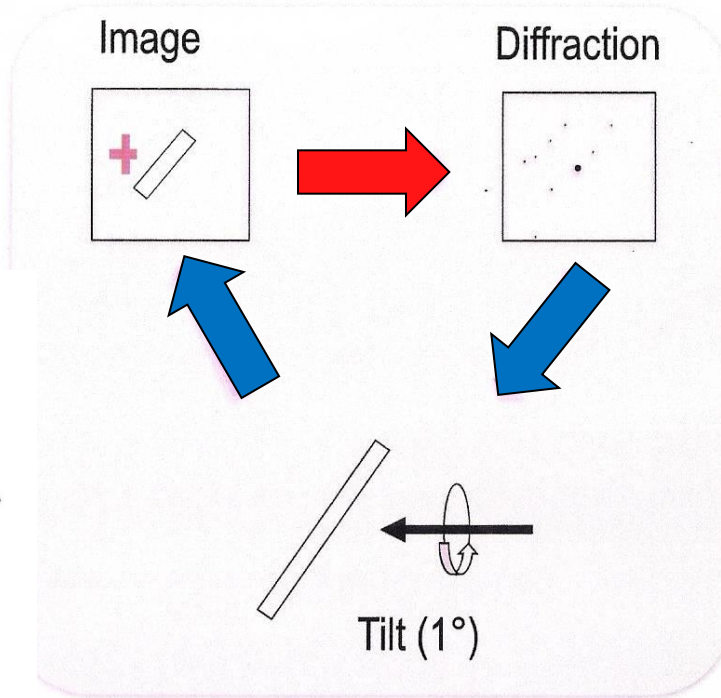
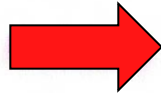


Data analysis by ADT3D
3D reconstruction of diffraction space

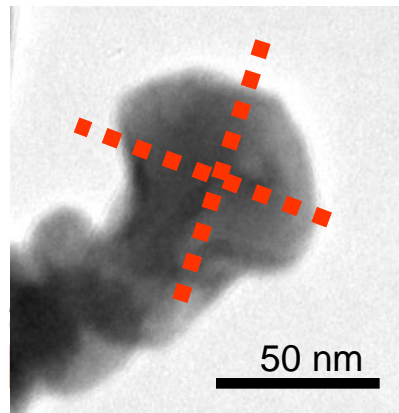
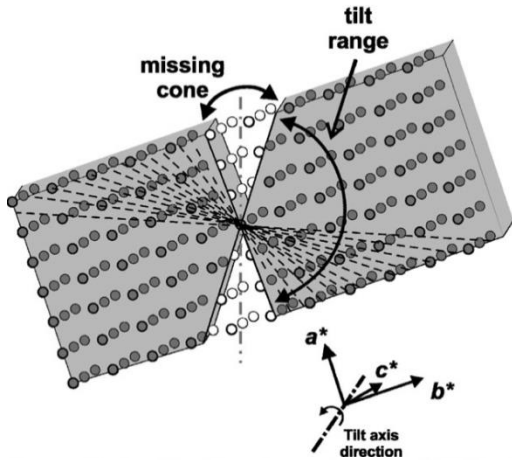


TEM - ADT3D : 3D sampling of reciprocal space

Select a crystal

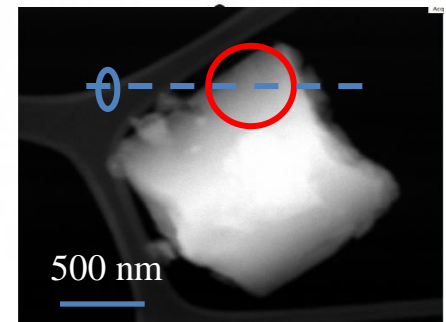


Tilt series



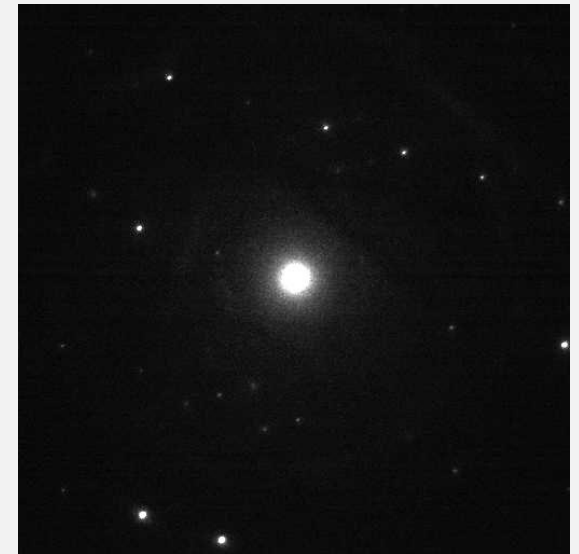
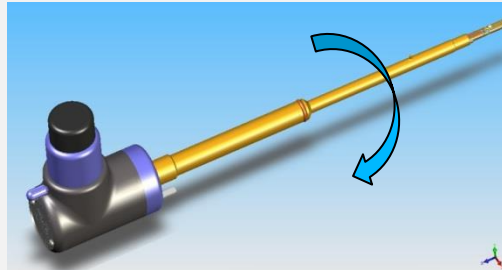
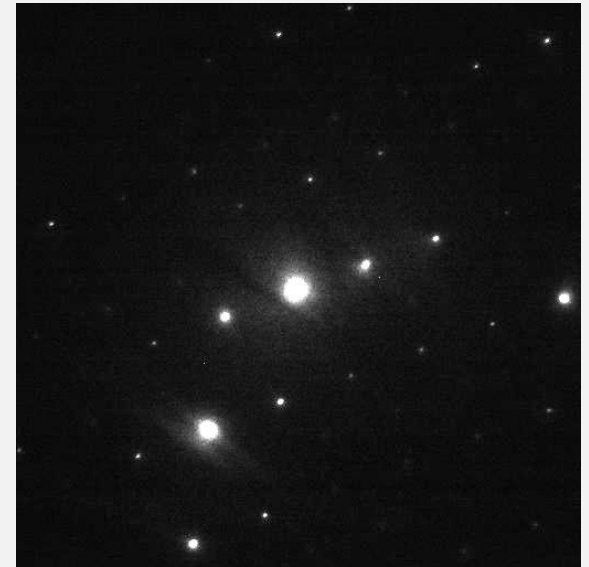
Arbitrary axis: Less dynamical effects,
More reflections
Easier to learn

Data collection: Any TEM using SAED or NED,
~30° for unit cell parameter
≥ 100° for structure solution

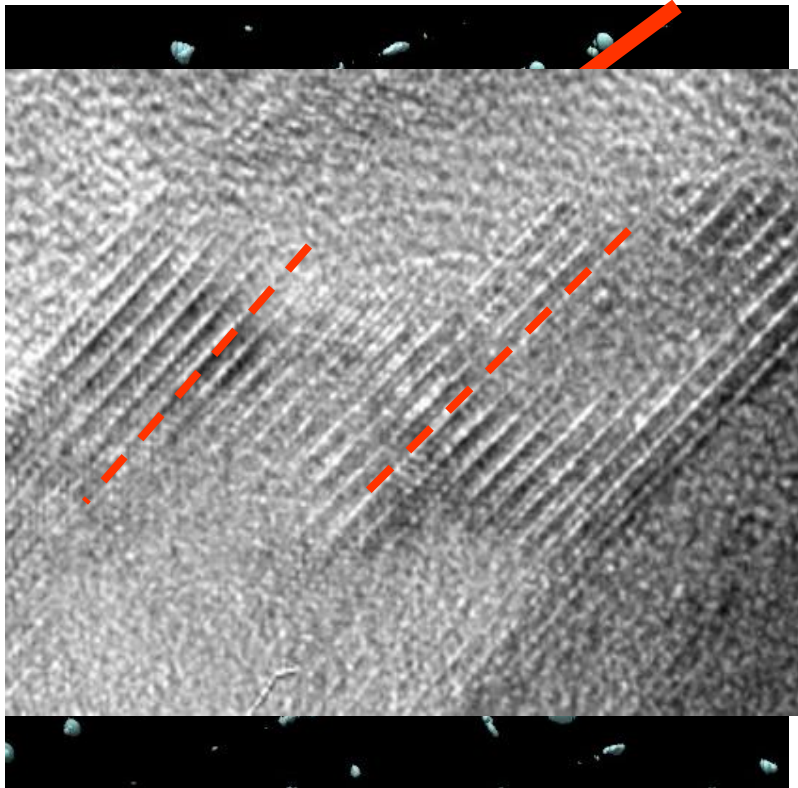


3D sampling of reciprocal space

Tilt angle
 $\pm 30^\circ$
(max. $\pm 70^\circ$)
In steps of 1°

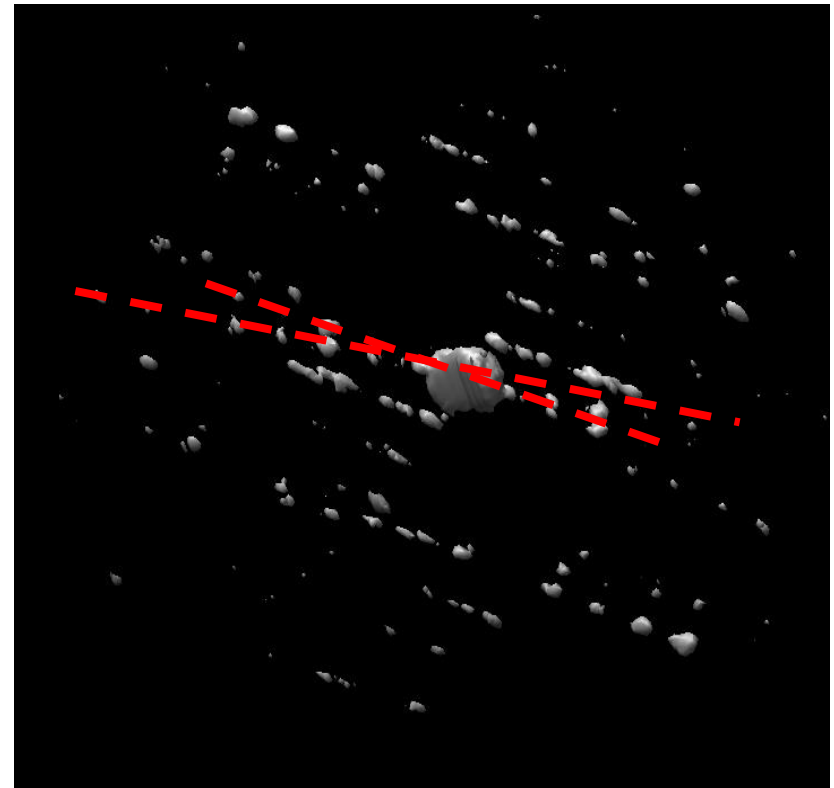


TEM ADT3D : Disorder & polycrystallinity



DISORDER

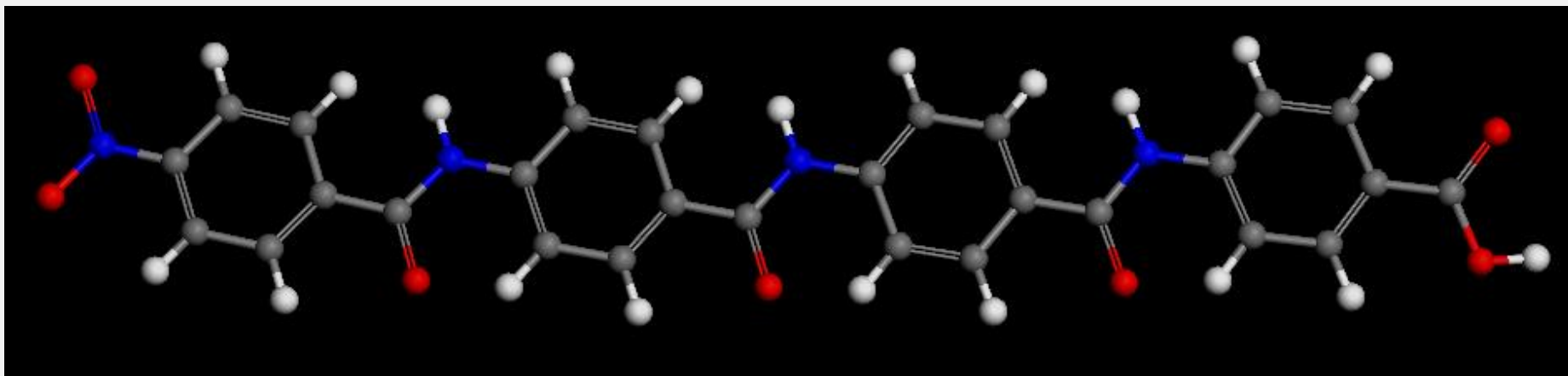
$0kl : k = 2N+1$



POLYCRYSTALS

c^* tilted $\sim 3^\circ$

ADT-3D solving organic (polymer) compounds NS4



$a=56.3\text{\AA}$ $b=5.8\text{\AA}$ $c=18.8\text{\AA}$ $\beta=75.53^\circ$

Unit cell content (asymm unit, $Z=4$)

28 C, 4 N, 7 O

Tilt range: $\pm 60^\circ$

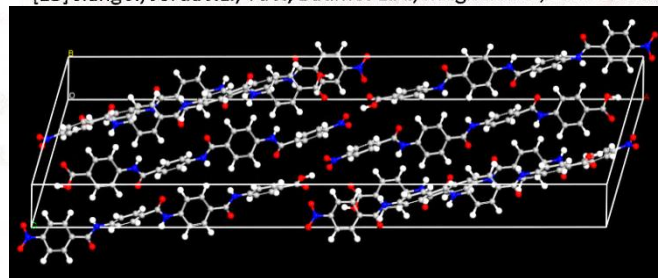
0.8031 \AA Angstrom resolution

9410 total reflections 3818 independent reflections

Crystal Structures solved from ADT^[1,2] data (new structures are marked with *)

	Space group	N° ind. reflections	N° ind. atoms	Volume (Å ³)	Completeness (%)
Phosphates					
SrP ₃ N ₅ O ^{[3]*}	Pnam	1790	25	1900	86
Ba ₆ P ₁₂ N ₁₇ O ₉ Br ₃ *	P6 ₃ /m	1343	11	1530	99
Tungstates					
Na ₂ W ₄ O ₁₃ ^[4]	P-1	738	10	262	69
Na ₂ W ₂ O ₇	Cmce	454	9	1264	91
K ₂₀ Al ₄ W ₂₄ O ₈₈ *	C2	1307	36	1983	84
Layered materials					
Sodium titanate (Na ₂ Ti ₆ O ₁₃) ^[5]	C2/m	517	11	510	72
Sodium titanate (NaTi ₃ O ₇ ·2H ₂ O) ^{[6]*}	C2/m	628	13	670	79
Hydrous silicate*	P-4m2	121	8	540	84
Ca-compounds					
Calcite (CaCO ₃) ^[7]	R-3c	106	3	120	97
Calcium silicate hydrate (Ca ₅ Si ₆ O ₁₇ ·5H ₂ O)*	Cm	689	19	930	69
High pressure phases					
Hydrous Al-pyroxene (Mg ₂ Al(OH) ₂ AlSiO ₆) ^{[8]*}	C2/c	498	8	560	87
Minerals					
Barite (BaSO ₄) ^[9]	Pnma	355	5	350	82
Mullite (Al ₆ Si ₂ O ₁₃)	Pbam	213	5	180	86
Charoite ₉₆ ((K,Sr) ₁₆ (Ca,Na) ₃₂ [(Si ₇₀ (O,OH) ₁₈₀)](OH,F) ₄ ·nH ₂ O) ^{[10]*}	P2 ₁ /m	3353	89	4430	96
Charoite ₉₀ ((K,Sr) ₁₆ (Ca,Na) ₃₂ [(Si ₇₀ (O,OH) ₁₈₀)](OH,F) ₄ ·nH ₂ O) ^{[11]*}	P2 ₁ /m	2878	90	4450	97
Metal Organic Frameworks (MOF)					
MFU_4large (Cl ₄ Zn ₅ N ₁₈ C ₃₆ O ₆ H ₁₂) ^{[12]*}	Fm-3m	655	8	32770	100
Basolite (C ₆ H ₄ CuO ₅)	Fm-3m	384	7	18640	99
Bi-MOF*	Pca2 ₁	1158	34	3560	67
Inorganic nanophasess					
Intermetallic nanoparticles (ZnSb) ^[13]	Pbca	106	2	440	70
Intermetallic nanoparticles (Zn ₈ Sb ₇) ^{[13]*}	P-1	3651	30	1610	57
Intermetallic matrix (NiTe)	P6 ₃ /mmc	37	2	150	93
Intermetallic nanodomains (Ni ₃ Te ₂)*	P6 ₃ /mc	57	5	300	95
Semiconductor 6H-SiC	P6mm	52	6	130	100
Pseudo-spinel (Li ₂ Ti ₃ NiO ₈) ^[14]	P-3c1	187	11	720	91
Zeolites					
ZSM-5 (Na _x Al _x Si _{96-x} O ₁₉₂)	Pnma	2288	39	5490	79
IM-5 (Si ₂₈₈ O ₅₇₆)	Cmcm	2170	71	16380	68
Natrolite (Na ₄ Al ₃ Si ₉ O ₃₈ ·2H ₂ O) ^[5]	Fdd2	719	10	2250	92
ITQ_43 (Si ₁₉₂ O ₃₈₄) ^{[15]*}	Cmmm	2735	39	14040	91
EC3-3 ((Na,K) ₃ Al ₃ Si ₄ C ₁₂ H ₈ O ₁₂ ·nH ₂ O) ^{[16]*}	Cc	4417	62	5040	72
Organic					
NLO-active material 10-CNBA (C ₂₉ NH ₁₇) ^[17]	P2 ₁ /c	1871	30	2000	90
Oligo p-benzamide OPBA3 ^[18]	P2 ₁ /c	3078	30	1755	81
Oligo p-benzamide OPBA4 ^{[18]*}	C2/c	3576	39	4545	77

- [1] Kolb U., Gorelik T., Kübel C., Otten M. T., Hubert D. (2007) *Ultramicroscopy* **107**, 507.
- [2] Kolb U., Gorelik T., Otten M. T. (2008) *Ultramicroscopy* **108**, 763.
- [3] Sedlmaier S.J., Mugnaioli E., Oeckler O., Kolb U., Schnick W. (2011) *Chem. – Eur. J.*, DOI:10.1002/chem.201101545.
- [4] Gorelik T.E., Stewart A., Kolb U. (2011) *J. Microscopy*, in print.
- [5] Mugnaioli E., Gorelik T.E., Stewart A., Kolb U. (2011) In Krivovichev S.V. (ed.): *Minerals as Advanced Materials II*, Springer, Berlin Heidelberg, in print.
- [6] Andrusenko I., Mugnaioli E., Gorelik T.E., Koll D., Panthöfer M., Tremel W., Kolb U. (2011) *Acta Cryst.* **B67**, 218.
- [7] Kolb U., Gorelik T., Mugnaioli E. (2009) In Moeck P., Hovmoeller S., Nicolopoulos S., Rouvimov S., Petrok V., Gateshki M., Fraundorf P. (ed.): *Electron Crystallography for Materials Research and Quantitative Characterization of Nanostructured Materials*, Materials Research Society Symposia Proceedings Volume 1184, Warrendale PA, USA, GG01-05.
- [8] Gemmi M., Fischer J., Merlini M., Poli S., Fumagalli P., Mugnaioli E., Kolb U. (2011) *Earth Planet. Sci. Lett.*, in print.
- [9] Mugnaioli E., Gorelik T., Kolb U. (2009) *Ultramicroscopy*, **109**, 758.
- [10] Rozhdestvenskaya I., Mugnaioli E., Czank M., Depmeier W., Kolb U. (2011) *Min. Mag.*, in print.
- [11] Rozhdestvenskaya I., Mugnaioli E., Czank M., Depmeier W., Kolb U., Reinholdt A., Weirich T. (2010) *Min. Mag.*, **74**, 159.
- [12] Denysenko D., Grzywa M., Tonigold M., Schmitz B., Krkljus I., Hirscher M., Mugnaioli E., Kolb U., Hanss J., Volkmer D. (2011) *Chem. – Eur. J.*, **17**, 1837.
- [13] Birkel C.S., Mugnaioli E., Gorelik T., Kolb U., Panthöfer M., Tremel W. (2010) *J. Am. Chem. Soc.*, **132**, 9881.
- [14] Kolb U., Mugnaioli E., Gorelik T.E. (2011) *Cryst. Res. Technol.*, **46**, 542.
- [15] Jiang J., Jorda J.L., Yu J., Baumes L.A., Mugnaioli E., Diaz-Cabanias



3D diffraction tomography

Example on pharma API sample

API sample Nateglinide Form B

X-RAY DATA (from Synchrotron powder diffraction)

B: P2₁ with a=38.68198 Ang, b=57.94722 Ang, c=8.03988 Ang and
beta=95.15785 deg

work in collaboration with Dr. F.Gozo Excelsius Brussels

Unit cell Naterglinide

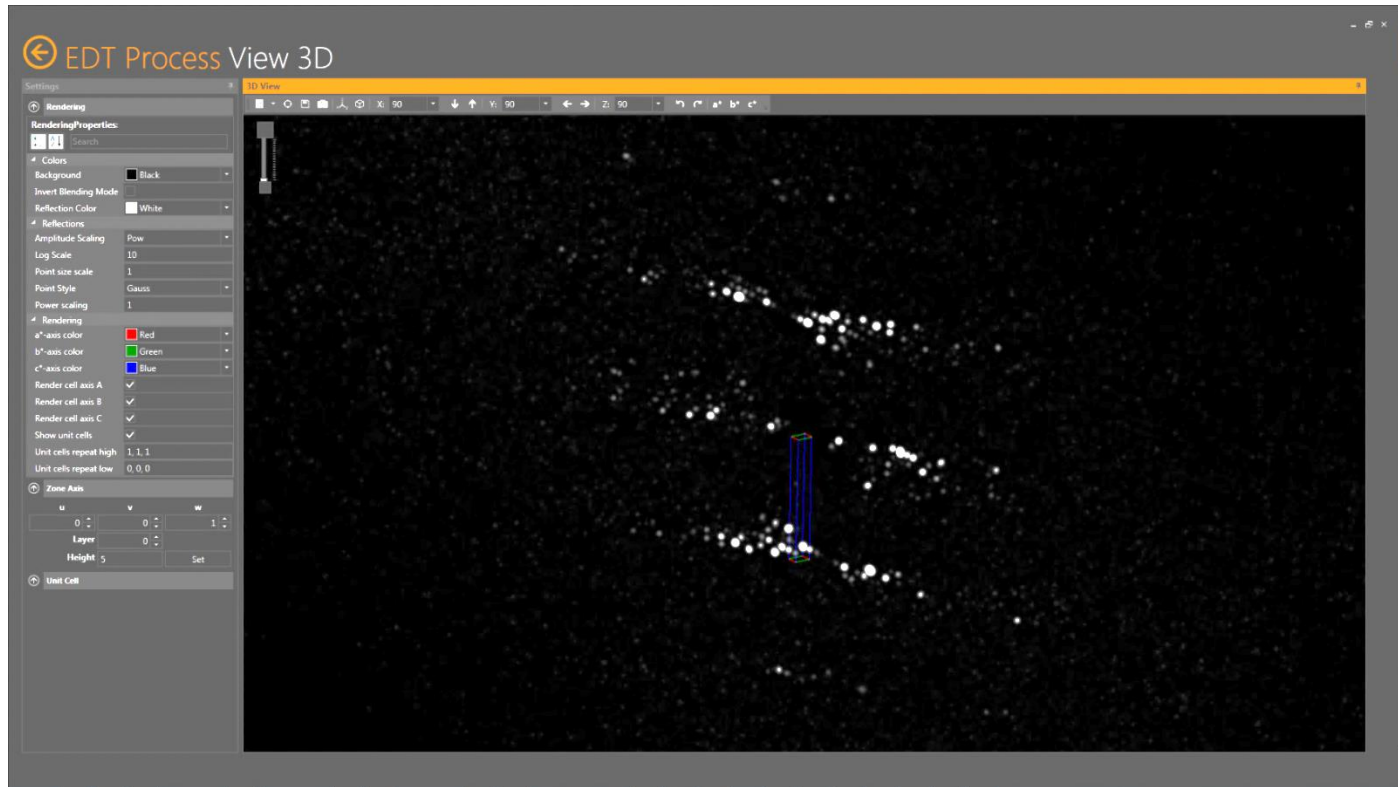
- **Data set 1: $a = 55.59\text{\AA}$, $b=37.13\text{\AA}$, $c=4.99\text{\AA}$, $\alpha=90.1$, $\beta=88.5$, $\gamma=90.2$**
- **Data set 2: $a = 56.7\text{\AA}$, $b=38.4\text{\AA}$, $c=4.92\text{\AA}$, $\alpha=89.2$, $\beta=90.7$, $\gamma=88.85$**
- **X-RAY DATA**

B: $P2_1$ with $a=38.68198$ Ang, $b=57.94722$ Ang, $c=8.03988$ Ang and $\beta=95.15785$ deg

**Work on progress
data consistent with X-Ray**

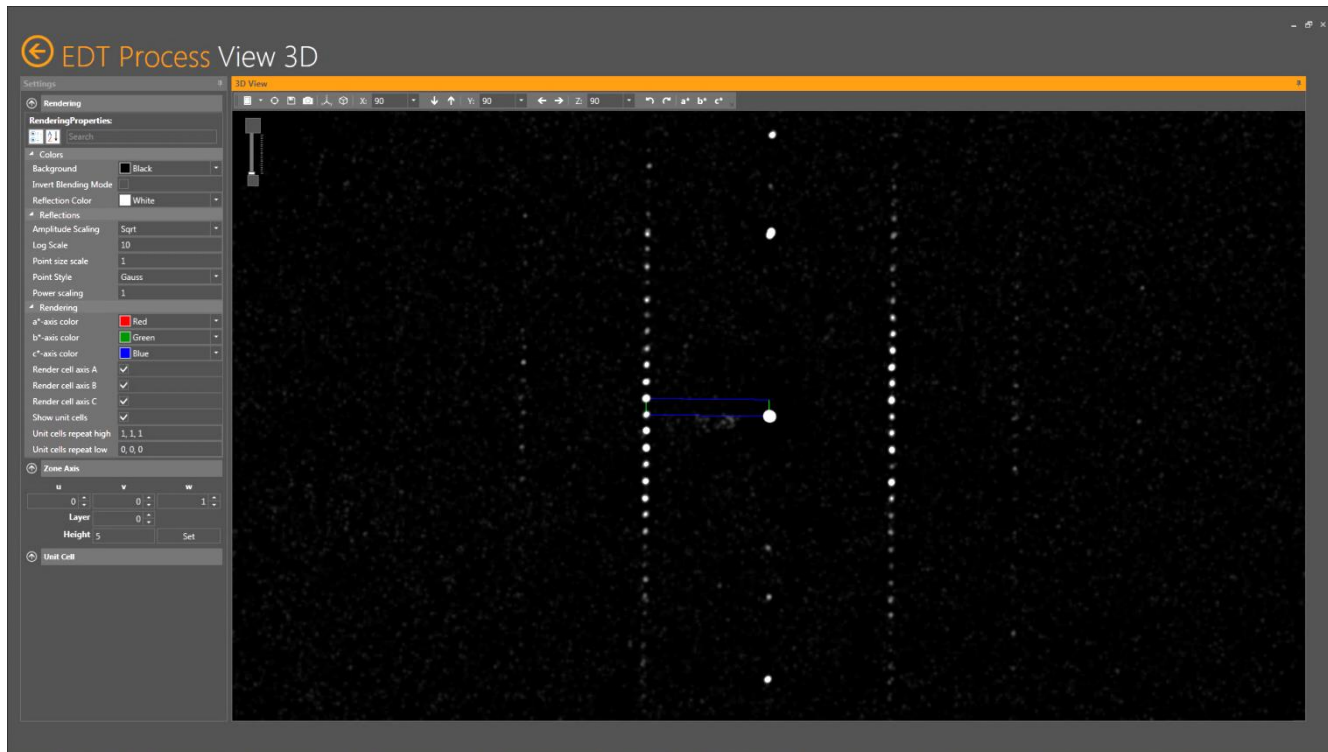
Unpublished work , analysis with EDT software
by Dr. Oleynikov Stockholm University

RESULTS 3D diffraction tomography on a single Naterglinide nanocrystal



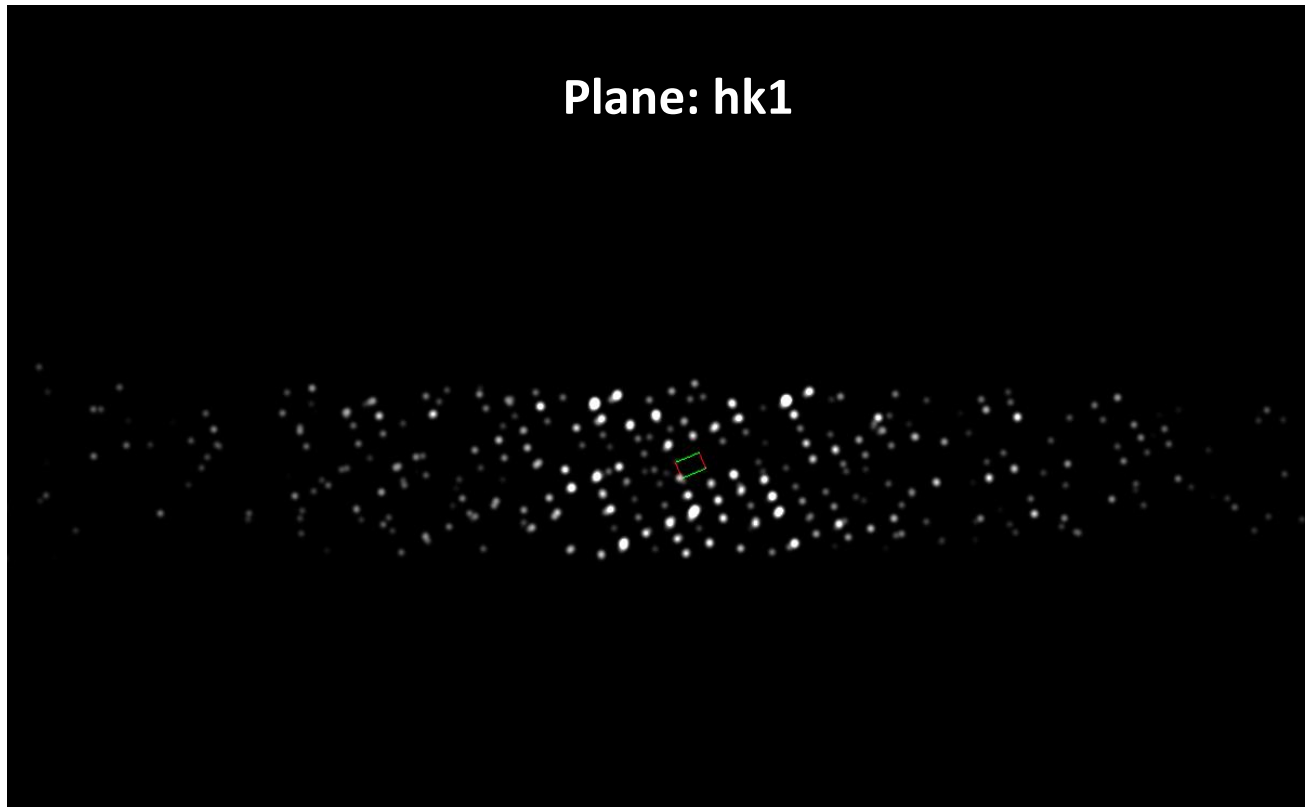
Unpublished work , analysis with EDT software by Dr. Oleynikov Stockholm University

RESULTS 3D diffraction tomography on a single Naterglinide nanocrystal



Unpublished work , analysis with EDT software by Dr. Oleynikov Stockholm University

RESULTS 3D diffraction tomography on a single Naterglinide nanocrystal



Unpublished work , analysis with EDT software by Dr. Oleynikov Stockholm University

Automatic 3D precession diffraction tomography

ADT-3D

Access to single nano-crystals with TEM

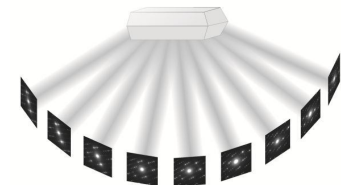
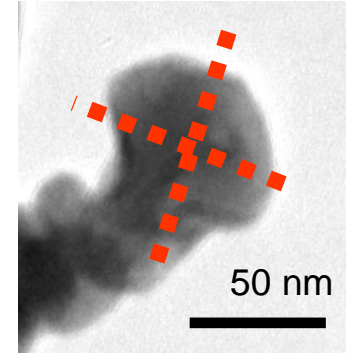
Data collection in 90-120 min

Reveal Unit cell & crystal symmetry

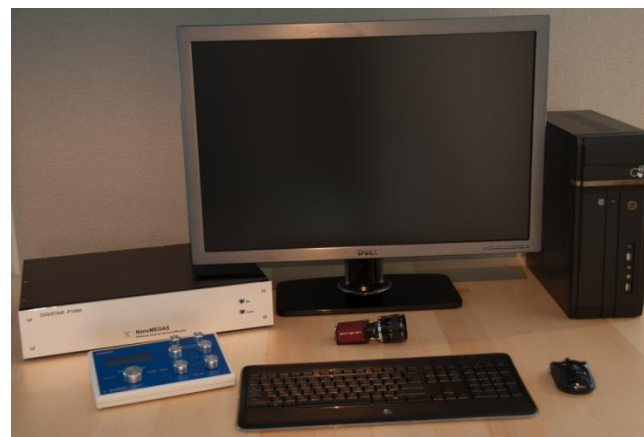
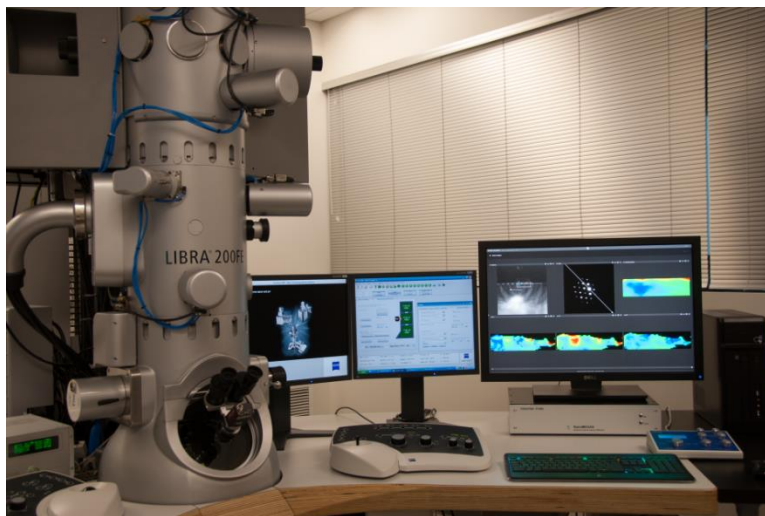
through 3D automatic reciprocal space acquisition and reconstruction

Solve ab-initio structures using 3D precession intensities

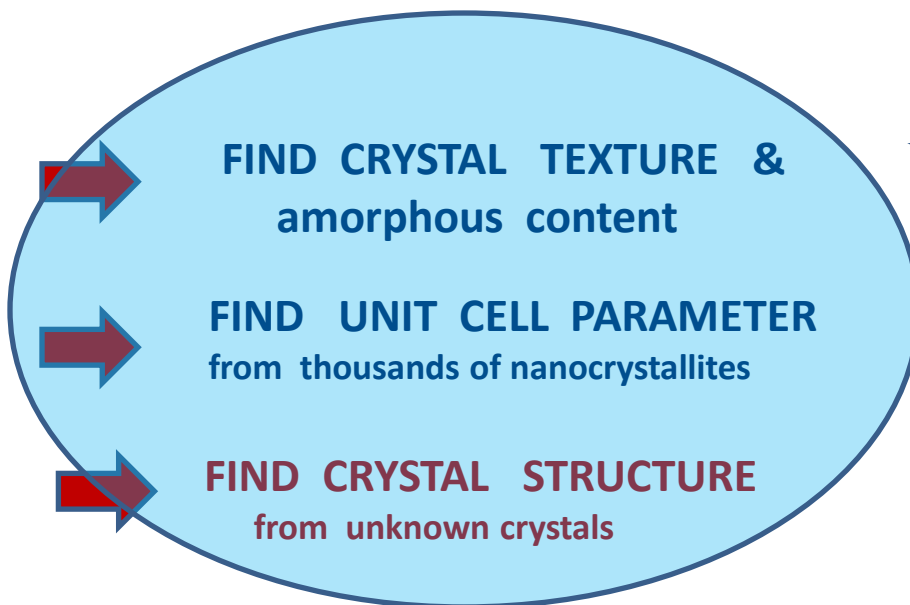
ADT 3D for beam sensitive samples (pharma) should be used with cryo-techniques



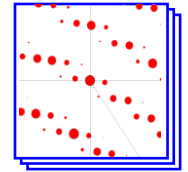
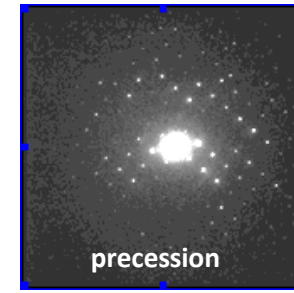
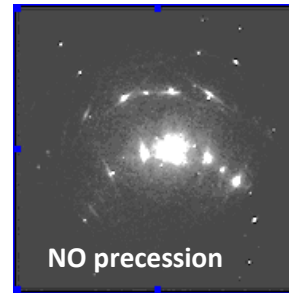
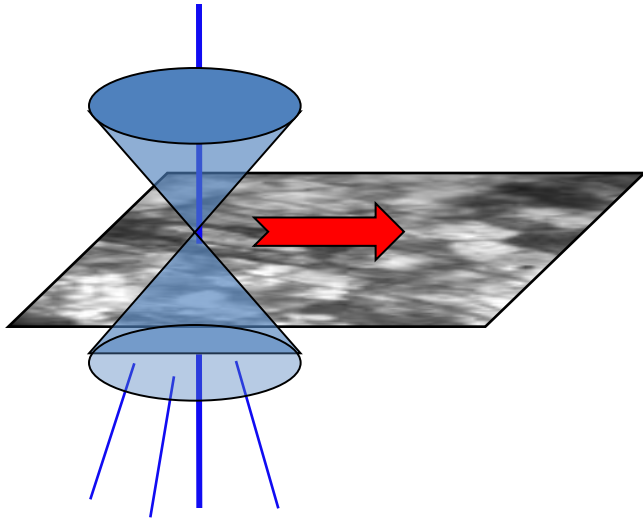
ORGANIC CRYSTALS : THE RANDOM TOMOGRAPHY METHOD



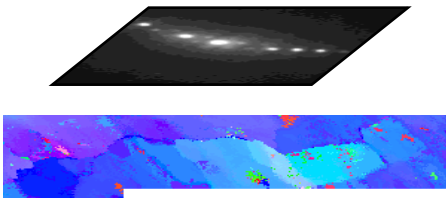
The challenge :



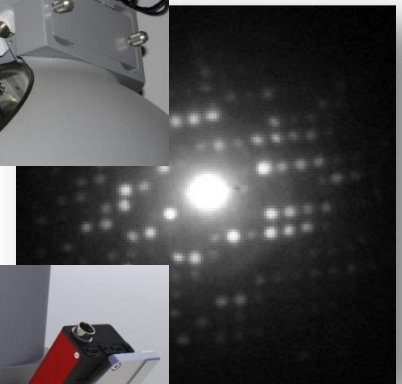
ASTAR (Orientation and phase imaging in TEM)



Using precession diffraction the number of ED spots observed increases (almost double) ; correlation index map becomes much more reliable when compared with templates

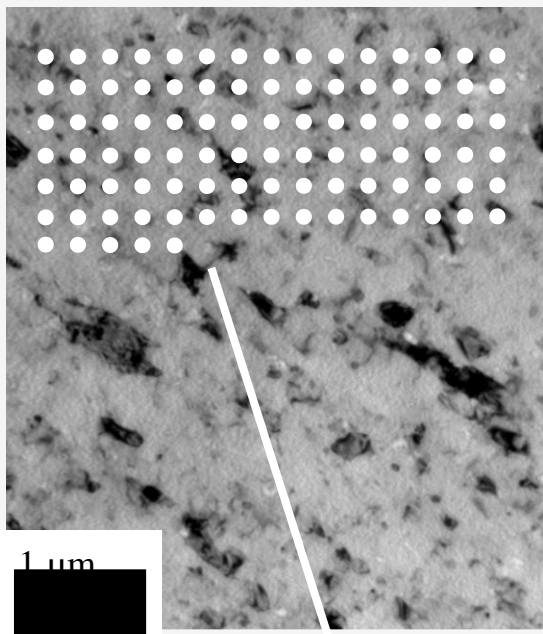


Orientation map

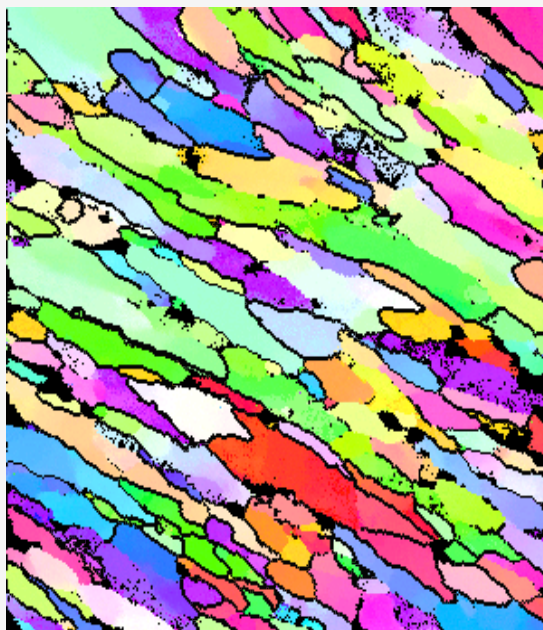
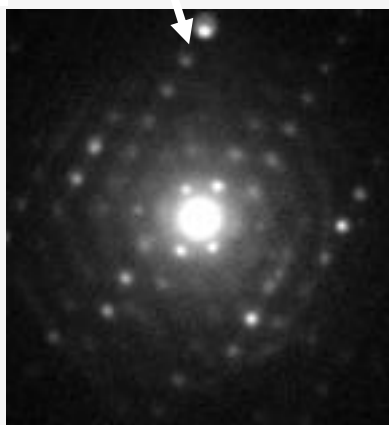


Scanning the TEM beam in precession mode
Step size 0.1 nm -100 nm
Dedicated CCD with > 100 frames/sec
Typical area 5 x 5 microns
Scanning times (typical) 5-10 min

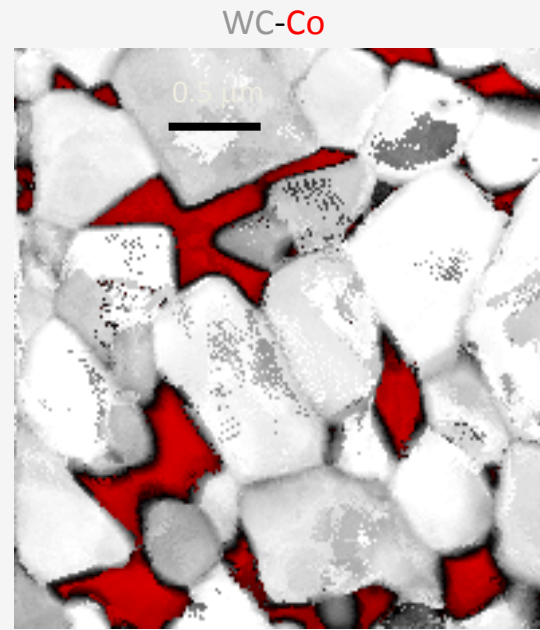
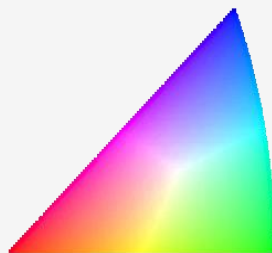
ASTAR : Automated Crystal Orientation Mapping



Severely deformed
7075 Al. Alloy



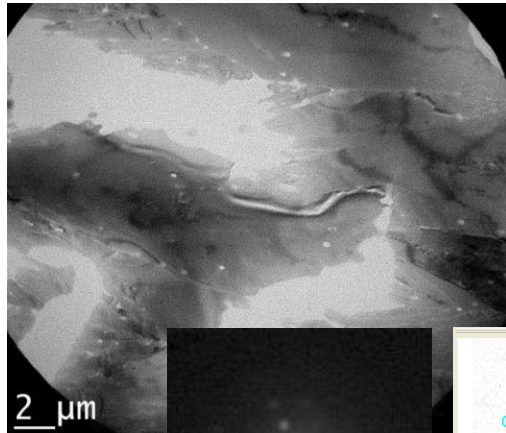
Orientation map



Phase map

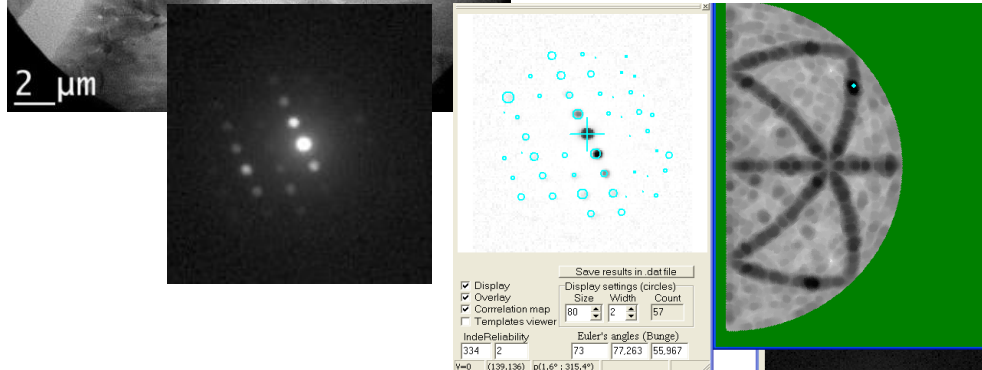


ASTAR : texture of organic structures

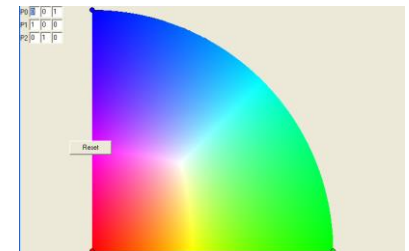
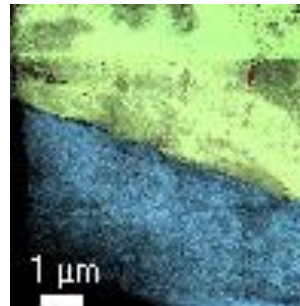
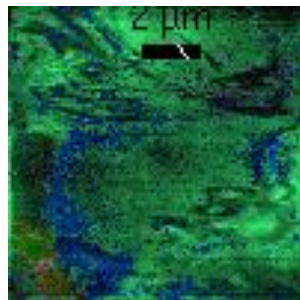
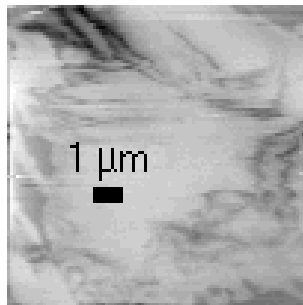


TRIS structure $C_{16}H_{48}N_4O_{12}$

Pna2₁ cell 0.7768 X 0.8725 X 0.8855 nm

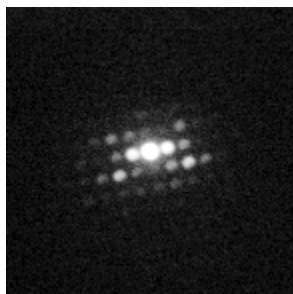


Fast scanning > 100 fps
prevent crystal
instant beam damage



ASTAR : texture of organic nanomagnets

Organic matter : $[\text{Fe}(\text{Htrz})_2(\text{trz})]\cdot\text{BF}_4$



Jeol 3010, 100fps,
spot 25nm,

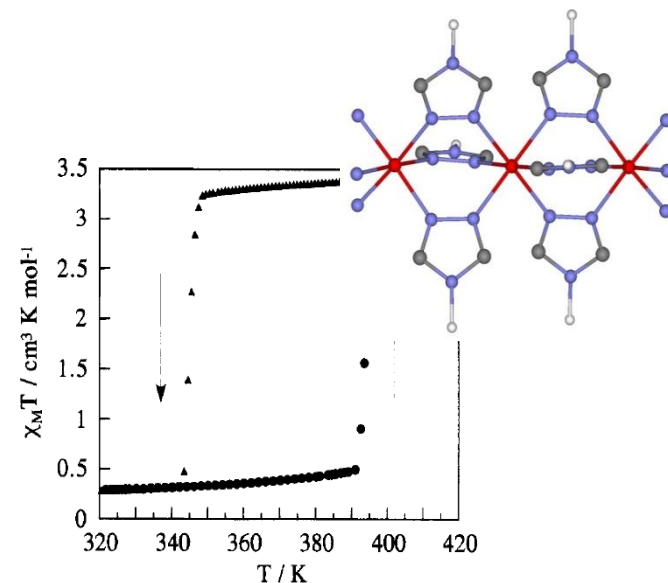
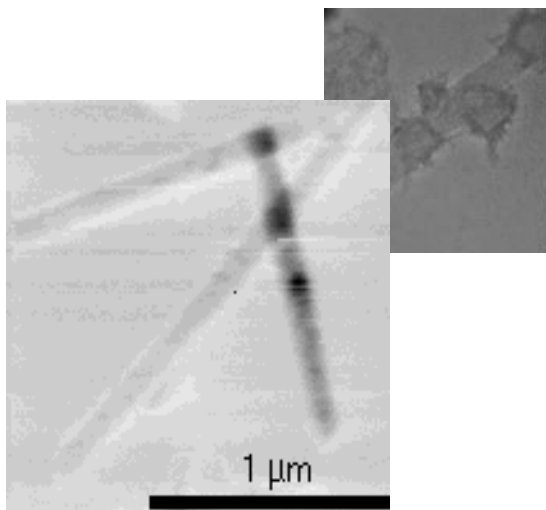
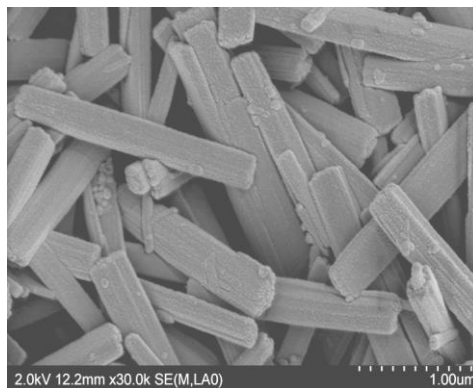
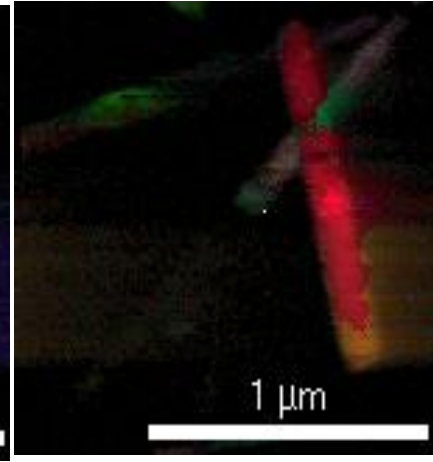
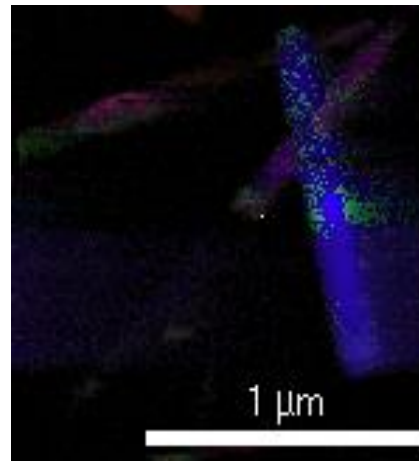
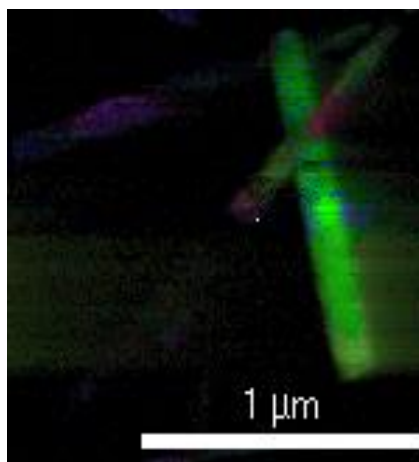


Figure 1. $\chi_M T$ versus T plots in the warming and cooling modes for $[\text{Fe}(\text{Htrz})_2(\text{trz})](\text{BF}_4)$ (1a).



What about the amorphous content in a sample ?

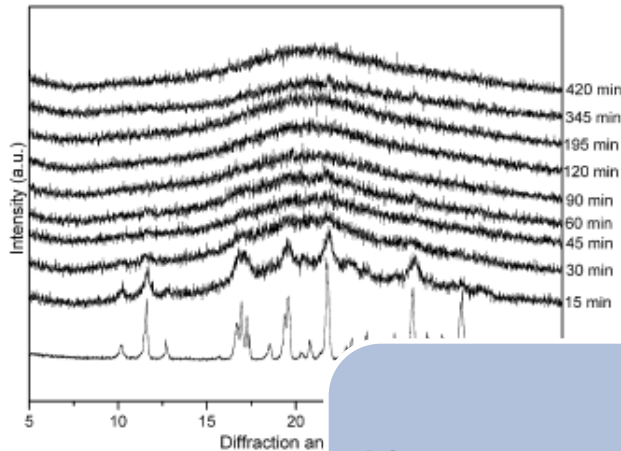
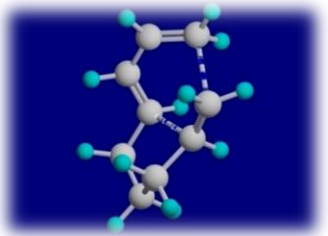
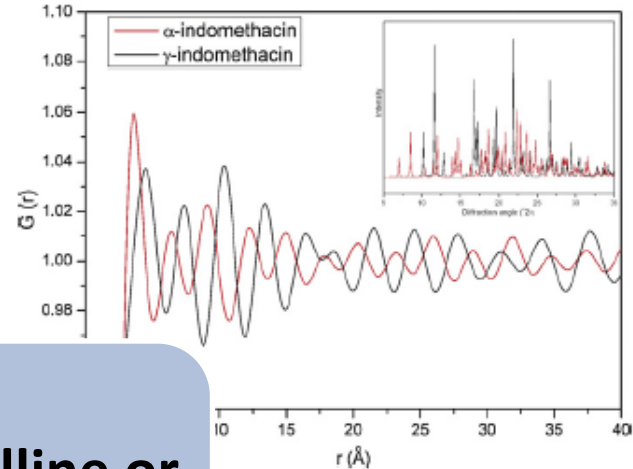


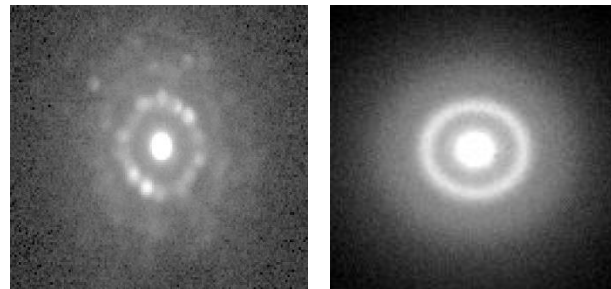
Fig. 2. XRPD diffractograms of the cryo-m for different times (time in the figure corre



and α -form of indomethacin. XRPD diffractograms of γ -ethacin are shown in the inset.

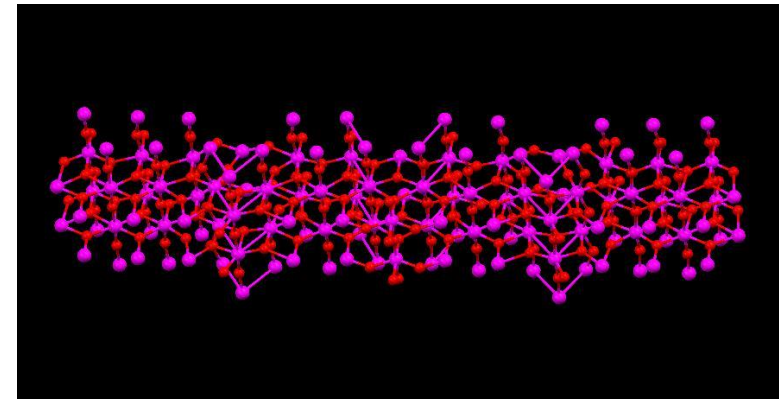
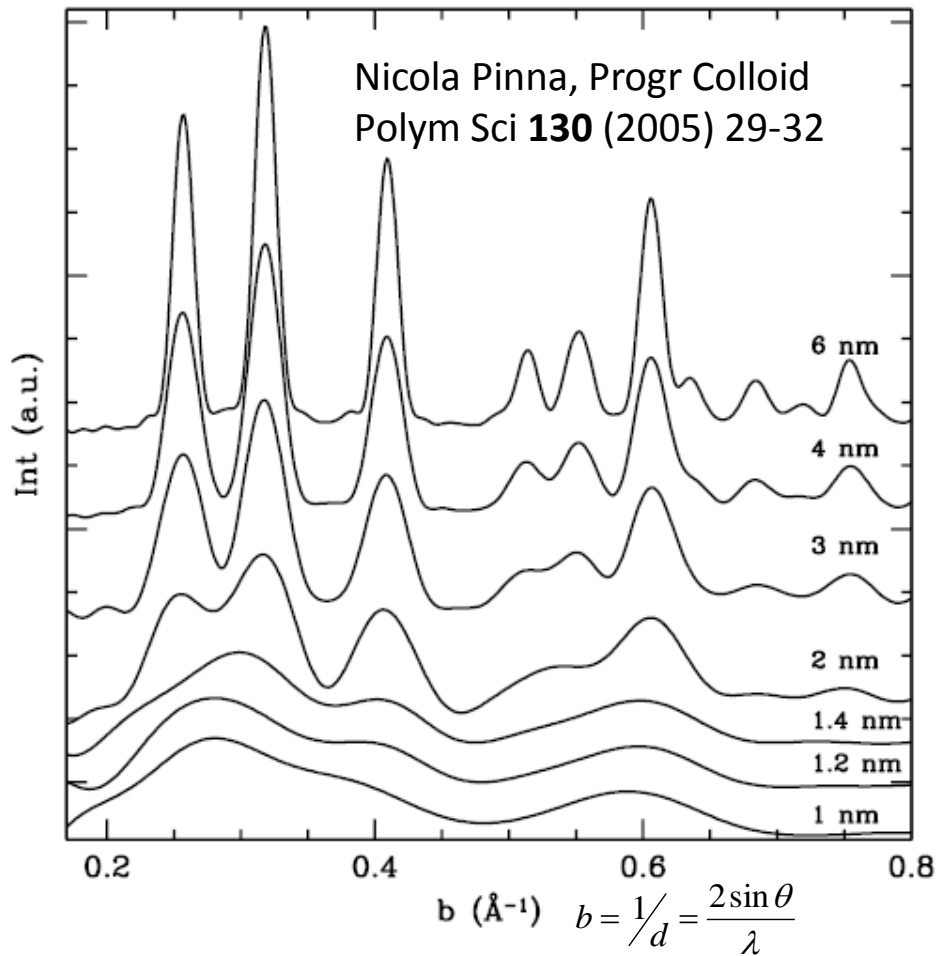
Nanocrystalline or Amorphous ?

ED pattern from overlapping nanocrystals < 10 nm



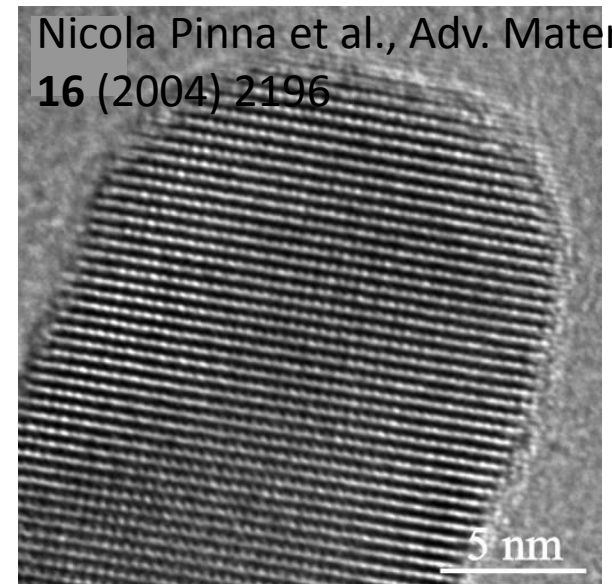
ED pattern from amorphous area

both may show "X-ray amorphous" pattern



Ta_2O_5
tantite

Nicola Pinna et al., Adv. Mater
16 (2004) 2196

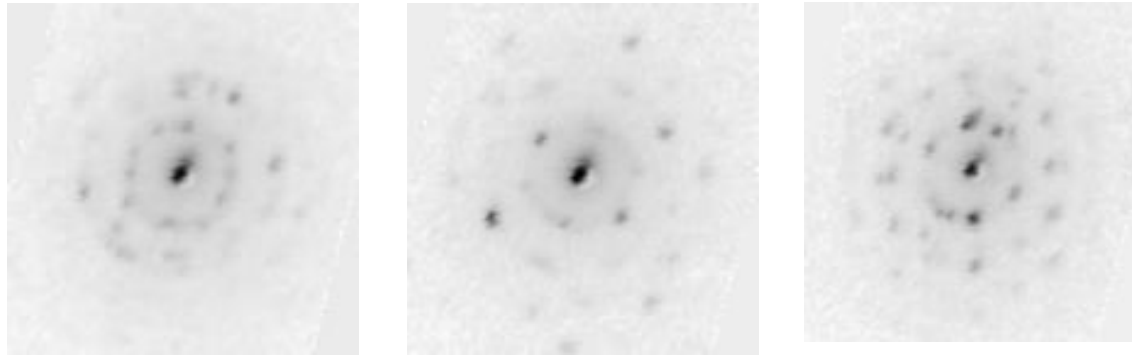


**Crystals < 5 nm look like “X-Ray amorphous”
but we can see them in TEM !**

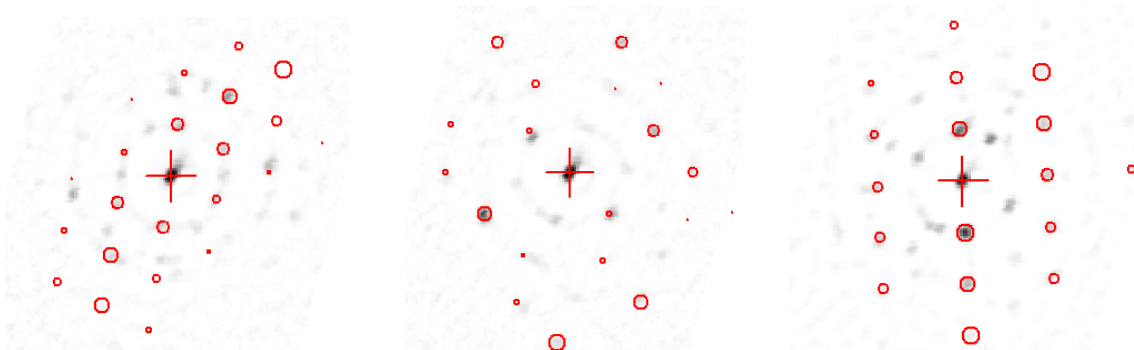
Nanocrystalline or Amorphous ?

Example: Polycrystalline thin film of Ni-Fe nanocrystals (average size 5-20 nm)

Data taken with JEOL JEM 2200F operating at 200 kV spot size 1-8 nm



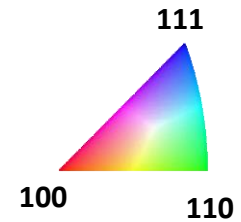
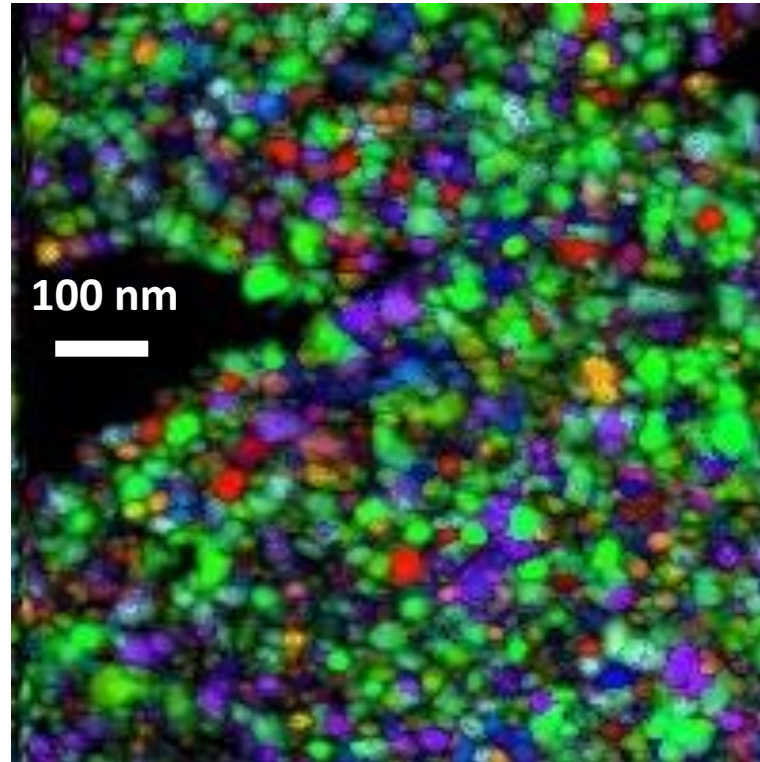
ASTAR can index even overlapping diffraction patterns from polycrystalline sample



Data taken with JEOL JEM 2200F operating at 200 kV spot size 1-8 nm

Results courtesy Prof. Dr. E.Rauch CNRS Grenoble

they are polycrystalline !

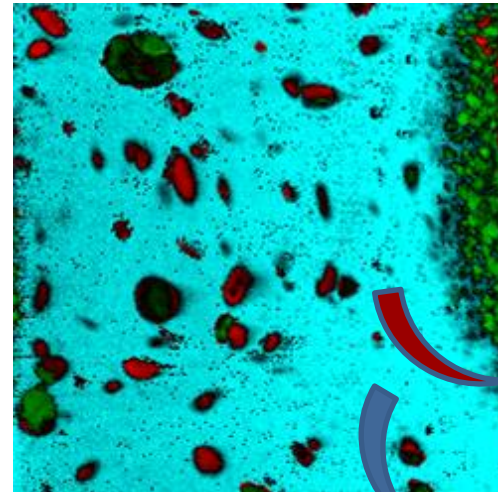
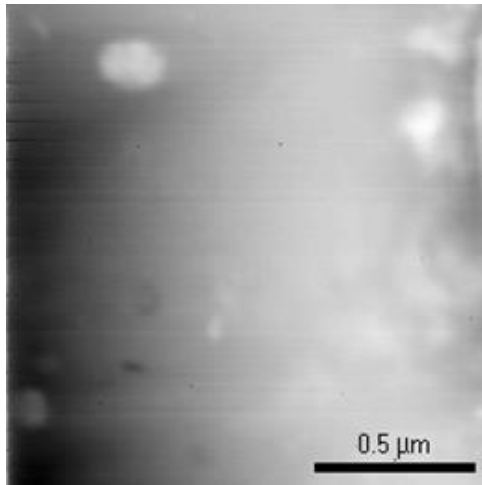
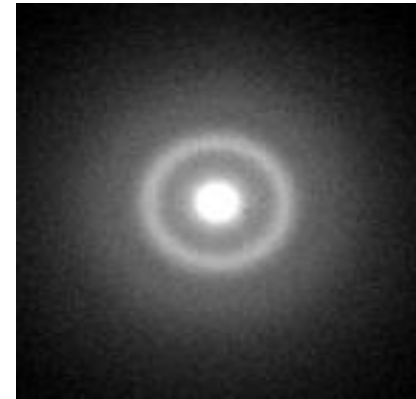
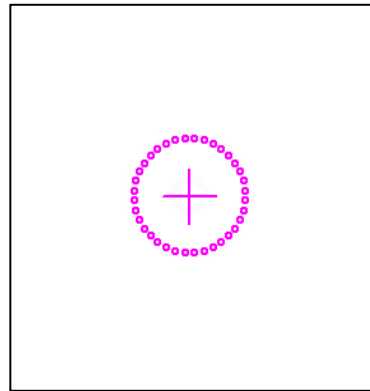
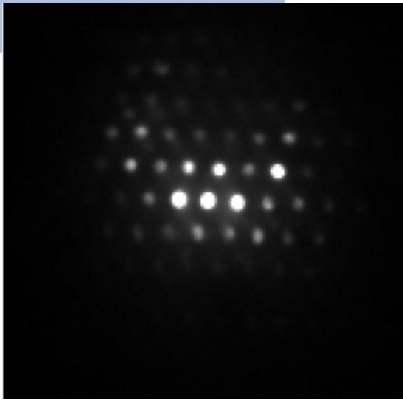


Orientation map (z)

ASTAR orientation image showing individual Ni-Fe orientations

Nanocrystalline or Amorphous ?

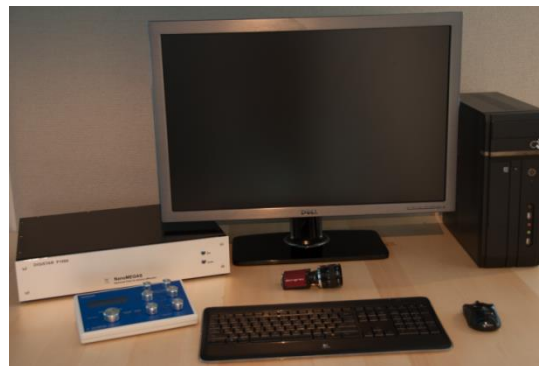
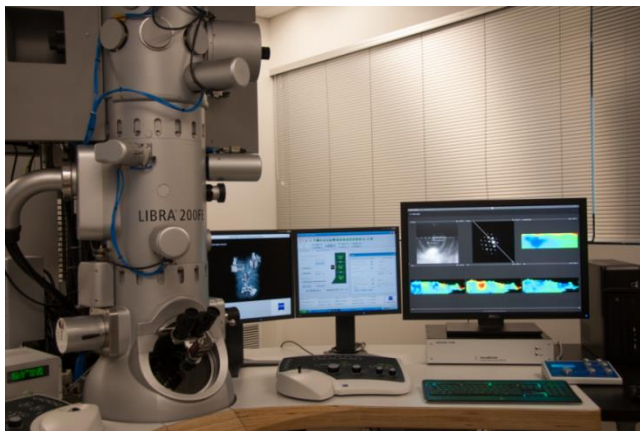
Example : Mg-Cu-Gd partly recrystallized metallic
glass with Mg_2Cu and Cu_2Gd crystalline precipitates



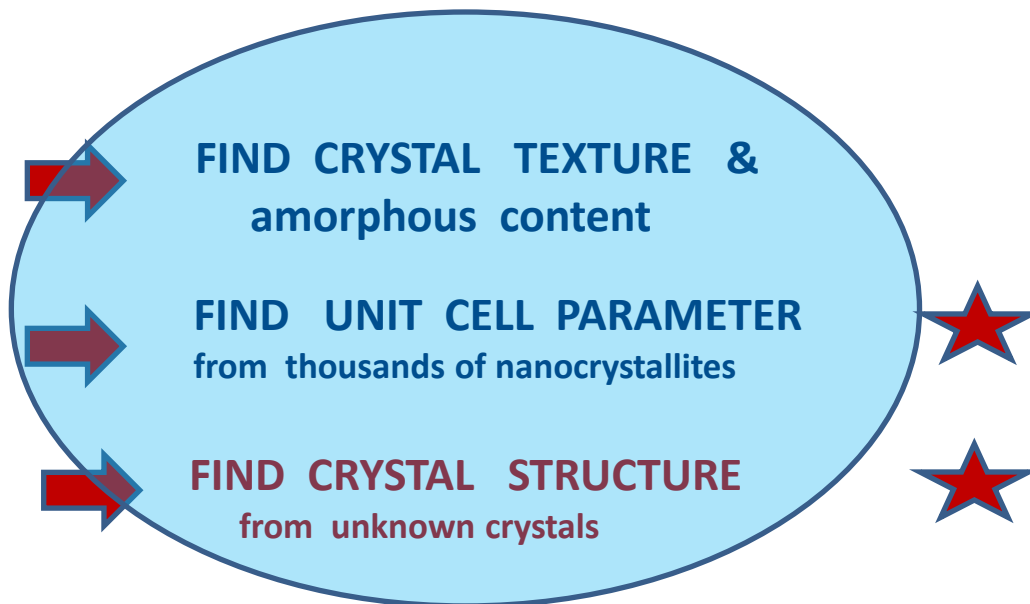
crystalline

amorphous

PHARMA CRYSTALS : THE RANDOM TOMOGRAPHY METHOD



The challenge :

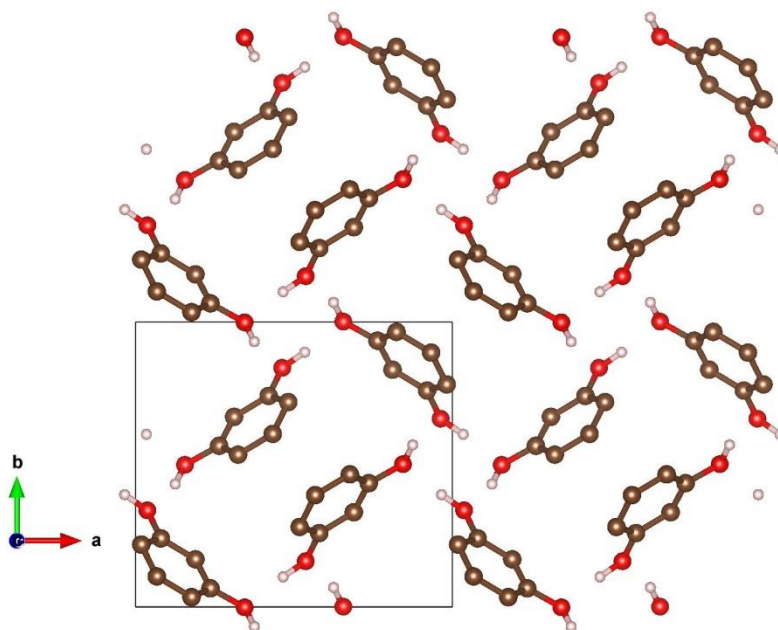


RESORCINOL crystal structure

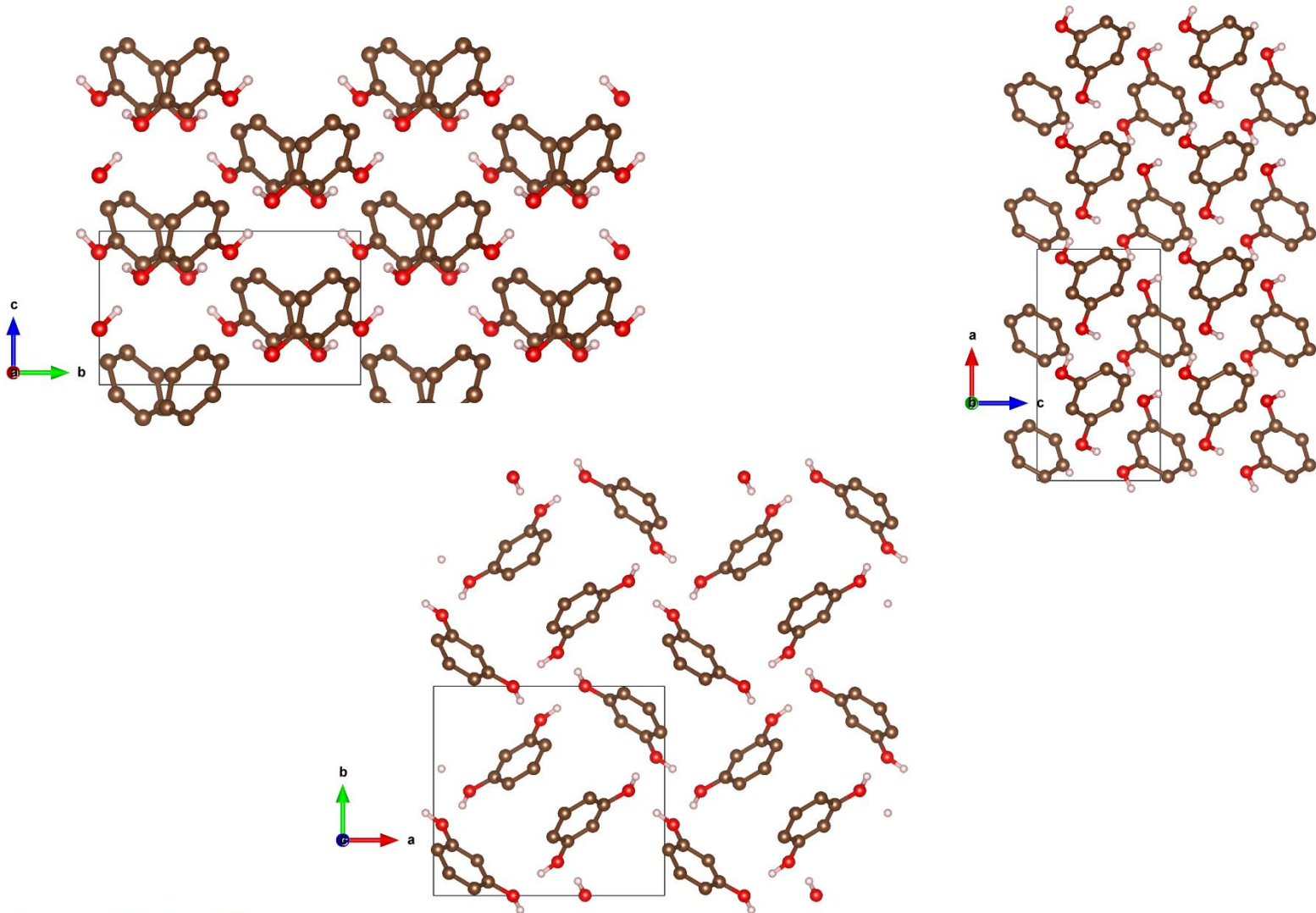
1,3-Dihydroxybenzene.

α -phase $a=10.447 \text{ \AA}$, $b=9.356 \text{ \AA}$, $c=5.665 \text{ \AA}$ $Pna2_1$

β -phase: $a=7.811 \text{ \AA}$ $b=12.615 \text{ \AA}$, $c=5.427 \text{ \AA}$ $Pna2_1$

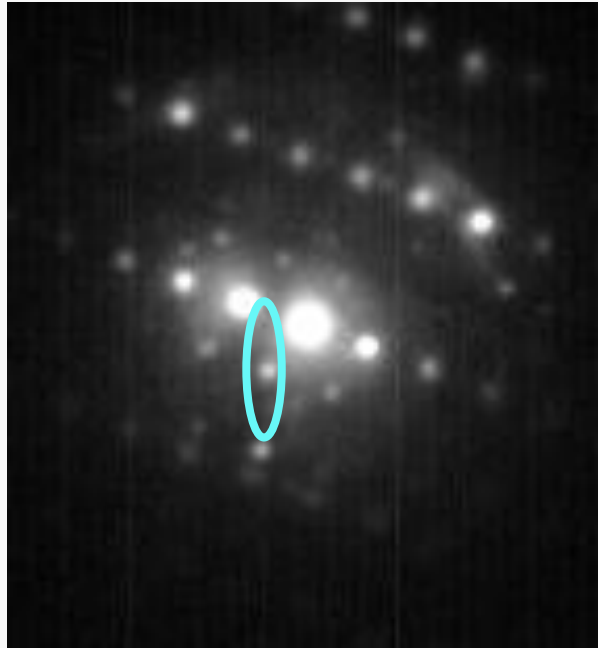


RESORCINOL crystal structure

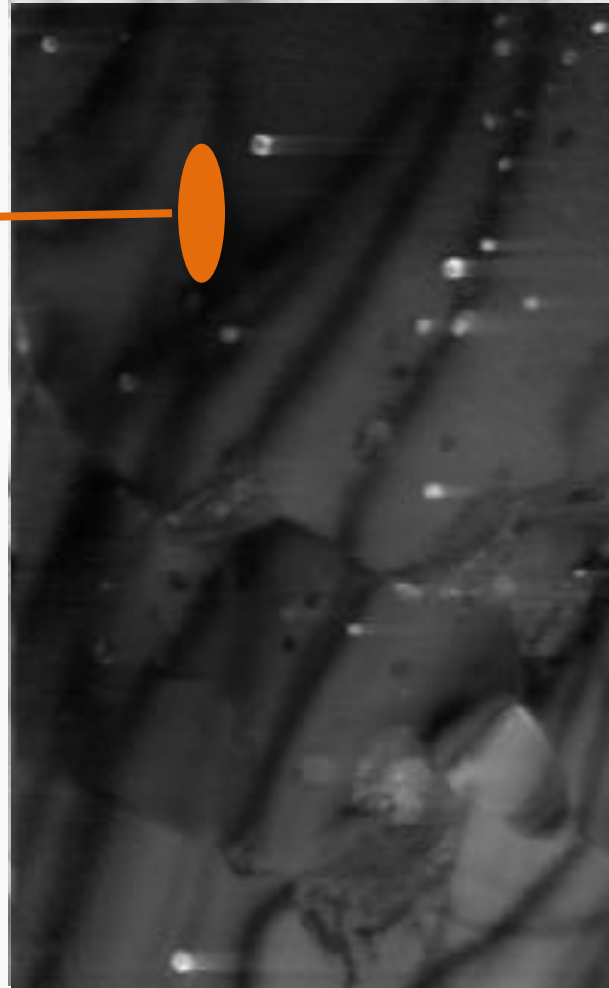


ASTAR : create virtual dark (VDF) maps from digital images

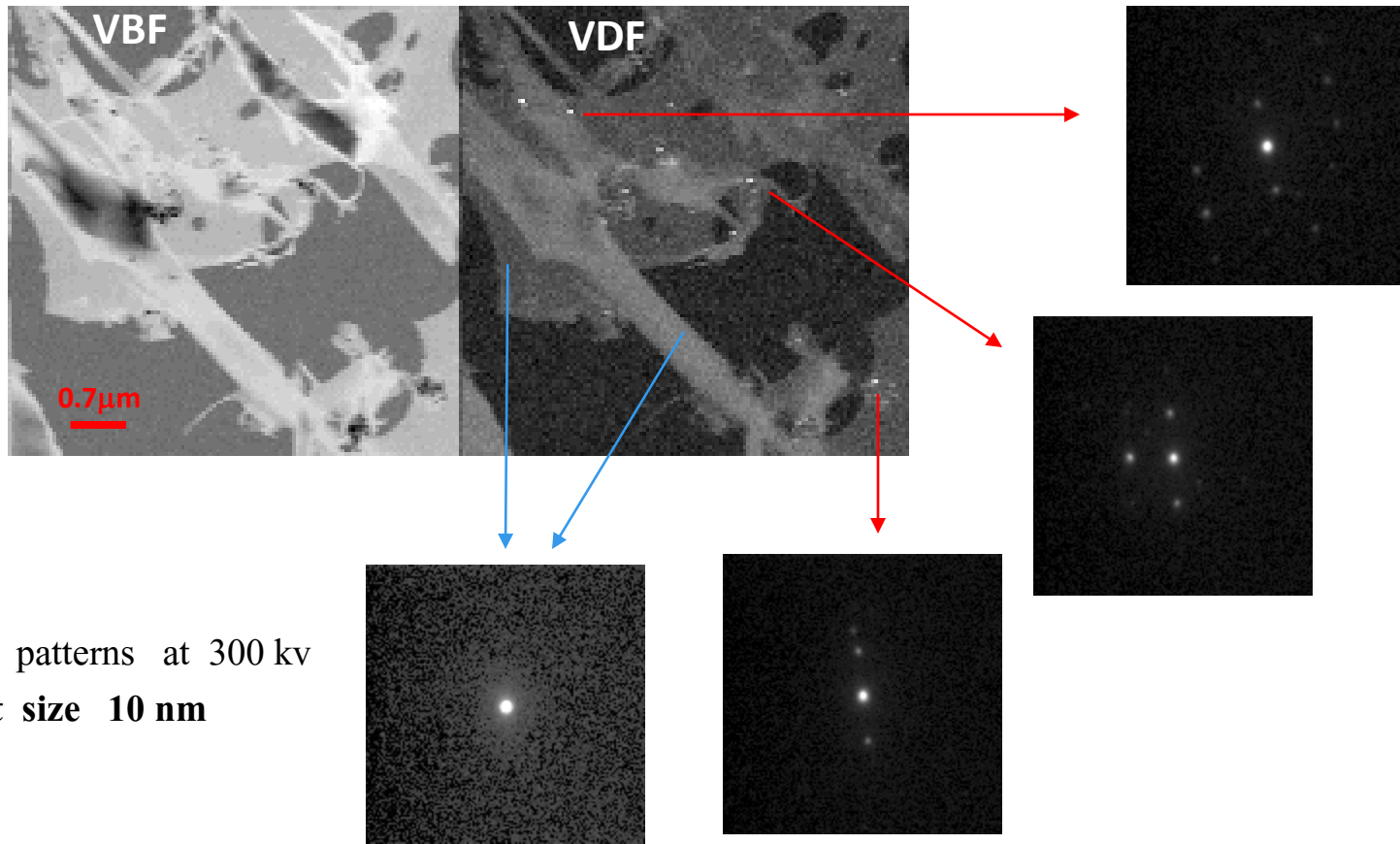
Diffraction pattern



Dark field image



ASTAR : Reveal crystalline – amorphous content



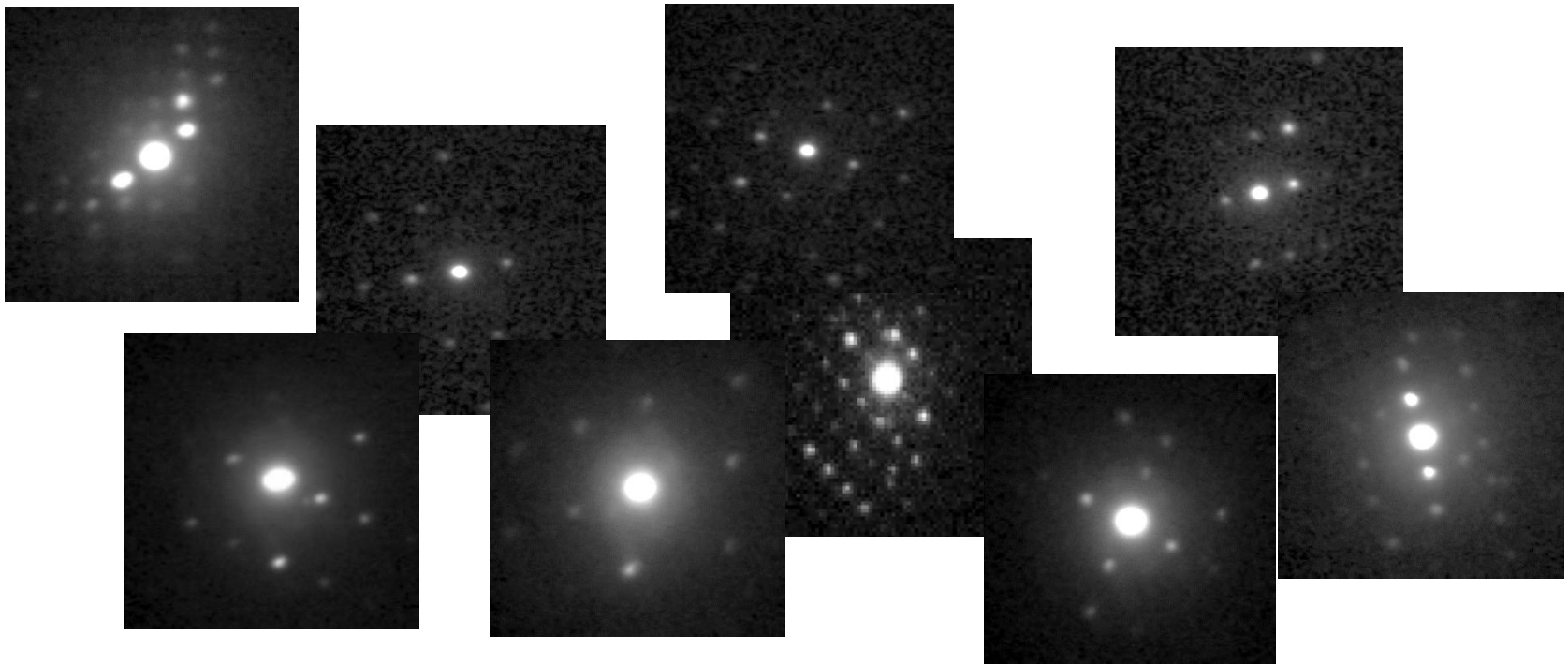
PED patterns at 300 kv
spot size 10 nm

**Crystals of resorcinol < 10 nm
clearly revealed
on amorphous background !**

ASTAR : Random precession diffraction tomography

UNIT CELL DETERMINATION

Collection of 12 random “quasi-oriented” PED patterns at 300 kv spot size 10 nm scanning at high speed rates > 50 fps

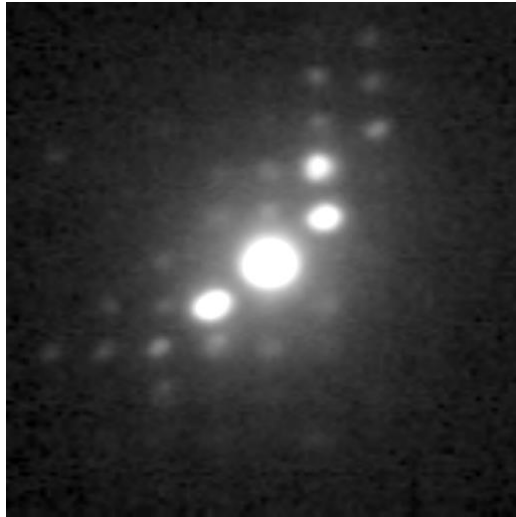


EDiff software after collection of 9 random PED patterns reveals the correct unit cell parameter of α phase

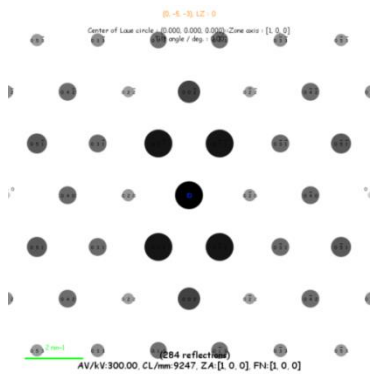
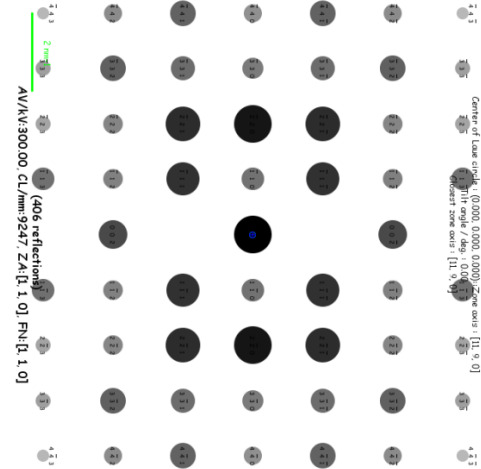
5.615 9.195 10.05 90 90 90

ASTAR : Random precession diffraction tomography

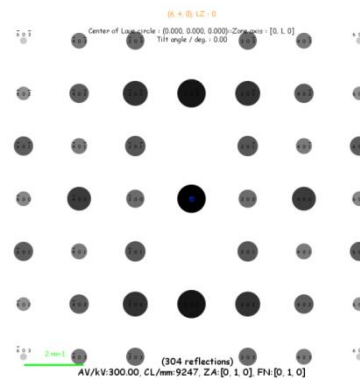
UNIT CELL DETERMINATION



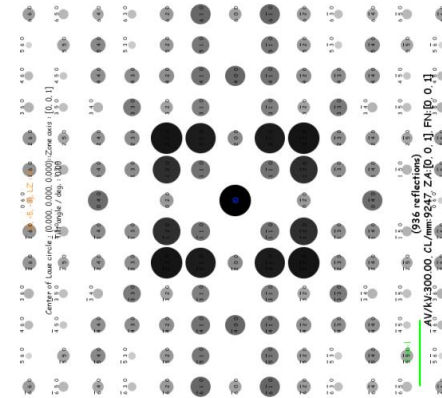
ZA 110



ZA 100



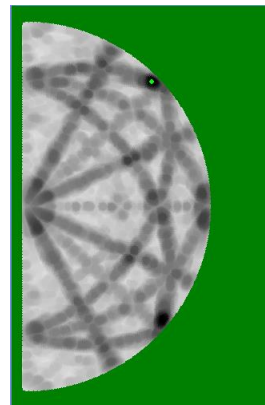
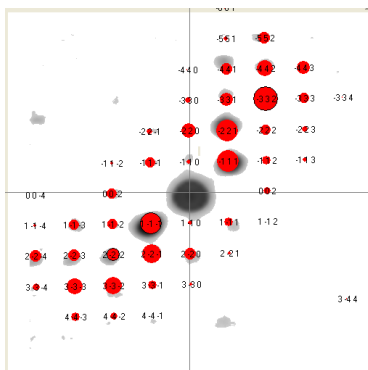
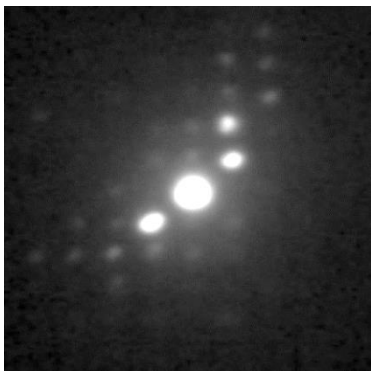
ZA 010



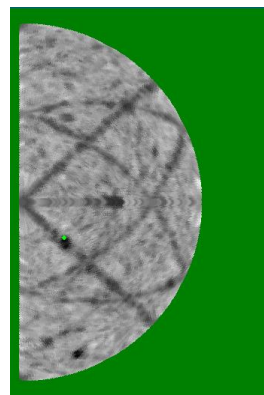
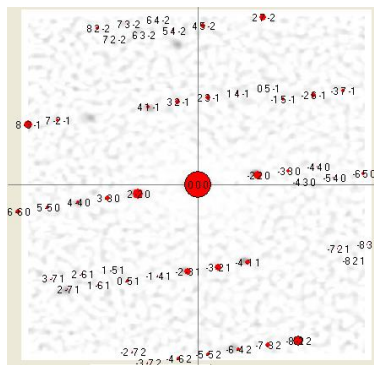
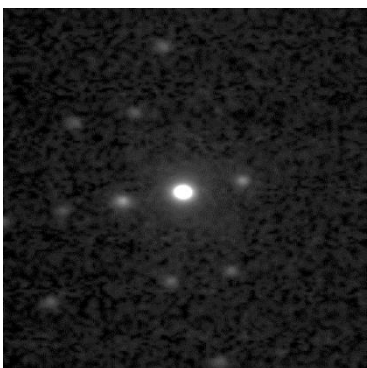
ZA 001

Diffraction simulation confirms correct ZA index

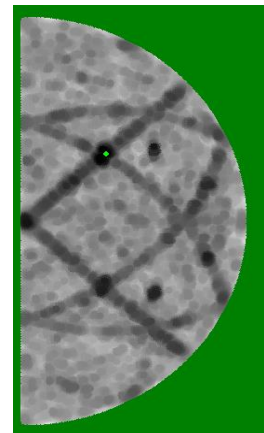
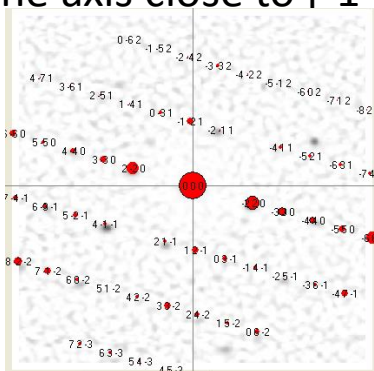
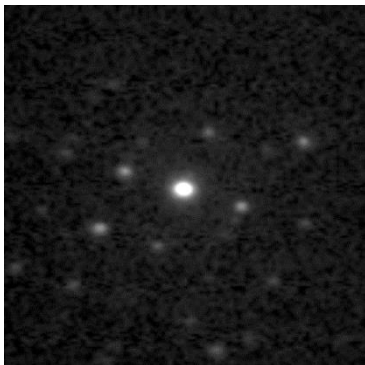
ASTAR : Random precession diffraction tomography



Zone axis close to $[110]$

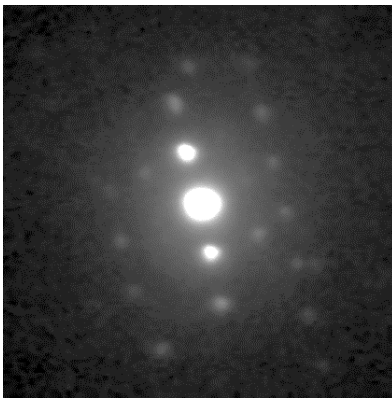
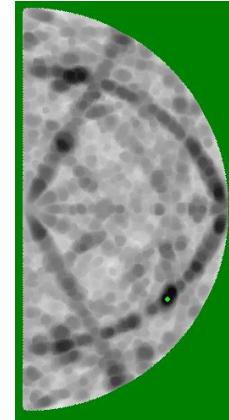
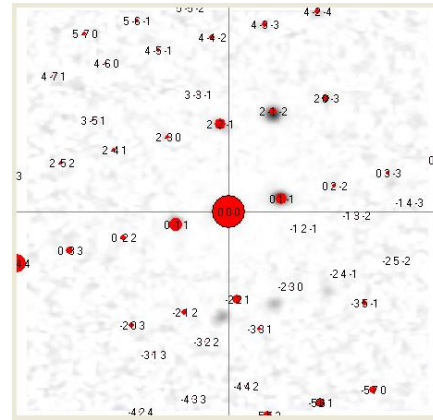
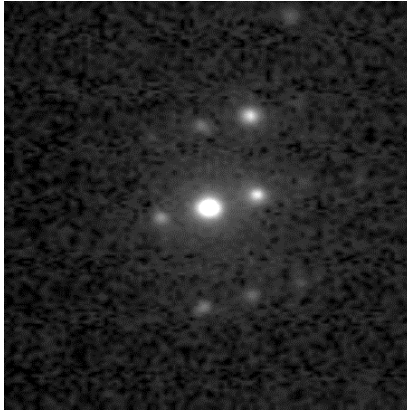


Zone axis close to $[-1-1-5]$

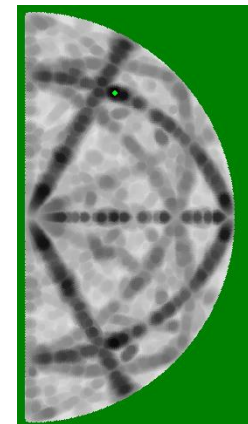
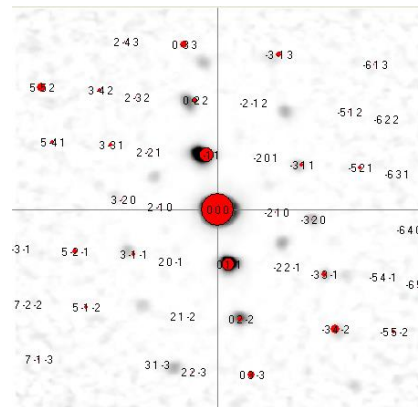


ASTAR : Random precession diffraction tomography

ZA close to $[-7 -7 -5]$

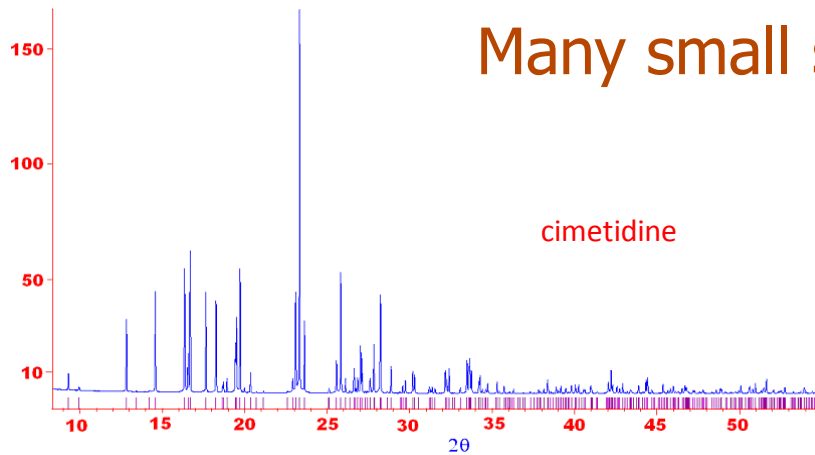


ZA close to $[5 8 8]$



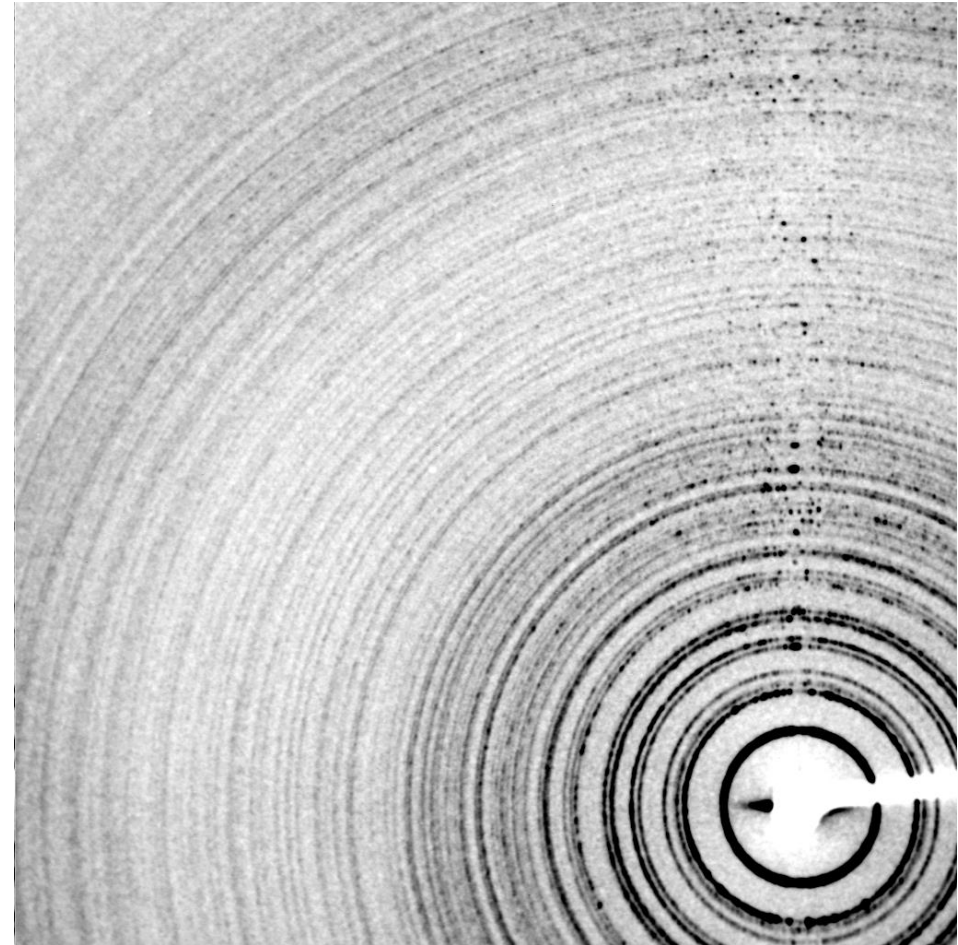
UNIT CELL DETERMINATION - SOLVE CRYSTAL STRUCTURE

Many small single crystals make a powder

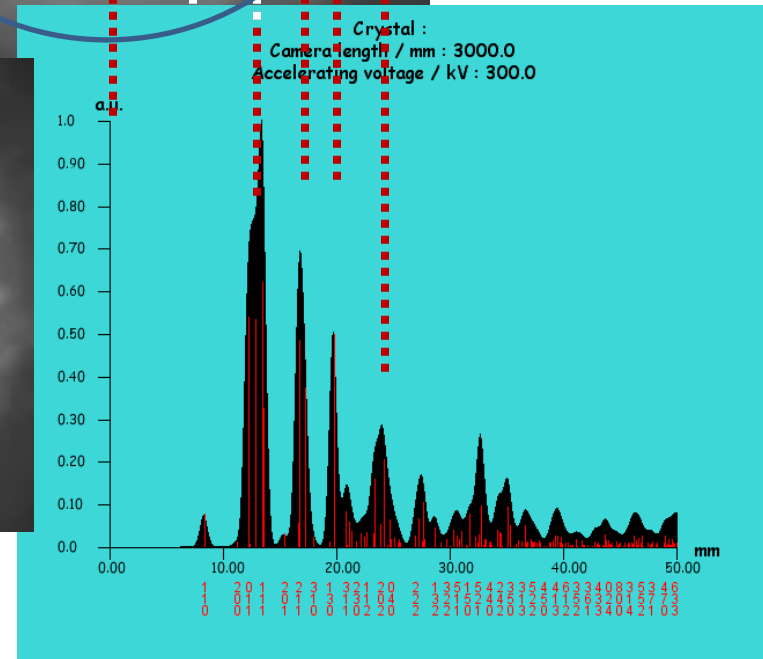
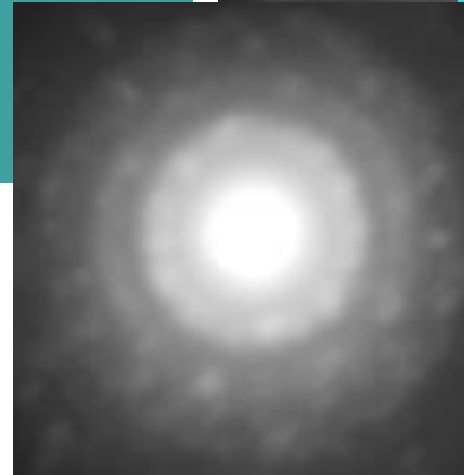
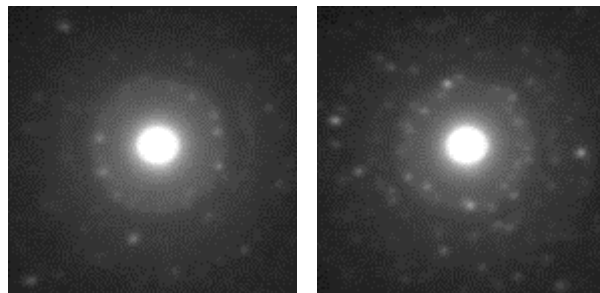
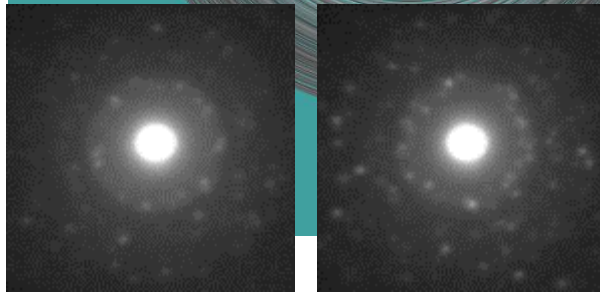
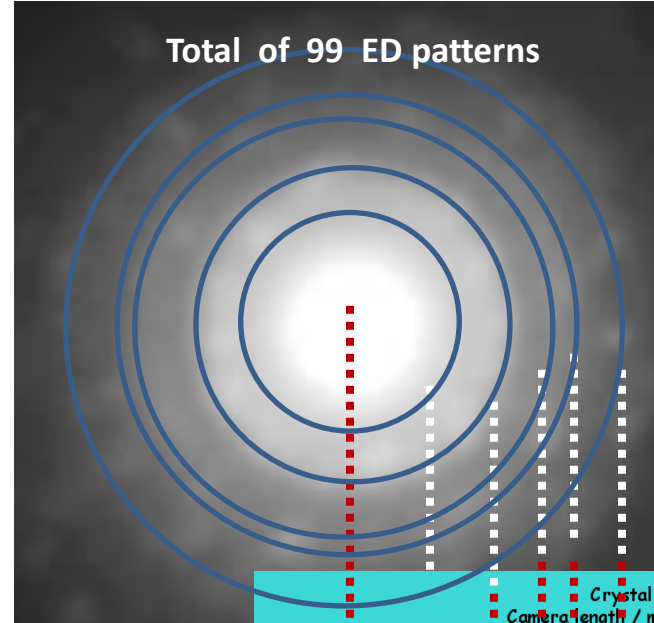
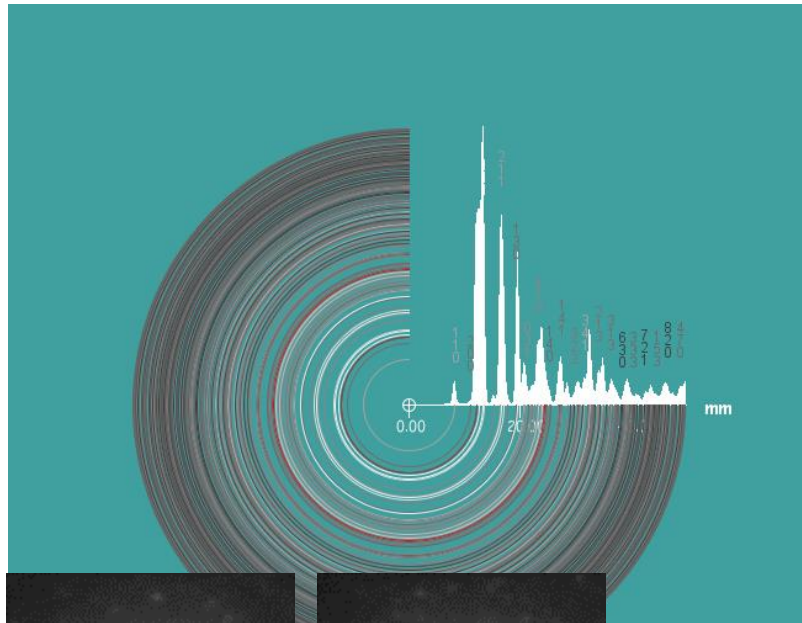


- » 1
- » 2
- » 3
- » 5
- » 10
- » 20
- » 50

- Spots cover spheres in 3D reciprocal space
- 2D area detector takes a slice
(on Ewald sphere)
- 1D powder scan measures distance from origin



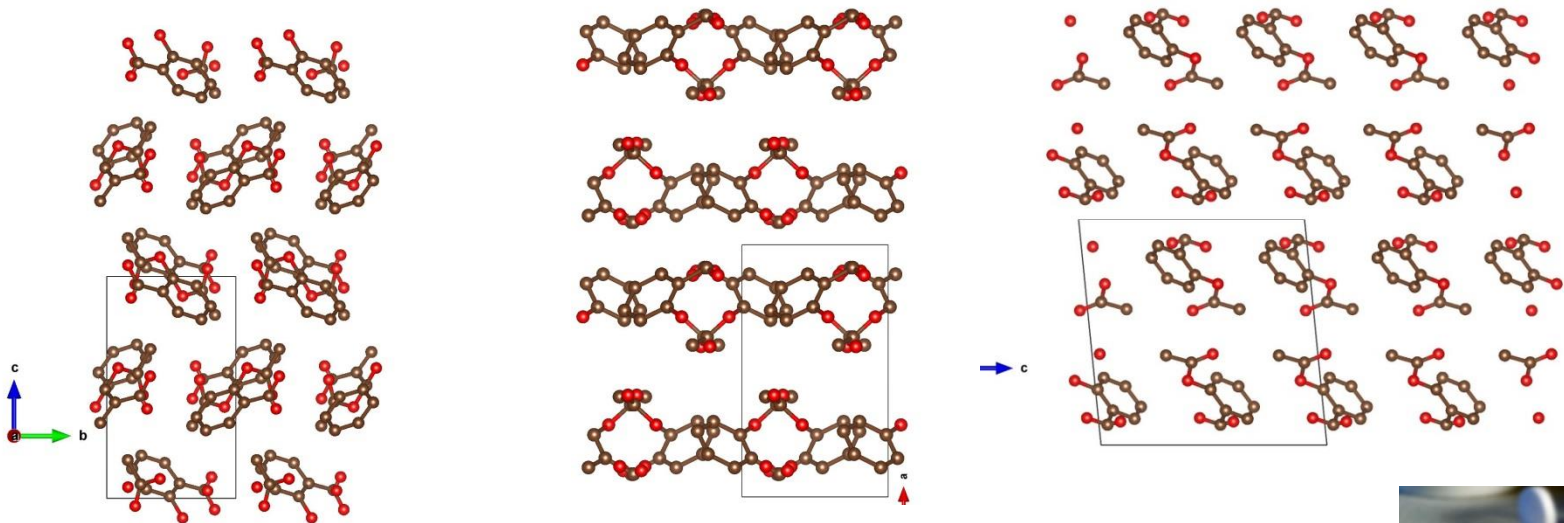
ASTAR : Adding random PED patterns to form a powder



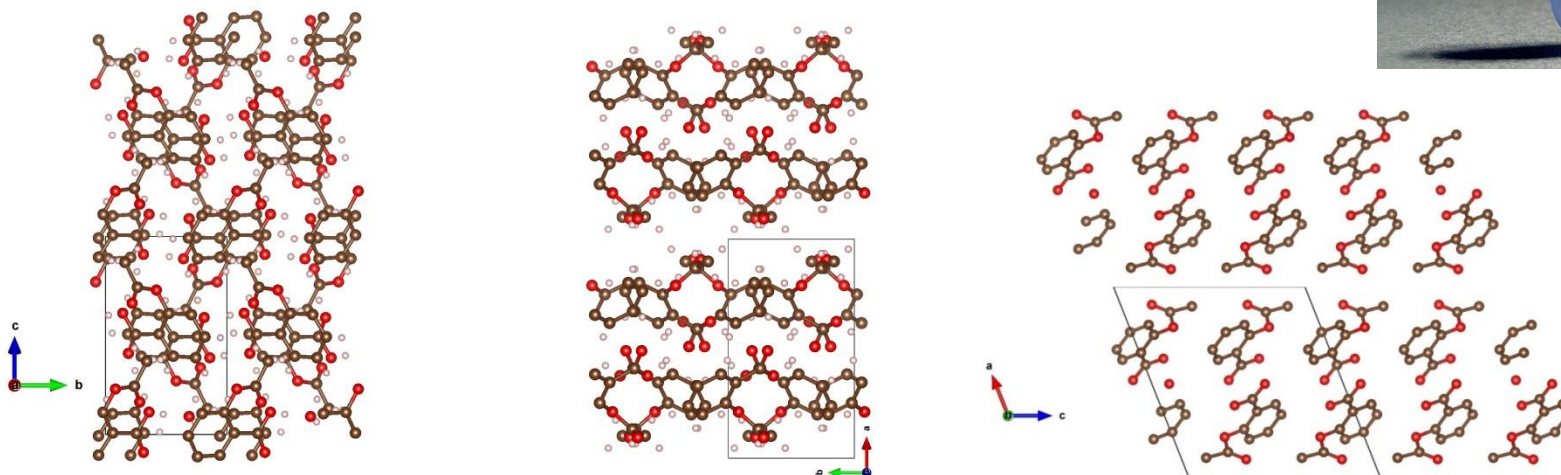


ASPIRIN

form I (P21/c): $a=11.233(3)$ Å, $b=6.544(1)$ Å, $c=11.231(3)$ Å, $\hat{a} = 95.89(2)^\circ$

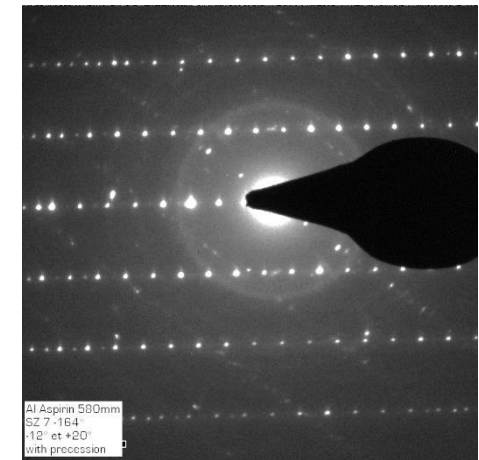
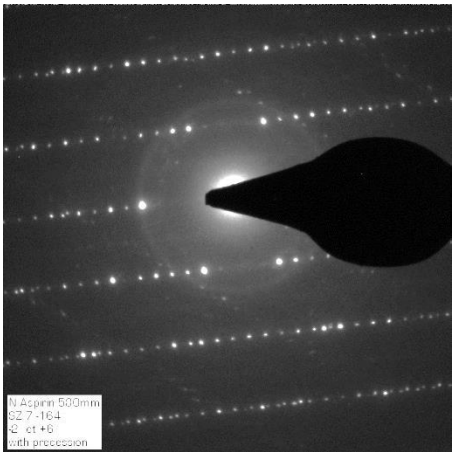
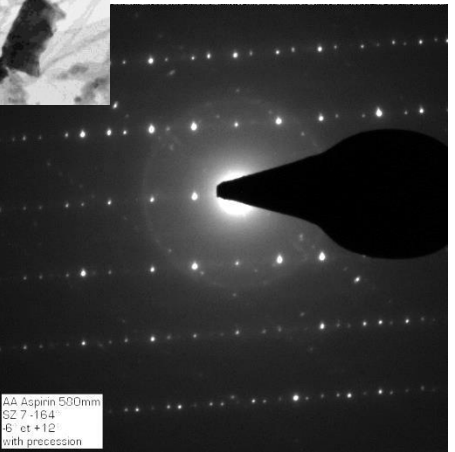
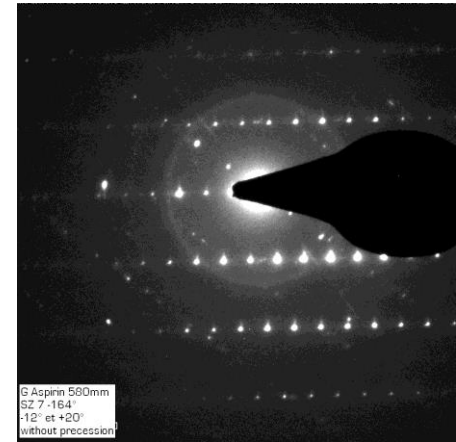
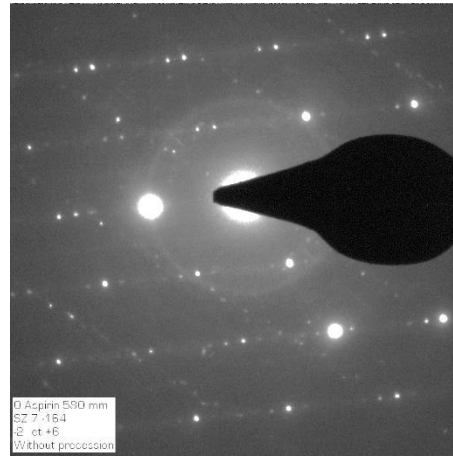
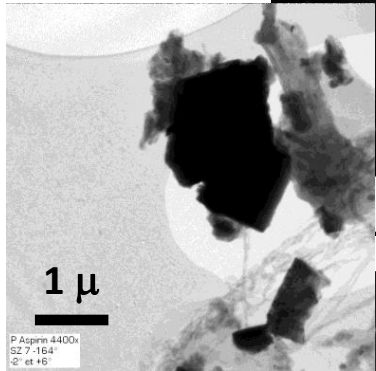


form II (P21/c): $a=12.095(7)$ Å, $b=6.491(4)$ Å, $c=11.323(6)$ Å, $\hat{a}=111.509(9)^\circ$

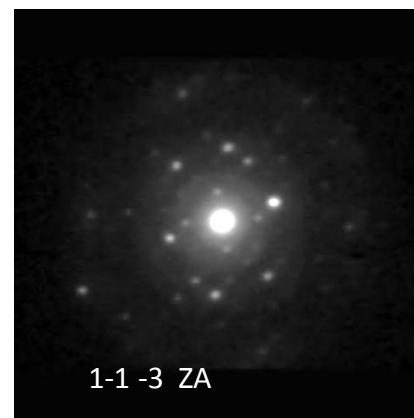
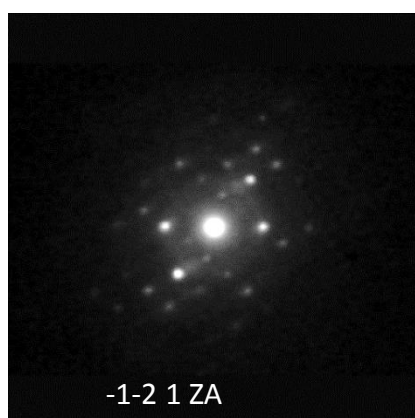
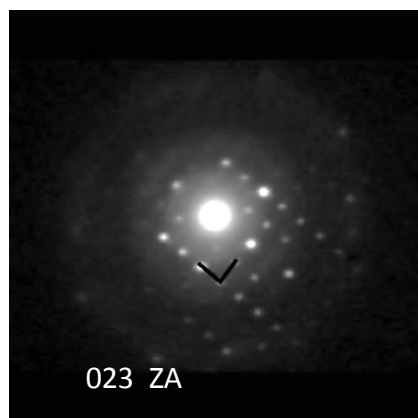
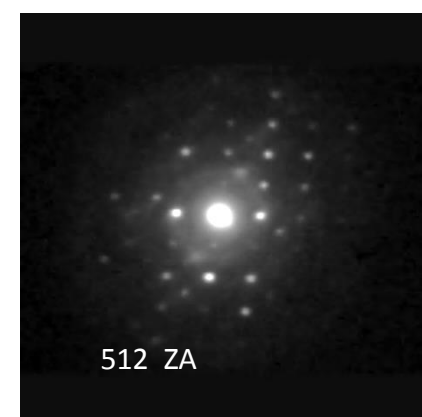
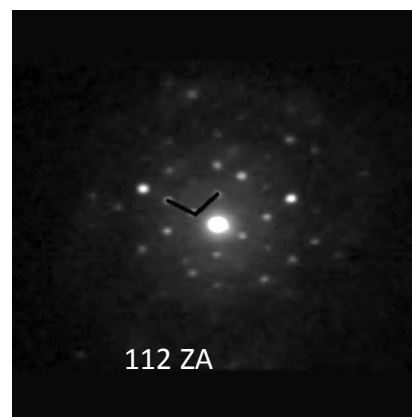
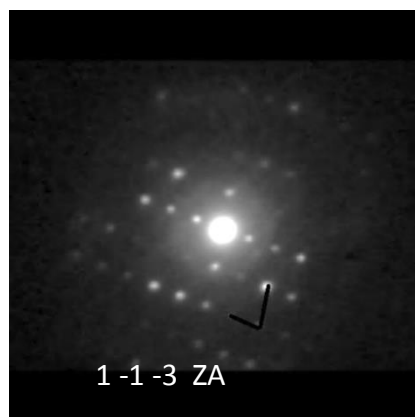
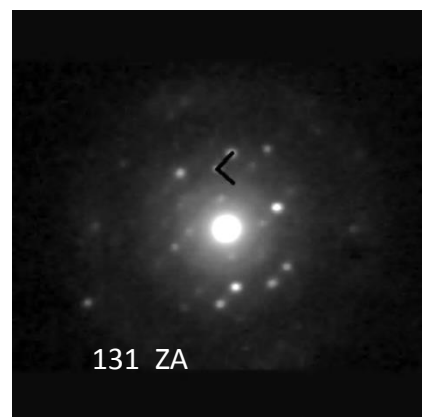


ASPIRIN

PED patterns improvement with precession



ASTAR : Random precession diffraction tomography

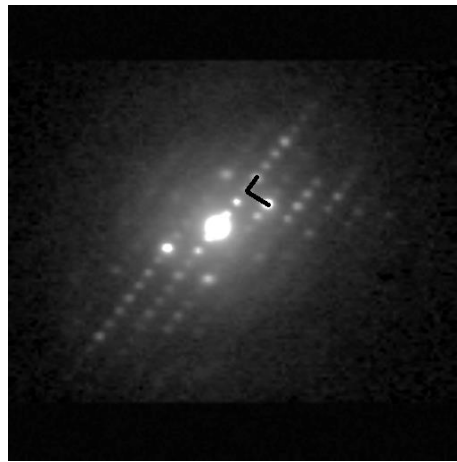


EDiff software : cell parameters are found from 11 random PED patterns

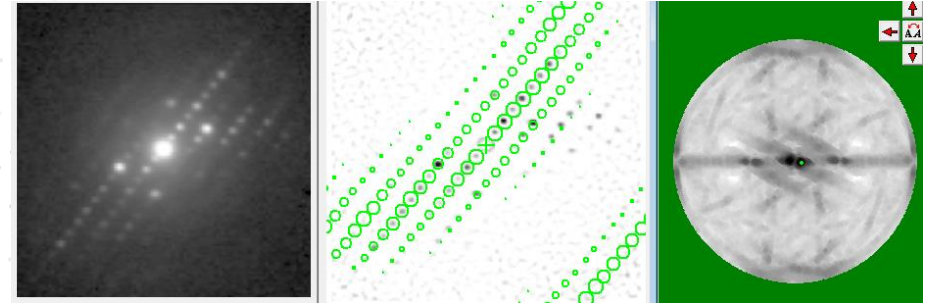
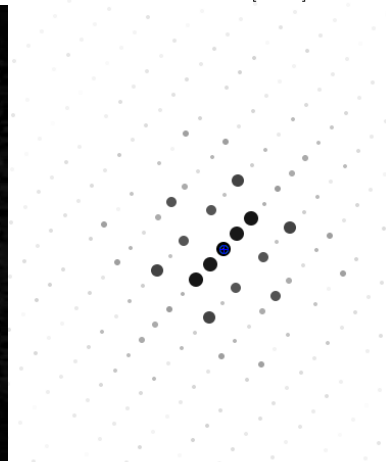
a	b	c	alpha	beta	gamma
6.663	10.68	11.75 97.5	89.3	91	95.000

Data collected with 120 kv TEM IIT Pisa

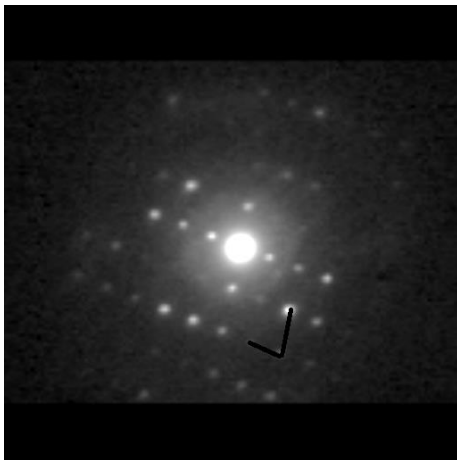
ASTAR : Random precession diffraction tomography



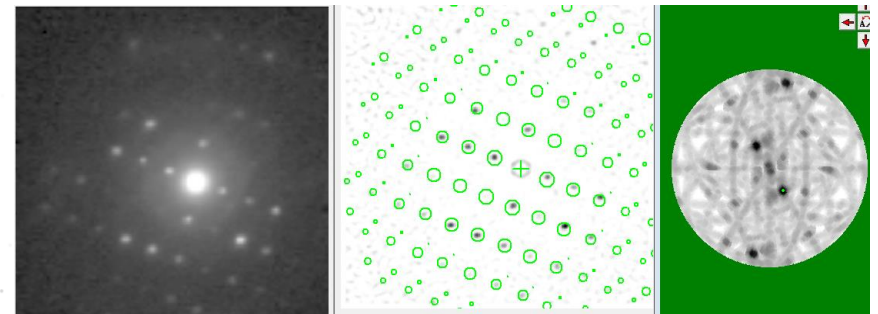
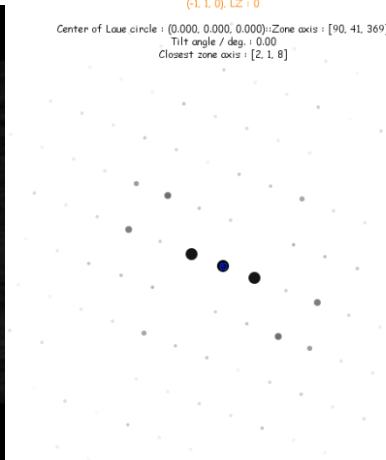
Center of Laue circle : (0.000, 0.000, 0.000):Zone axis : [-1, 0, 10]
Tilt angle / deg. : 0.00
Closest zone axis : [-1, 0, 10]



ZA 001, Best match



(-1, 1, 0), LZ : 0
Center of Laue circle : (0.000, 0.000, 0.000):Zone axis : [90, 41, 369]
Tilt angle / deg. : 0.00
Closest zone axis : [2, 1, 8]

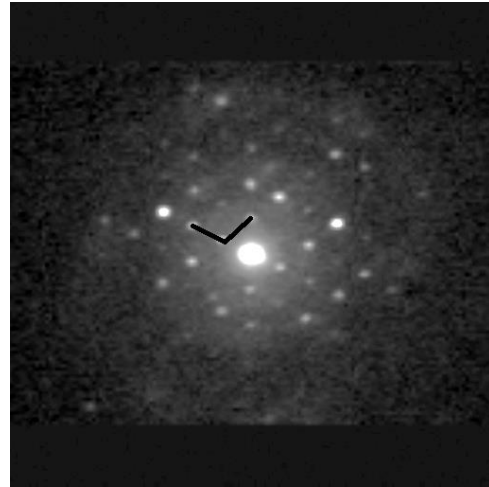


ZA 113 Best Match

5 nm⁻¹

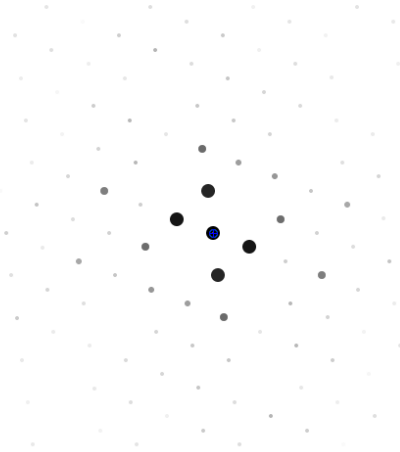
(124 reflections)
AV/kV:120.00, CL/mm:2366, ZA:[1, 1, 3], FN:[1, 1, 3]

ASTAR : Random precession diffraction tomography

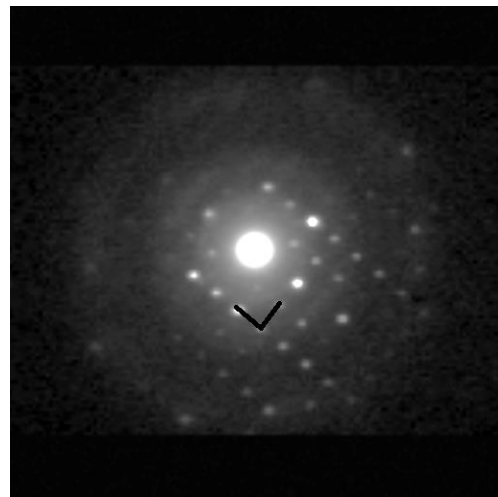


(8, -2, -3), LZ : 0

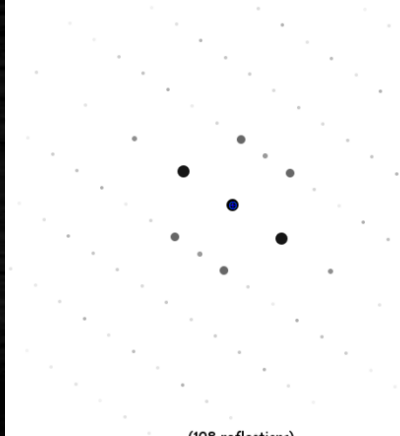
Center of Laue circle : (0.000, 0.000, 0.000); Zone axis : [51, 21, 119]
Tilt angle / deg. : 0.00
Closest zone axis : [18, 7, 42]



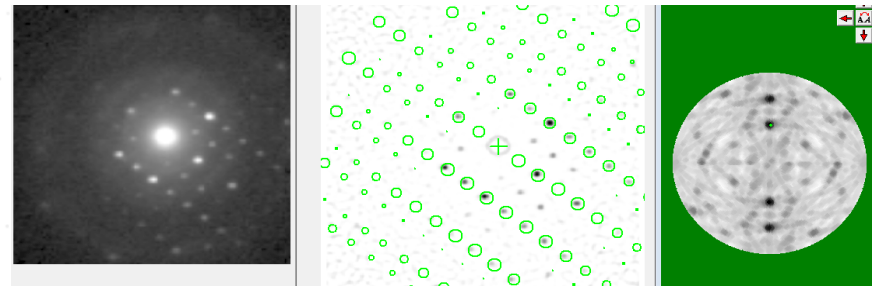
ZA 112 Best Match



Center of Laue circle : (0.000, 0.000, 0.000); Zone axis : [8, 0, 13]
Tilt angle / deg. : 0.00
Closest zone axis : [8, 0, 13]



(108 reflections)
AV/kV:120.00, CL/mm:2366, ZA:[2, 0, 3], FN:[2, 0, 3]



ZA 203 , Best Match

5 nm⁻¹

CONCLUSIONS

Try electron diffraction !

CONCLUSIONS

Most important reasons to use Electron Diffraction

- Nanocrystalline samples that give poor X-Ray patterns
- Inconclusive cell determination /crystal structure from X-Ray
- Detailed overview over crystalline vs amorphous content
- Solve crystal structures ab-intio from < 50 nm crystals

How Electron Diffraction can be used ?

- Use any TEM (120, 200, 300 kv LaB6 or FEG) with cryoholder
- **3D precession diffraction tomography (ADT-3D) can help to find ab-initio the unit cell /crystal structure of any unknown crystal > 50 nm**
- Random precession diffraction tomography (ASTAR) to find unit cell and crystal structure by reconstructing reciprocal space from quasi-oriented PED patterns
- **Reveal detailed local amorphous vs crystalline part in samples**

NanoMEGAS team



Thanks !

Acknowledgements

CNRS Grenoble

- Edgar Rauch
- Muriel Veron

NanoMEGAS

- Thanos Galanis
- Partha Pratim Das

IIT Pisa Italy

- Mauro Gemmi

Peter Oleynikov

Univ of Stockholm Sweeden

Univ of Pavia Italy

- Giovanna Bruni

Univ of Cambridge

- Alex Egermann

Excelsius Belgium

- Fabia Gozzo (next speaker)
- ICDD
- Chinese Academy of Science